

AN ABSTRACT OF THE DISSERTATION OF

Rongkun Shen for the degree of Doctor of Philosophy in Biochemistry and Biophysics presented on September 8, 2006.

Title: Protein-Protein Interactions in the Bacteriophage T4 dNTP Synthetase Complex

Abstract approved:

---

Christopher K. Mathews

The enzymes of dNTP synthesis in T4 infection associate to form a multienzyme complex, the T4 dNTP synthetase complex, facilitating the flow of metabolites *en route* to dNTPs, and their subsequent flow into DNA. Study of protein-protein interactions helps one to understand how the enzymes in the complex are organized and coordinated to function efficiently. By use of several approaches, namely, IAsys optical biosensing, fluorescence spectroscopy and analytical ultracentrifugation, a large number of direct protein-protein interactions among the proteins in the complex were detected. Those associations involved not only T4-encoded proteins but also two host-encoded enzymes, namely, *E. coli* NDP kinase and adenylate kinase. Quantitative analysis of some of those associations show that their equilibrium dissociation constants fall into the micromolar range, which is comparable to the estimated intracellular protein concentrations, suggesting that those interactions are significant *in vivo*. In addition, direct interactions between T4 single-strand DNA binding protein (gp32) and several proteins in the

complex suggest a linkage between the dNTP synthetase complex and DNA replisome.

We also found that some nucleotides, especially ATP, enhanced most of the direct protein-protein interactions. Quantitative analysis shows that, in the presence of 1 mM ATP, the dissociation constants were an order of magnitude lower than that in the absence of ATP. The intracellular concentration of ATP was determined in millimolar range, suggesting that *in vivo* the associations are even more significant.

IASys analysis shows the self-association of *E. coli* NDP kinase and its enhancement by ATP. Equilibrium sedimentation indicates that, in the absence of ATP, the dissociation constant between dimers and tetramers was 0.8  $\mu$ M. However, in the presence of 0.5 mM ATP, NDP kinase appeared completely in tetramer, suggesting that ATP might exert its effect through influence upon the quaternary structure of NDP kinase.

A mixture of purified T4 enzymes was assayed for activity of a three-step sequence (dCTP $\rightarrow$ dCMP $\rightarrow$ dUMP $\rightarrow$ dTMP), sequentially catalyzed by dCTPase/dUTPase, dCMP deaminase and thymidylate synthase. Kinetic coupling behavior was observed. Other proteins in the complex that are not catalytically involved in this pathway enhanced the kinetic coupling, suggesting positive cooperativity among interactions stabilizing the complex.

© Copyright by Rongkun Shen  
September 8, 2006  
All Rights Reserved

Protein-Protein Interactions in the Bacteriophage T4  
dNTP Synthetase Complex

by  
Rongkun Shen

A DISSERTATION

submitted to

Oregon State University

in partial fulfillment of  
the requirements for the  
degree of

Doctor of Philosophy

Presented September 8, 2006  
Commencement June 2007

Doctor of Philosophy dissertation of Rongkun Shen presented on September 8, 2006.

APPROVED:

---

Major Professor, representing Biochemistry and Biophysics

---

Chair of Department of Biochemistry and Biophysics

---

Dean of the Graduate School

I understand that my dissertation will become part of the permanent collection of Oregon State University libraries. My signature below authorizes release of my dissertation to any reader upon request.

---

Rongkun Shen, Author

## ACKNOWLEDGEMENTS

I would like to express my grateful thanks to my advisor and mentor, Dr. Christopher K. Mathews, for his great ideas, extensive help and constant support during this research. His enthusiasm for and serious attitude towards science always inspires my strong interests in science, which will benefit me for my lifetime. I would also like to thank all the members in Mathews' lab during my stay, especially Linda J. Wheeler (Benson) and Dr. Indira Rajagopal for their kind technical advice and support, Dr. Michael C. Olcott for his great and generous help on protein purification, Dr. Shiwei Song for his help on ribonucleotide reductase activity assay and more, Dr. JuHyun Kim for useful discussion, and Dr. Korakod Chimploy for her help on the preparation of ATP affinity column.

I would like to appreciate Drs. Sonia R. Anderson (committee member) and Dean A. Malencik for their helpful advice and generous help on fluorescence spectroscopy and analytical ultracentrifugation experiments. I also thank other committee members, Drs. Stephen Giovannoni, Michael Penner, Ken E. van Holde, Thomas Savage for their time and suggestion on my dissertation.

I am greatly indebted to my wife – Li Li, my son – Chris (Lu), and my parents for their love, encouragement, support and patience.

## TABLE OF CONTENTS

	<u>Page</u>
Chapter 1 Introduction and Literature Review.....	1
1.1 Protein-Protein Interactions .....	1
1.2 Multifunctional Enzymes, Multienzyme Complexes and Metabolons .....	3
1.3 Bacteriophage T4 and Its Life Cycle .....	4
1.4 T4 dNTP Synthesis Pathway .....	6
1.5 T4 Ribonucleotide Reductase .....	10
1.6 T4 dNTP Synthetase Complex .....	13
1.7 dNTP compartmentation in other organisms .....	20
1.8 Known Protein-Protein Interactions in T4 dNTP Synthetase Complex .....	22
1.9 <i>E. coli</i> NDP Kinase Function and Structure, and Oligomeric Structure of NDP Kinases from Other Organisms .....	25
1.10 New Approaches to Study Protein-Protein Interactions .....	30
1.10.1 IAsys Optical Biosensor .....	31
1.10.2 Fluorescence Spectroscopy .....	35
1.10.3 Analytical Ultracentrifugation .....	36
1.11 Dissertation Aims .....	37
Chapter 2 Materials and Methods .....	55
2.1 Overview of Recombinant Proteins and Their Expression Systems .....	55
2.2 Overexpression and Purification of T4 Aerobic Ribonucleotide Reductase (RNR) .....	55
2.3 Preparation of $\gamma$ -PO <sub>4</sub> -Linked dATP Sepharose Column .....	58
2.4 Overexpression and Purification of T4 Thymidylate Synthase (TS) .....	59
2.5 Thymidylate Synthase Activity Assay .....	61

## TABLE OF CONTENTS (Continued)

	<u>Page</u>
2.6 Overexpression and Partial Purification of T4 dCMP Hydroxymethylase (gp42) .....	62
2.7 Overexpression and Purification of T4 dCTPase/dUTPase (gp56) .....	63
2.8 dUTPase/dCTPase Activity Assay .....	66
2.9 Overexpression and Purification of T4 dCMP Deaminase (CD) .....	66
2.10 dCMP Deaminase Activity Assay .....	68
2.11 Overexpression and Partial Purification of <i>E. coli</i> NDP Kinase .....	69
2.12 <i>E. coli</i> NDP Kinase Activity Assay .....	70
2.13 Overexpression and Purification of T4 dNMP kinase (gp1) .....	70
2.14 T4 dNMP Kinase Activity Assay .....	71
2.15 Overexpression and Purification of T4 Anaerobic Ribonucleotide Reductase Subunit (NrdD) .....	72
2.16 Other Proteins .....	73
2.17 Kinetic Coupling Assay for dCTP→dCMP→dUMP→dTMP Pathway .....	74
2.18 Immobilization of Protein onto an IAsys Cuvette .....	75
2.19 Real-Time Interaction Measurement and Data Analysis on an IAsys Optical Biosensor .....	76
2.20 Fluorescence Spectroscopy .....	76
2.21 Analytical Ultracentrifugation .....	77
Chapter 3 Direct Protein-Protein Interactions in the T4 dNTP Synthetase Complex ....	84
3.1 Protein-Protein Interactions Involving T4 Phage-Encoded Proteins in Bacteriophage T4 dNTP Synthetase Complex .....	85
3.2 Protein-Protein Interactions Involving <i>E. coli</i> NDP Kinase .....	87

## TABLE OF CONTENTS (Continued)

	<u>Page</u>
3.3. Protein-Protein Interactions Involving <i>E. coli</i> Adenylate Kinase .....	90
3.4 Protein-Protein Interactions Involving T4 Anaerobic Ribonucleotide	
Reductase Subunit (NrdD) .....	92
Chapter 4 Nucleotide Effects upon Protein-Protein Interaction .....	110
4.1 Nucleotide Effects upon Protein-Protein Interactions Involving T4-Encoded	
Proteins .....	111
4.2 Nucleotide Effects upon Protein-Protein Interactions Involving Host-	
Encoded Enzymes .....	112
4.3 Protein-Protein Interactions Involving T4 Anaerobic Ribonucleotide	
Reductase Subunit (NrdD) .....	114
Chapter 5 Tetramerization and Self-Association of <i>Escherichia coli</i> NDP Kinase .....	123
5.1 Self-Association of <i>E. coli</i> NDP Kinase Detected by Optical Biosensing ....	124
5.2 Tetramerization of <i>E. coli</i> NDP Kinase Detected by Analytical	
Ultracentrifugation .....	126
5.3 Self-Association of <i>E. coli</i> NDP Kinase Detected by Fluorescence	
Spectrophotometry.....	127
5.4 Self-Association of Other Proteins in the T4 dNTP Synthetase Complex ....	128
Chapter 6 Kinetic Coupling Assay for a Three-Step dCTP→dCMP→dUMP→dTMP	
Pathway .....	137
6.1 Kinetic Coupling Assay for a Three-Step dCTP→dCMP→dUMP→dTMP	
Pathway .....	138
6.2 Effects on Kinetic Coupling by Other Proteins That Are Not Catalytically	
Involved in the Pathway .....	140

## TABLE OF CONTENTS (Continued)

	<u>Page</u>
Chapter 7 Discussion and Conclusions .....	146
7.1 Direct Protein-Protein Interactions in the T4 dNTP Synthesis Complex .....	146
7.2 Nucleotide Effects upon Protein-Protein Interactions .....	150
7.3 Tetramerization and Self-Association of Escherichia coli NDP Kinase .....	152
7.4 Merits of IAsys Optical Biosensing on Protein-Protein Interaction Study ....	154
7.5 Kinetic Coupling Assay for a Three-Step dCTP→dCMP→dUMP→dTMP Pathway .....	154
7.6 Merits of the T4 dNTP Synthetase Complex Model .....	155
Bibliography .....	160
Appendices .....	181
A. Hm-dCTP Preparation Protocol .....	182
A.1 Enzymatic Production and Purification of hm-dCMP .....	182
A.2 Enzymatic Production and Purification of hm-dCTP .....	186
B. Raw Data from Analytical Ultracentrifugation.....	188
C. Computer Simulation of Non-Coupled Assay for Three-Step Pathway: Program in Perl .....	190
D. Repeatability of IAsys cuvettes .....	194

## LIST OF FIGURES

<u>Figure</u>	<u>Page</u>
1.1 Overview of T4 developmental program .....	45
1.2 A chronology of major events in the T4 infective life .....	46
1.3 dNTP biosynthesis pathways in T4 phage-infected <i>E. coli</i> host .....	47
1.4 Structure of <i>E. coli</i> ribonucleoside diphosphate reductase .....	48
1.5 A “funnel” model of dNTP biosynthesis in T4 infection where T4 dNTP synthetase complex is juxtaposed with the DNA replication apparatus .....	49
1.6 Protein-protein interaction model identified within the T4 dNTP synthetase complex as of 2000 .....	50
1.7 Comparison of subunit assembly of the NDP kinases of human NDP kinase B and <i>Myxococcus</i> .....	51
1.8 Configuration of the IAsys optical biosensor device and principles of Resonant Mirror technology .....	52
1.9 A typical biosensing experiment .....	53
1.10 Monophasic association (theoretical) .....	54
1.11 Typical binding curve analysis (theoretical) .....	54
2.1 Highly purified proteins in SDS-PAGE .....	80
2.2 Activity assay for dUTPase/dCTPase (gp56) coupled with a TS assay .....	81
2.3 Activity assay for dCMP deaminase coupled with a TS assay .....	81
2.4 Kinetic coupling assay for dCTP→dCMP→dUMP→dTMP pathway .....	82
2.5 Chemistry for immobilization of proteins to CMD or carboxylate cuvette by EDC/NHS chemistry .....	83
3.1 Interactions of T4 ribonucleotide reductase (RNR), T4 single-strand DNA binding protein (gp32), T4 dihydrofolate reductase (DHFR) with T4 thymidylate synthase (TS) that was immobilized on an IAsys carboxylate cuvette .....	94
3.2 Interactions of T4 TS, T4 DHFR, T4 gp32 with T4 RNR that was immobilized on an IAsys carboxylate cuvette .....	95
3.3 Fluorescence spectra of T4 RNR and T4 TS (excitation at 290 nm) .....	96

## LIST OF FIGURES (Continued)

<u>Figure</u>	<u>Page</u>
3.4 Fluorescence spectra of T4 gp56 and T4 TS (excitation at 290 nm) .....	97
3.5 Binding curve of T4 RNR to T4 TS immobilized on IAsys carboxylate cuvette in the absence or presence of ATP .....	98
3.6 Interactions of T4 RNR, T4 TS, T4 gp32, T4 gp56 or <i>E. coli</i> TS, <i>E. coli</i> CTP synthetase with <i>E. coli</i> NDPK immobilized on an IAsys carboxylate cuvette ..	99
3.7 Protein-protein interactions as inferred by fluorescence enhancement .....	101
3.8 Quantitative analysis of the interaction of T4 gp32 (A), T4 dCMP deaminase (B), or T4 thymidylate synthase (C) in solution with immobilized <i>E. coli</i> NDP kinase on an IAsys carboxylate cuvette .....	103
3.9 Protein-protein interactions involving <i>E. coli</i> adenylate kinase .....	105
3.10 Quantitative analysis of protein-protein interactions .....	106
3.11 Fluorescence spectra of T4 NrdD with T4 TS (A), T4 gp56 (B) or <i>E. coli</i> NDPK (C) (excitation at 290 nm) .....	108
3.12 ATP effects on the association of T4 anaerobic ribonucleotide reductase (NrdD) to <i>E. coli</i> NDPK immobilized on an IAsys carboxylate cuvette .....	109
4.1 Interaction between T4 ribonucleotide reductase (RNR) and T4 thymidylate synthase (TS) and ATP effects on their interaction .....	116
4.2 Nucleotide effects on interaction of T4 RNR to T4 TS immobilized on an IAsys carboxymethyl dextran (CMD) cuvette .....	117
4.3 ATP enhances the association of T4 RNR to <i>E. coli</i> NDPK immobilized on IAsys carboxylate cuvette .....	118
4.4 ATP effects on the association of T4 TS (A), or gp56 (B) to <i>E. coli</i> NDPK immobilized on an IAsys carboxylate cuvette .....	119
4.5 ATP and hm-dCTP effects on the association of T4 CD to <i>E. coli</i> NDPK immobilized on IAsys carboxylate cuvette .....	120
4.6. dCTP effect on the association of T4 CD to <i>E. coli</i> ADK immobilized on IAsys carboxylate cuvette .....	121

## LIST OF FIGURES (Continued)

<u>Figure</u>	<u>Page</u>
4.7. ATP and hm-dCTP effects on the association of T4 CD to <i>E. coli</i> ADK immobilized on IAsys carboxylate cuvette .....	122
5.1 Association of <i>E. coli</i> NDPK to <i>E. coli</i> NDPK immobilized on an IAsys carboxylate cuvette .....	130
5.2 Quantitative analysis of NDP kinase-NDP kinase interactions in the absence or presence of ATP .....	131
5.3 NDP kinase quaternary structure as a function of protein concentration generated by global fitting analysis .....	132
5.4 The apparent equilibrium association constant determination between dimer-tetramer species in <i>E. coli</i> NDP kinase generated by 10,000 iterations of Monte Carlo analysis .....	133
5.5 Effect of ATP titration to <i>E. coli</i> NDP kinase on fluorescence spectra .....	134
5.6 Self-association of <i>E. coli</i> adenylate kinase .....	135
5.7 Self-association of T4 aerobic ribonucleotide reductase .....	136
6.1 Kinetic coupling assay for the three-step dCTP→dCMP→dUMP→dTMP pathway sequentially catalyzed by dCTPase/dUTPase, dCMP deaminase and thymidylate synthase .....	143
6.2 Effects on kinetic coupling by enzymes that do not catalytically participate in the three-step dCTP→CMP→dUMP→dTMP pathway – I .....	144
6.3. Effects on kinetic coupling by enzymes that do not catalytically participate in the three-step dCTP→CMP→dUMP→dTMP pathway – II .....	145
7.1 An interactome model for the organization of the T4 dNTP synthetase complex around DNA .....	159
A.1 Schema for enzymatic preparation of hm-dCTP .....	182
A.2 Hm-dCMP production checked by TLC .....	185
A.3 Hm-dCTP production checked by TLC .....	187

LIST OF FIGURES (Continued)

<u>Figure</u>	<u>Page</u>
B.1 All residual errors in sedimentation equilibrium distribution of <i>E. coli</i> NDP kinase .....	188
B.2 Scan overlays of sedimentation equilibrium distribution of <i>E. coli</i> NDP kinase ...	189
C.1 The calculated concentrations of dCTP, dCMP, dUMP and dTMP .....	193
D.1 The repeatability of an IAsys cuvette .....	194

## LIST OF TABLES

<u>Table</u>	<u>Page</u>
1.1 Enzymes in the <i>de novo</i> synthesis of dNTP precursors of T4 DNA .....	40
1.2 Overview of the characteristics of the ribonucleotide reductase classes .....	41
1.3 Regulation of T4 ribonucleotide reductase activity .....	42
1.4 Proteins retained on protein affinity columns where dCMP hydroxymethylase was immobilized .....	43
1.5 Proteins retained on protein affinity columns .....	44
2.1 Recombinant proteins and their expression systems .....	79
4.1 Nucleotide effects on interaction of T4 RNR to T4 TS immobilized on an IAsys carboxymethyl dextran (CMD) cuvette .....	115
5.1 Interactions involving <i>E. coli</i> NDP kinase and T4-encoded proteins plus <i>E. coli</i> adenylate kinase .....	129
7.1 Direct protein-protein interactions and ATP enhancement upon their interactions observed in this thesis comparing with previous results .....	157
7.2 Proteins in the T4 dNTP synthetase complex and their available crystal structure information .....	158

## DEDICATION

To my wife, my son and my parents.

# **Protein-Protein Interactions in the Bacteriophage T4 dNTP Synthetase Complex**

## **Chapter 1**

### **Introduction and Literature Review**

#### **1.1 Protein-Protein Interactions**

Protein-protein interactions exist in virtually all biological processes (Walhout and Vidal, 2001). Any major process in biology involves protein complexes. These processes, for example, include DNA replication and repair, transcription, translation, cell cycle control, cell movement, signal transduction, cell growth, and metabolic pathways (Srere and Mathews, 1990; Mathews, 1993a; Mathews, 1993b; Mathews *et al.*, 2000). Protein-protein interactions play pivotal roles in those processes. Understanding biological processes largely depends on understanding interactions among the proteins involved in those processes.

There are three types of protein-protein interactions (Phizicky and Fields, 1995). First, subunit-subunit associations in multi-chain proteins are clear since the proteins are purified as multi-subunit complexes. For instance, the R1 and R2 subunits interact with each other in bacteriophage T4 ribonucleotide reductase R1-R2 holoenzyme (Hanson and Mathews, 1994). Second, some well-known assemblies contain multiple tightly associated proteins. These complexes include pyruvate dehydrogenase (Mathews *et al.*,

2000), the ribosome (Mathews *et al.*, 2000) and bacteriophage T4 tail assembly (Kostyuchenko *et al.*, 2005). Third, what is more interesting to many researchers is the transient protein-protein interactions that control most cellular processes, for example, DNA replication apparatus in phage T4 and *Escherichia coli* (Trakselis *et al.*, 2001; Benkovic *et al.*, 2001; O'Donnell, 2006). Some proteins undergo chemical modifications such as phosphorylation by protein kinases, acylation by acyl transferases, cleavage by proteases, and so forth. These processes include signal transduction, cell cycle control and cell growth. Other transient protein-protein interactions do not involve modifications, but dynamic associations, such as protein folding assisted by chaperonins, transcription complex interacting with different promoters, initiation, elongation and termination of translation, protein transport across membranes (Mathews, 1997; Mathews *et al.*, 2000), and so on. Because these interactions are specific to their microenvironment and process phase *in vivo*, they are more difficult to study using the approaches from traditional biochemistry.

Protein-protein interactions can result in some measurable biochemical and biophysical effects (Phizicky and Fields, 1995). First, proteins can change their kinetic properties, such as altering an enzyme's  $K_M$  or allosteric properties. Second, protein-protein association can facilitate substrate channeling. Channeling is a kinetic facilitation of a metabolic pathway, usually involving preferential transfer of an intermediate from the catalytic site of one enzyme to the next, in preference to its release to the surrounding milieu (Mathews, 1985; Mathews, 1997). Third, they can form a new binding site for

another protein or new substrate. Fourth, they can also inactivate a protein through interaction. Fifth, protein-protein interactions can change the specificity of a protein, e.g., an enzyme, for its substrates.

## **1.2 Multifunctional Enzymes, Multienzyme Complexes and Metabolons**

Multifunctional proteins juxtapose the active sites of enzymes catalyzing sequential reactions so that intermediates can be channeled directly from site to site. Fatty acid synthase (Mathews *et al.*, 2000) is a classical example of multifunctional proteins. However, in many other cases, multiple enzymes rather than a single-chain protein catalyze sequential reactions. These separate proteins associate with each other strongly enough to form a multienzyme complex. Some of these complexes are tightly but noncovalently bound aggregates, while others are loosely associated complexes, which are called “metabolons” in metabolic pathways (Srere, 1987). The high concentration dependence of these associations within the cell implied that “metabolons” are often difficult to detect following the dilution that usually occurs when enzymes are isolated from cells.

Like multifunctional proteins, multi-enzyme complexes also benefit from metabolic channeling. Metabolic channeling possesses at least two apparent advantages. First, channeling prevents diffusion of intermediates away from their sites and provides

efficient utilization of substrates and delivers them to the next site. Second, channeling keeps average concentrations of most intermediates low and prevents the accumulation of intermediates from exerting adverse osmotic pressure in the cell. A multienzyme complex from T4 bacteriophage-infected *E. coli* has been highly purified and kinetically characterized (Tomich *et al.*, 1974; Reddy *et al.*, 1977; Mathews and Allen, 1983; Mathews, 1993b; Greenberg *et al.*, 1994). This multienzyme aggregate, called T4 dNTP synthetase complex, conducting the conversion from ribonucleoside diphosphates to dNTPs through a series of enzymatic reactions, will be further discussed in the following sections.

### **1.3 Bacteriophage T4 and Its Life Cycle**

Bacteriophage T4 has been among the most important model systems in the study of modern genetics and molecular biology (Mathews, 1994). Although phage T4 has been intensively studied over the past sixty years or so, it still has the ability to answer important questions through its further study and continues to contribute to the paradigms of genetics and biochemistry. T4 phage is a particularly powerful system for analyzing dNTP biosynthesis and DNA replications, and the relationship between them, since it encodes almost all the enzymes for these two fundamental processes and most of enzymes have already been well-characterized. Because its DNA replication is

comparable to that of prokaryotes and eukaryotes, it possesses broad biological significance.

Bacteriophage T4 is a virus to *Escherichia coli*. It contains a large linear double-stranded DNA with genome size of 168,903 base pairs – one of the longest DNAs in phages, which encodes about 300 gene products: 289 probable proteins, 8 tRNAs and at least 2 small and stable RNAs of unknown function (Miller *et al.*, 2003). Phage T4 can finish DNA replication, protein synthesis, capsid structure package and host cell lysis within about 25 to 30 minutes at 37°C from its infection through the release of mature progeny. Figures 1.1 and 1.2 show the major events of phage T4's life cycle. Unlike  $\lambda$  phage, T4 is only capable of undergoing a lytic lifecycle and not the lysogenic life cycle. At first, T4 phage adsorbs to host *E. coli* outer cell membrane through its baseplate. The conformational change of the baseplate promotes the contraction of the tail sheath and pushes the inner tube through the cell's outer membrane. After the tail lysozyme (gp5 or gene 5 product) digests the peptidoglycan layer, the inner tube reaches the inner membrane. T4 DNA is injected into the host cell cytoplasm with the aid of electrochemical potential (Miller *et al.*, 2003; Kostyuchenko *et al.*, 2005). T4 phage utilizes entirely the host core RNA polymerase throughout its infection. Immediately after infection, the unmodified bacterial RNA polymerase transcribes a set of T4 genes through their promoters that share some common features with yet are stronger than those of *E. coli*. T4 redirects the transcriptional machinery to T4 promoters with high efficiency (Mathews, 1994). Among those early proteins, *gpalc*, an RNA polymerase-binding

protein, prevents the host RNA polymerase from transcriptional elongation of RNA using the cytosine-containing host DNA as template. In addition to *gpalc*, three different ADP-ribosyltransferases – *gpalt*, ModA and ModB – involve in ADP-ribosylation on  $\alpha$  subunits of *E. coli* RNA polymerase so that host RNA polymerase further prefers T4 promoters to host ones.

During the early stage of T4 phage life cycle, proteins involved in dNTP synthesis, DNA replication, recombination, repair, host cell DNA degradation, and dNTP synthesis are synthesized. Expression of all these proteins are complete within 10 minutes after infection. Meanwhile, DNA synthesis starts at around 5 minutes. T4 life cycle enters the middle stage around 5 minutes. Middle transcription is activated by AsiA – heterodimerizing with  $\sigma^{70}$  – and MotA – a transcriptional activator. Late transcription occurs at around 9 minutes after infection and late proteins include components required for T4 head, tail, fiber, and several virion assembly factors (Mathews, 1994; Miller *et al.*, 2003). Around 25 minutes, 200 or more phage particles are released and ready to infect other host cells.

#### **1.4 T4 dNTP Synthesis Pathway**

In the T4 phage life cycle, one of the major biological activities is DNA synthesis. Following infection, phage T4 shuts off all the host RNA synthesis and redirects

ribonucleotides to the flow into pools of DNA precursors. In the early stages of the T4 life cycle, proteins required for dNTP and DNA synthesis are synthesized within the first 5 minutes (Figures 1.2) (Mathews, 1994; Miller *et al.*, 2003). T4 phage encodes almost all of the proteins needed for dNTP and DNA biosynthesis. DNA synthesis starts at around 5 minutes after infection at 37°C and dNTPs as DNA precursors are on demand simultaneously. Figure 1.3 shows the T4 dNTP biosynthesis pathway. There are at least 10 enzyme activities contributing to dNTP synthesis in T4-infected host, 8 of which are encoded by T4 and 2 of which are from preexisting host, i.e., nucleoside diphosphate kinase (NDP kinase, or NDPK) and adenylate kinase (ADK) (Mathews and Allen, 1983). What's unique in the pathway is dCMP hydroxymethylase (gp42 or gene 42 product), which modifies dCMP to hm-dCMP (hydroxymethyl-dCMP). Hm-dCMP will be further discussed below. Table 1.1 lists the basic information of those 10 enzymes involved in *de novo* DNA precursor synthesis.

The nucleotide source directly from the degradation of host DNA is about 20 phage-equivalent genomes (169 K base pairs) per *E. coli* chromosome (3 M base pairs). About half of the nucleotides released are actually incorporated into progeny phage DNA. Therefore, host DNA provides approximately 5% of total dNTPs contained in phage progenies released from each infected host cell. The remaining 95% of dNTPs are *de novo* synthesized from ribonucleotides released from host mRNA degradation or synthesized *de novo* (Figure 1.3) (Mathews and Allen, 1983; Mathews, 1994; Greenberg *et al.*, 1994).

Phage T4 incorporates 5-hydroxymethyl dCMP (hm-dCMP) in its genome completely replacing the unmodified dCMP. Hm-dCMP residues in DNA are further glucosylated: 70% of them are  $\alpha$ -glucosylated, and 30%,  $\beta$ -glucosylated, catalyzed by DNA  $\alpha$ - and  $\beta$ -glucosyltransferases, respectively (Mathews and Allen, 1983). The glucosylation of hm-dCMP residue of phage DNA protects its DNA from restriction by host endonucleases, and improves the stability of phage double stranded DNA as well. The hydroxymethylation from dCMP to hm-dCMP is catalyzed T4 dCMP hydroxymethylase (abbreviated to be dCMP HMase, also called gp42 (gene 42 product)), which is an essential enzyme.

After T4 phage infection, the rate of DNA synthesis in the infected *E. coli* increases up to 10-fold higher than in uninfected cells. However, dNTP pools are not augmented substantially (Mathews, 1972). Meanwhile, the dCTP pool disappears and is completely replaced by hm-dCTP. To fulfill the higher demand of dNTP synthesis, phage T4 employs several approaches (Mathews and Allen, 1983; Mathews, 1994). First, T4 synthesizes enzymes such as T4 aerobic ribonucleotide reductase (RNR) and thymidylate synthase (TS), duplicating preexisting activities in the host cell, but enhancing them greatly. Second, T4 encodes dUTPase/dCTPase (gp56 or gene 56 product) to replace its host counterpart – *E. coli* dUTPase that lacks dCTPase. Third, T4 synthesizes its unique dCMP hydroxymethylase to convert dCMP to hm-dCMP to meet the uniqueness of T4 DNA nucleotide composition. Fourth, due to the disappearance of the dCTP pool, the *E.*

*coli* dCTP deaminase, which works on dCTP as its substrate, becomes useless. Instead, T4 replaces it with dCMP deaminase, encoded by gene *cd*, to carry out an important function in thymine nucleotide biosynthesis. Finally, T4 directly makes use of two host-encoded nucleotide kinases: NDP kinase and adenylate kinase.

In the T4 dNTP biosynthesis pathways, there are several other noteworthy features. First, T4 aerobic ribonucleotide reductase (RNR), encoded by genes *nrda* and *nrdB*, and dCMP deaminase are two key enzymes allosterically regulating the whole pathway. T4 RNR will be further discussed in detail in the next section. T4 phage-encoded dCMP deaminase activity is almost completely dependent on the presence of hm-dCTP as an allosteric activator *in vivo* (Fleming and Bessman, 1967) although *in vitro* dCTP is a more effective activator (Maley and Maley, 1982a; Maley and Maley, 1982b). On the other hand, dCMP deaminase is inhibited by dTTP (Fleming and Bessman, 1967). It plays an important role in maintaining the 2:1 ratio of synthesis rates of dTMP (thymidine monophosphate) to hm-dCMP *in vivo* (Flanegan and Greenberg, 1977). Chiu *et al* (Chiu *et al.*, 1977) observed that *E. coli* cells infected by dCMP deaminase-defective T4 phage can synthesize dTMP and hm-dCMP at about 0.6:1 ratio. This further suggests the regulating function of dCMP deaminase.

Second, another essential enzyme for phage T4 growth is dNMP (deoxynucleoside monophosphate) kinase, gene product 1 (abbreviated as gp1). Gp1 exclusively converts three dNMPs, i.e., hm-dCMP, dTMP and dGMP (deoxyguanosine monophosphate), to

their corresponding dNDPs (Brush *et al.*, 1990; Brush and Bessman, 1993; Teplyakov *et al.*, 1996). However, it does not act upon dCMP and dAMP. dAMP is phosphorylated to dADP by *E. coli* ADK. dCMP need not be phosphorylated since it will be converted into either dUMP (deoxyuridine monophosphate) by T4 dCMP deaminase or hm-dCTP by T4 dCMP hydroxymethylase.

Third, T4 thymidylate synthase not only methylates dUMP at 5-carbon to dTMP using tetrahydrofolate (THF) as the one-carbon group donor, but oxidizes methylene-THF to dihydrofolate (DHF). DHF reductase, another enzyme in the pathway, is responsible to reduce DHF to THF.

Finally, the pathway also includes two host-encoded enzymes. Adenylate kinase, as mentioned above, phosphorylates dAMP to dADP. The other is NDP kinase, which has extremely high activity and low specificity for NDP substrates. In crude extracts, NDP kinase activity is as much as 20-fold higher than that of T4 dNMP kinase, thus obviating a need for a T4-coded NDP kinase (Mathews and Allen, 1983). NDP kinase will be further discussed in the later sections.

### **1.5 T4 Ribonucleotide Reductase**

Ribonucleotide reductase (RNR) is an essential enzyme in DNA synthesis, catalyzing all

*de novo* synthesis of deoxyribonucleotides. In all organisms, the remarkable ribonucleotide reductase represents the branch point between RNA and DNA precursor biosynthesis. Ribonucleotide reductase reduces all the four ribonucleoside diphosphates (rNDPs) – i.e., ADP, GDP, CDP, UDP – to their corresponding deoxyribonucleoside diphosphates (dNDPs) – i.e., dADP, dGDP, dCDP, dUDP – by reducing the hydroxyl at carbon 2 to a hydrogen via a free radical mechanism (Jordan and Reichard, 1998). Unlike ribonucleotides that are utilized in all compartments of the cell, deoxyribonucleotides play their sole role to provide DNA synthesis as precursors. The enzyme ribonucleotide reductase is the point that is closely regulated to control the right ratio of four different dNDPs and subsequent dNTPs. The rates of synthesis of four dNTPs must also be controlled to avoid unbalanced dNTP pools. dNTP pool imbalance could cause enhanced mutagenesis, chromosomal abnormalities, induction of endogenous viruses, enhanced genetic recombination and cell death (Mathews, 1997; Mathews, 2006). The enzymes from all organisms possess the regulatory patterns of activation and inhibition with different nucleoside triphosphates – rNTPs and dNTPs – as allosteric effectors.

There are three classes of ribonucleotide reductases, namely, Class I, Class II and Class III shown in Table 1.2 (Thelander and Reichard, 1979; Reichard, 1985; Reichard, 1988; Reichard, 1993; Jordan and Reichard, 1998; Reichard, 2002; Nordlund and Reichard, 2006). Class I ribonucleotide reductases are most widely distributed. Class I enzymes act upon ribonucleoside diphosphates (rNDPs). The enzyme generates a free radical on a tyrosine residue with the aid of a diferric oxygen bridge. Therefore they are limited to

aerobic conditions. Class II enzymes are found in cyanobacteria and some bacteria, and have either aerobic or anaerobic forms. The Class II enzyme acts on ribonucleoside triphosphate substrates (rNTPs). It uses adenosylcobalamin, a B<sub>12</sub> coenzyme to generate a free radical. Class III ribonucleotide reductases are found only in facultative or obligate anaerobes. The Class III enzyme acts on ribonucleoside triphosphate substrates (rNTPs). It uses S-adenosylmethionine and an iron-sulfur center to generate the catalytically essential radical on a glycine residue.

The most common form, Class I, is an  $\alpha_2\beta_2$  dimer. Both *E. coli* and T4 aerobic RNRs belong to Class Ia. The structure of *E. coli* RNR is shown in Figure 1.4. The two  $\alpha$  subunits form the large subunit of the protein called R1 containing the activity and specificity sites. Table 1.3 shows the details of allosteric regulation on T4 RNR. The activity site, binding either ATP (adenosine triphosphate) or dATP (deoxyadenosine triphosphate), increases or decreases all the reduction activities, respectively. However, unlike the enzymes from other organisms that inhibit all four activities, dATP only shows a weak inhibition on GDP reduction (Berglund, 1972). The specificity site, binding ATP, dATP, dTTP (thymidine triphosphate) or dGTP (deoxyguanosine triphosphate), regulates the reduction activities for particular ribonucleoside diphosphates. In addition, the unique hm-dCTP in T4 is also a potent activator for UDP and CDP reduction (Berglund, 1975). The counterpart of hm-dCTP in the host cell, dCTP, plays little or no role in regulating T4 RNR. The two  $\beta$  subunits make up the small subunit of the protein called R2, which contains the free radical. Hydroxyurea (HU), an inhibitor of ribonucleotide reductase,

destroys the free radical (Thelander and Reichard, 1979; Reichard, 1985; Reichard, 1988; Reichard, 1993; Jordan and Reichard, 1998; Reichard, 2002; Nordlund and Reichard, 2006).

Besides aerobic ribonucleotide reductase (abbreviated as RNR), both *E. coli* and T4 also encode a Class III ribonucleotide reductase, the anaerobic form (Young *et al.*, 1994a; Olcott *et al.*, 1998; Fontecave *et al.*, 2002).

### **1.6 T4 dNTP Synthetase Complex**

After phage T4 infection, the DNA synthesis rate per infected *E. coli* cell is up to 10-fold higher than that of the uninfected cell while dNTP pools do not increase substantially (Mathews, 1972; Mathews and Sinha, 1982; Mathews and Allen, 1983). Unlike the rNTPs, which are utilized in all compartments of the cell, dNTPs have extremely limited functions other than acting as DNA precursors and need to be in the close vicinity of the place where DNA is synthesized. It is necessary to organize and regulate the synthesis of deoxyribonucleotides in order to deliver to DNA replication sites as needed. Moreover, deoxyribonucleoside triphosphates must be provided at the same relative rates as the composition of DNA to be synthesized to avoid dNTP imbalance.

However, the chain growth rate at each replication fork in infected cells is about the same as that of the uninfected cell, that is, about 800 nucleotides per second at 37°C. Werner (1968) observed that the number of replication forks increases dramatically to about 60 forks in T4 phage-infected cells, from the original 2-6 forks in uninfected cells. Since replicative DNA polymerases operate at maximum velocity (Mathews, 1976), it is essential that the cell be organized so that dNTPs can be delivered to these replication sites fast enough to meet the tremendous demand for DNA precursors and to maintain saturating concentrations in the vicinity of DNA replication forks (Mathews, 1976). Therefore, in a T4 phage-infected host cell, the dNTP pools must turn over at up to 10 times the rate of an uninfected cell (Ji and Mathews, 1991). All these factors suggest that there exist dNTP concentration gradients at replication sites *in vivo*. Furthermore, Mathews' lab proposed that enzymes of dNTP synthesis form a multi-enzyme complex and this complex is juxtaposed with replication sites (Reddy *et al.*, 1977). Several years earlier, Greenberg's lab had already suggested a similar model based on indirect evidence (Tomich *et al.*, 1974). They devised an innovative technique to simultaneously measure the activity of dCMP hydroxymethylase and thymidylate synthase *in vivo* by assaying the release of tritium from [5-<sup>3</sup>H]uridine administered to a Thy<sup>-</sup> host. [5-<sup>3</sup>H]uridine is converted to labeled substrates by both enzymes, each of which displaces the tritium from the 5-position. Tritium is then released to the solution. Tomich *et al.* found that, *in vivo*, these enzymes start to be active about 5 minutes after enzyme activities can be detected in the cell extract, and their activation starts at the same time as DNA replication. They suggested that these enzymes and others must assemble into a multi-enzyme complex and

become activated *in vivo*. Flanagan and Greenberg also modified this method to estimate flux rates *in vivo* for dCMP hydroxymethylase and thymidylate synthase. They found the flux rate ratio was 1:2, which is very close to the ratio of hm-dCMP to dTMP residues in T4 DNA (Flanagan and Greenberg, 1977; Flanagan *et al.*, 1977; Chiu *et al.*, 1982). They proposed that individual activities in the multi-enzyme complex are closely controlled so that all four dNTPs can be synthesized at the same rates that the T4 DNA is replicated. This helps to explain how balanced dNTP pools can be controlled.

The concept of a T4 dNTP synthetase complex (Tomich *et al.*, 1974; Reddy *et al.*, 1977; Mathews and Allen, 1983; Mathews *et al.*, 1993; Mathews, 1993a; Greenberg *et al.*, 1994) is further supported by the following evidence. First, evidence from our laboratory suggests that T4 phage-infected cells might have two distinct pools of dNTPs.

Subcellular compartmentation means the maintenance within a cell of two or more distinct pools of a particular metabolite where pools may be separated either physically or kinetically. A small pool, believed to be near the replication sites, is rapidly turned over, and a large pool, distributed throughout the rest of the cell, is slowly replenished (Pato, 1979; Mathews, 1993a). Reddy and Mathews (1978) studied T4 phage-infected host cells permeabilized by sucrose plasmolysis. The infected cells incorporate distal DNA precursors, i.e., rNDPs or dNMPs, into DNA seven-fold faster than they incorporate proximal precursors, i.e., dNTPs. This suggested that the replication apparatus preferentially utilizes dNTPs from the small pool *in situ* rather than free dNTPs (Mathews and Allen, 1983; Mathews, 1993a). dNTPs might be subject to the process of

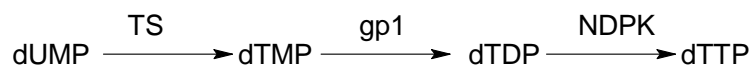
dephosphorylation and then phosphorylation before incorporation into DNA. This hypothesis is further supported by other experiments showing that permeabilized cells infected with T4 phage with a gene 42 (encoding dCMP hydroxymethylase) or gene 1 (encoding dNMP kinase) mutation synthesize little or no DNA even if they were administered with exogenous dNTPs, including the T4-unique hm-dCTP (North *et al.*, 1976; Stafford *et al.*, 1977). In addition, inhibition of NDP kinase inhibits direct incorporation of dNTP into DNA in permeabilized cells (Reddy and Mathews, 1978).

Second, both Mathews' and Greenberg's laboratories isolated a multienzyme aggregate using sucrose gradient centrifugation or gel filtration chromatography (Reddy *et al.*, 1977; Chiu *et al.*, 1982; Allen *et al.*, 1983). There are eight T4 enzymes and two host enzymes in the aggregate that are capable of synthesizing dNTPs *in vitro* (Allen *et al.*, 1983; Thylén and Mathews, 1989). These enzymes are: dCMP hydroxymethylase (gp42), thymidylate synthase (TS), dNMP kinase (gp1), dCTPase/dUTPase (gp56), dCMP deaminase (CD), ribonucleotide reductase (RNR), thymidine kinase (TK), and *E. coli* NDP kinase (NDPK), *E. coli* adenylate kinase (ADK), shown in Figure 1.3. Interestingly, only about 5% of the total host NDP kinase activity was detected in the large aggregate. The aggregate has roughly 0.7-1.0 and 1.0 mDa of molecular mass from sedimentation experiments and gel filtration chromatography, respectively. These numbers are close to the sum of molecular weights of those 10 enzymes above, assuming the complex contains one molecule of each enzyme (Allen *et al.*, 1983; Moen *et al.*, 1988). The possibility of artefactual aggregation after lysis of the cells was ruled out by a mixing experiment

(Allen *et al.*, 1983). A pre-isolated mixture of radiolabeled T4 proteins was added to phage-infected host cells just before lysis and sucrose gradient analysis, none of those radiolabeled proteins sedimented rapidly. This indicates that artefactual aggregation did not occur.

Finally, kinetic coupling assays provide more evidence for the hypothesis. Kinetic coupling reduces the transient time for catalysis in a multi-step reaction pathway. The transient time is defined as the zero time intercept of the plot of product concentration versus time (Welch and Gaertner, 1975). In other words, the time interval required to fill all intermediate pools. Because the two enzymes are juxtaposed, the intermediates released by the first enzyme need not diffuse to reach the catalytic site of the second enzyme. This greatly reduces the time required for accumulation of substrate for the second enzyme to reach the saturating level. Meanwhile, the overall average concentration of intermediates is kept much lower than those in uncoupled systems, even though local concentrations near catalytic sites are relatively high enough to saturate the enzyme.

Mathews' laboratory first analyzed kinetic coupling in the three-step pathway as follows:



where TS is thymidylate synthase, gp1 is dNMP kinase and NDPK is NDP kinase. The pathway was analyzed with the rapidly sedimenting enzyme fraction from a cell extract of the T4 phage-infected host cells. The steady-state concentration of dTDP

(deoxythymidine diphosphate), one of the intermediates, was found to be reduced to about one-tenth and the transient time was lowered to about one-twentieth the values calculated for uncoupled enzyme mixtures. A computational simulation suggested that the local concentrations of intermediates were concentrated 50-fold (Reddy *et al.*, 1977). The longest sequence that demonstrated kinetic coupling involves five enzyme activities, including the key enzyme ribonucleotide reductase, catalyzing a series of reactions from UDP to dTTP (Allen *et al.*, 1980).



where RNR is ribonucleotide reductase and gp56 is dCTPase/dUTPase.

Of great interest is the three-step pathway, dCTP→dCMP→dUMP→dTMP, sequentially catalyzed by gp56, dCMP deaminase and thymidylate synthase. The pathway was analyzed with a partially purified multiple-enzyme complex from *E. coli* infected with the wild-type or gene 42 *amber* mutants of T4 phage by a gel filtration chromatography. Although gp42 (dCMP hydroxymethylase) is not directly involved in catalyzing the pathway, the highly truncated dCMP hydroxymethylase at C-terminus abolishes kinetic coupling in the above three-step pathway, while the mutants of almost full length of dCMP hydroxymethylase give the normal kinetic coupling (Mathews *et al.*, 1988; Thylén and Mathews, 1989; Mathews, 1993a). This suggests that the enzymes within the complex are functionally and physically associated with each other and any structural and functional mutation could disrupt the integrity of the complex.

To sum up, a “funnel” model of dNTP biosynthesis by the T4 dNTP synthetase complex in T4 phage-infected *E. coli* juxtaposed with the replication machinery is given in Figure 1.5 (Mathews, 1993a). Although the breakdown of host cell DNA provides about 5% of total DNA in progeny phages, all the remaining 95% source of dNTP comes from ribonucleotides. Ribonucleotides are sequentially converted to dNTPs as DNA precursors, catalyzed by a series of enzymes initialized with the key enzyme ribonucleotide reductase. Those dNTPs produced in the dNTP synthetase complex directly are released in the intermediate vicinity of DNA replication sites. All the processes are carried out like a “funnel” since almost no intermediates could leak out from the complex.

Since the isolated dNTP synthetase complex does not contain DNA polymerase or other replication proteins, there is no direct evidence supporting the hypothesis that the dNTP synthetase complex is localized near replication sites. New approaches were carried out, including protein affinity chromatography, which had been earlier applied in gp32 (T4 single-strand DNA-binding protein) column (Formosa *et al.*, 1983). Formosa *et al.* (1983) immobilized gp32 on an Affi-Gel-10 column and applied a cell lysate of T4-infected host cells on to the column. The eluates at different NaCl concentrations were analyzed by two-dimensional gel electrophoresis to identify proteins specifically retained by the immobilized gp32. Formosa *et al.* identified nine T4 proteins involved in DNA replication or recombination, including gp43 – T4 DNA polymerase. Our laboratory applied the same approach to immobilize T4 dCMP hydroxymethylase (gp42) (Wheeler *et al.*, 1992). Several proteins of the dNTP synthetase complex and a few proteins of

DNA replication and repair/recombination were retained in the columns. Those DNA replication proteins include gp43 (DNA polymerase), gp44 (clamp-loader subunit), gp45 (sliding clamp), gp61 (primase) and gp62 (clamp-loader subunit). In subsequent protein affinity chromatography experiments, where eight T4 proteins of dNTP synthetase complex were individually immobilized, gp32 was retained by each of these columns (Wheeler *et al.*, 1996). This implies a potent linkage between the dNTP synthetase complex and DNA replication apparatus.

### **1.7 dNTP compartmentation in other organisms**

Although the concept of phage T4 dNTP synthetase complex was proposed more than 30 years ago, it is surprising that there is relatively little work done with higher organisms, including the host of T4 phage – *E. coli*, one of the model systems of prokaryotes. First evidence of dNTP compartmentation in *E. coli* is from Werner's laboratory (Werner, 1971). He found that radiolabeling of DNA at maximal rates was observed long before the dTTP pool was fully radiolabeled when *E. coli* cells were treated with radiolabeled thymine. In 2002, Guzmán *et al.* (Guzman *et al.*, 2002) reported an interesting finding. They used an *E. coli* strain with *nrdA* 101 allele encoding a temperature-sensitive ribonucleotide reductase (RNR), whose activity is completely destroyed at 42°C within 2 minutes. Surprisingly, incubation of this strain at 42°C allows DNA replication for about 40 minutes, which is almost the lifetime of *E. coli*, while hydroxyurea stops DNA

synthesis immediately. This suggests that mutant RNR is protected by some replication hyperstructure from thermal inactivation and RNR is a component of the replication complex. A more recent publication by Molina and Skarstad (Molina and Skarstad, 2004) suggests the existence of a replisome-forming hyperstructure. Replication factories, consisting of 4 polymerases, are organized into higher order structures comprising 8 or 12 polymerases. In addition, the replication factories were dissociated due to lack of nucleotide supply or mutant thymidylate synthase. These findings suggest that the nucleotide synthesis apparatus/complex co-localizes with the hyperstructure formed by DNA replisome factories and further suggest that nucleotide metabolism is closely responsible for keeping the integrity of the replication factories and hyperstructure.

The situation in eukaryotic cells is much more complicated than that in prokaryotic cells. In eukaryotic cells, although some aggregated forms of the enzymes of dNTP biosynthesis were reported (Mathews and Slabaugh, 1986), direct coupling of dNTP synthesis to DNA replication seems unlikely, if only because the enzymes of dNTP synthesis are found largely in the cytosol while DNA replication occurs inside the nucleus (Mathews, 1997). There are two properties in which DNA replication in eukaryotic cells is distinct from that in prokaryotic cells. First, DNA chain growth is about an order of magnitude slower in eukaryotic cells than that in prokaryotic cells. Second, the  $K_M$  values of DNA polymerase for dNTPs in mammalian cells are at least an order of magnitude lower than those of prokaryotic enzymes. For example, the polyoma virus-infected nuclear system saturates at as low as 5  $\mu$ M dNTPs. However, the

intracellular dNTP concentrations are estimated to be higher than this value. For instance, the least abundant dNTP pool, that of dGTP, is about 10  $\mu\text{M}$  (Zhang and Mathews, 1995). Thus the kinetic coupling and substrate channeling is evidently rendered unnecessary since substrates can saturate DNA polymerase by simple diffusion (Mathews and Allen, 1983; Mathews, 1997).

The third category of dNTP compartmentation falls into organelles of eukaryotic cells, such as mitochondria and chloroplast. Since these organelles possess their own DNA distinct from nuclear DNA, they also have their dNTP pools. Song *et al.* (Song *et al.*, 2003; Song *et al.*, 2005) in our laboratory reported that mitochondrial dNTP pools were quite different from those in cytosol in that dGTP pool is unexpectedly higher than other dNTP pools. This suggests dNTP compartmentation in mitochondria. However, there are no reported data on dNTP pools in chloroplast up to date.

### **1.8 Known Protein-Protein Interactions in T4 dNTP Synthetase Complex**

Although several lines of evidence support the concept of the T4 dNTP synthetase complex in T4 phage-infected *E. coli* cells, which is one of the best understood of dNTP metabolic machines, the way enzymes are organized and they coordinate to function as a multi-enzyme complex are not clear. Our laboratory made efforts to better understand the complex by employing various approaches to study protein-protein interactions, which

would definitely provide indispensable and valuable information. Protein affinity chromatography is one of the early methods as mentioned in earlier section. Gp42 – dCMP hydroxymethylase – was immobilized on an Affi-Gel column (Wheeler *et al.*, 1992). More than a dozen proteins from an extract of T4-infected *E. coli* cells were retained on the column relatively strongly (bound at 0.2 M NaCl and eluted at 0.6 M NaCl), implying specific interactions with gp42 (might be indirect association). Among those proteins as shown in Table 1.4, five are enzymes involved in dNTP synthesis, and several are DNA replication proteins, such as gp43 and gp32. This suggests the linkage between the dNTP synthetase complex and DNA replication apparatus. Furthermore, the number of proteins retained on the column is reduced when an extract from phage T4 with amber mutant gp32 or thymidylate synthase was applied on the column under the same condition. This implies that some of the observations are not direct protein-protein associations or the full length proteins are required for their associations.

Following the success of gp42 affinity column, more proteins in the T4 dNTP synthetase complex were individually immobilized on columns to identify the protein-protein interactions. Table 1.5 summarizes the results obtained by 1996 (Wheeler *et al.*, 1996). Since gp32, T4 single-stranding DNA-binding protein, was retained by all eight proteins, Mathews' laboratory suggested that T4 gp32 could be a candidate organizing factor for the dNTP synthetase complex.

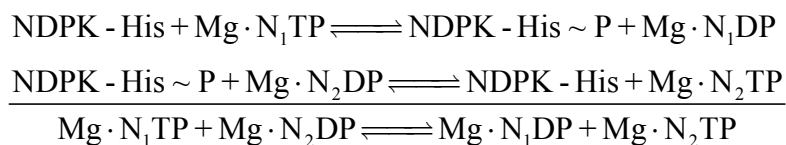
Gp32, the DNA double-helix-destabilizing protein, binds to single-strand DNA (ssDNA) unwound by primosome before being replaced by DNA replisome and is known to be required for T4 DNA replication, recombination and repair (Alberts and Frey, 1970; Nossal and Peterlin, 1979; Sinha *et al.*, 1980; Jarvis *et al.*, 1989). Gp32 binds to ssDNA as the replications forks move and stimulates replisome processivity and accuracy by about 700-fold. Gp32 consists of three domains: B domain, core domain and A domain, in order from N-terminus to C-terminus (Shamoo *et al.*, 1995b). The B domain is responsible for cooperative binding to ssDNA (Villemain and Giedroc, 1996; Villemain *et al.*, 2000). The A domain is essential for its interaction with other proteins. The core domain has a DNA binding site. Gp32 is suggested to be responsible for recruiting the dNTP synthetase complex proteins and leading the complex to the vicinity of DNA replication forks (Wheeler *et al.*, 1996). In addition, several replication proteins were also specifically retained on these columns. All these findings imply that the dNTP synthetase complex is juxtaposed to DNA replication apparatus to provide relatively high localized dNTP concentration to sustain the rapid DNA replication rate after phage infection.

Apart from protein affinity chromatography, some other methods were also employed. Those approaches include analysis of an anti-idiotypic antibody (Young and Mathews, 1992; Wheeler *et al.*, 1996), band shift non-denaturing gel electrophoresis (Wheeler *et al.*, 1996; Bernard *et al.*, 2000), cross-linking (Mathews *et al.*, 1987), and amber mutant and temperature-sensitive mutant and coimmunoprecipitation (Mathews and Allen, 1983;

Hanson and Mathews, 1994; Bernard *et al.*, 2000). The protein-protein interactome was proposed as shown in Figure 1.7 according to the results obtained as of 2000.

### **1.9 *E. coli* NDP Kinase Function and Structure, and Oligomeric Structure of NDP Kinases from Other Organisms**

Because of its role as one of very few host-cell enzymes involved in T4 DNA metabolism, *E. coli* NDP kinase is of particular interest. Nucleoside diphosphate kinase (NDP kinase or NDPK) catalyzes the reaction in which the terminal  $\gamma$ -phosphate group from nucleoside triphosphate (NTP) is transferred to a nucleoside diphosphate (NDP) (Lascu and Gonin, 2000). Like almost all other reactions involving nucleotides, the reaction requires  $Mg^{2+}$  as a cofactor. The enzyme exhibits broad substrate specificity and utilizes any kind of nucleoside (or 2'-deoxynucleoside) di- and triphosphates (Parks and Agarwal, 1973). The catalytic mechanism is an ordered bi-molecular ping-pong type by forming a covalent high-energy phosphoenzyme intermediate through its catalytic histidine residue. The reaction scheme is shown as following:



where nucleotides are chelated with  $Mg^{2+}$ . The reaction is very efficient and rapid and the phosphorylated enzyme is very stable even if there is no NDP acceptor for a couple of hours (Lascu and Gonin, 2000).

Although the reaction is theoretically fully reversible, it is highly prone to move to the right *in vivo* when ATP is abundant. The intracellular levels of ATP, the most common high-energy phosphate donor, are considerably higher than other nucleoside triphosphates. In addition, ATP is far more abundant than ADP or AMP, so there is a strong thermodynamic tendency for the potential energy of ATP to be used in the synthesis of other high-energy compounds (Mathews *et al.*, 2000).

Since NDP kinase functions on both ribo- and deoxyribonucleotides, it is considered to play an important role in maintaining the NTP and dNTP pools for RNA and DNA biosynthesis, respectively. A null mutation of *E. coli ndk* gene, however, causes dNTP pool imbalance, where dCTP pool increased 23-fold and dGTP pool, 7-fold, and a high mutation frequency resulted (Lu *et al.*, 1995). This implies that *E. coli ndk* is not just a housekeeping gene. As mentioned in the previous sections, *E. coli* NDP kinase, as part of T4 dNTP synthetase complex juxtaposed to the T4 DNA replication machinery, is physically and functionally involved in dNTP synthesis. Although most of the mispairs generated by an *E. coli* strain lacking NDP kinase could be corrected by mismatch repair system, double mutants of both *ndk* and *mutS* significantly increased base substitution and frameshift mutations (Miller *et al.*, 2002). It is of great surprise that *E. coli ndk* gene, encoding NDP kinase, is not essential, and the knockout of this gene does not cancel the normal cell growth and can sustain the growth of T4 phage-infected *E. coli* (Hama *et al.*, 1991a; Zhang *et al.*, 1996). But *Myxococcus xanthus* NDP kinase is essential for cell growth (Munoz-Dorado *et al.*, 1990). Later, *E. coli* ADK was reported to complement the

deficient NDPK kinase activity in nucleotide metabolism (Lu and Inouye, 1996).

NDP kinase is a ubiquitous enzyme found in many organisms. Interestingly, NDP kinases share high level of sequence and structure similarity across organisms from prokaryotes to eukaryotes. All NDP kinases are composed of four or six identical subunits of about 150 residues (16-20 kDa each). Eukaryotic NDP kinases are hexamers and some bacterial enzymes are tetramers (Figure 1.7). Each subunit has an independent active center with a nucleophilic histidine and a nucleotide-binding site capable of binding both NDPs and NTPs (Lascu *et al.*, 2000). Each subunit has an  $\alpha/\beta$  sandwich or ferredoxin fold (Janin, 1993; Janin *et al.*, 2000). The fold features a surface  $\alpha$ -helix hairpin, the Kpn (Killer-of-prune) loop and a C-terminus. The  $\alpha$ -helix hairpin and the Kpn loop form the nucleotide-binding site (Lascu *et al.*, 1992), and the C-terminal segment is largely divergent throughout the NDP kinase family (Milon *et al.*, 2000). Prokaryotic NDP kinases from *Myxococcus xanthus* (Williams *et al.*, 1993) and *E. coli* (Ohtsuki *et al.*, 1984; Almaula *et al.*, 1995) are 5-7 residues shorter at the C-terminus than that from eukaryotic enzymes (Mesnildrey *et al.*, 1998). In eukaryotic NDP kinase, the C-terminus (about 20 residues) protruding from the  $\alpha$ -helix is important for stabilizing the subunit-subunit interactions (Chiadmi *et al.*, 1993; Morera *et al.*, 1994; Webb *et al.*, 1995).

The hexameric and tetrameric NDP kinases are constructed by assembling identical dimers (Figure 1.7). The dimer, which is relatively thermostable in solution (Karlsson *et al.*, 1996), is made up by  $\beta$ -sheet extension where subunits sit side by side with their

central  $\beta$ -sheets effectively forming an inter-subunit eight-stranded antiparallel  $\beta$ -sheet between two monomers. However, the thermodynamic behavior of hexameric NDP kinases is distinct from that of tetrameric enzymes. The hexameric NDP kinases directly unfold without the release of natively folded monomer while tetrameric NDP kinases dissociate first and their corresponding monomer or dimer then unfold (Karlsson *et al.*, 1996; Lascu *et al.*, 2000). The hexameric structure ensures the full enzymatic activity while the dimeric form is inactive (Karlsson *et al.*, 1996; Mesnildrey *et al.*, 1998). Therefore, the thermodynamic behavior of NDP kinase is considered to be related to the enzyme activity although the active site in each subunit is independent (Lascu and Gonin, 2000).

In hexameric *Dictyostelium* NDP kinase, Pro-100 (P100), totally conserved in all NDP kinases, is responsible for contacting another dimer in the dimer-dimer interface. The P100S substitution makes the enzyme unstable due to the dissociation of the hexamer but has no effect on the catalytic activity (Lascu *et al.*, 1992; Karlsson *et al.*, 1996). But in the presence of 0.5-1.0 mM ATP, the P100S mutant of the *Dictyostelium* NDP kinase correctly assembled into an active hexameric format by approaches of fluorescence and analytical ultracentrifugation (Mesnildrey *et al.*, 1998). This suggests that the stabilization of oligomeric NDP kinase depends on the presence of nucleotides such as ADP and ATP. Giartosio and coworkers (Giartosio *et al.*, 1996) found that 1 mM ADP increases the thermostability of both tetrameric *E. coli* NDP kinase and the P105G mutant of *Dictyostelium* NDP kinase. Interestingly, while the active hexameric *Dictyostelium*

NDP kinase does not bind single-strand DNA, the dimeric mutant can bind ssDNA but is catalytically inactive (Mesnildrey *et al.*, 1997), suggesting that oligomeric states may be related to the diversified functions of NDP kinases.

In 2003, Postel's group reported that *E. coli* NDP kinase possessed a uracil-processing DNA repair nuclease activity (Postel and Abramczyk, 2003). However, a short time later the Mosbaugh laboratory (Bennett *et al.*, 2004) and followed by Varshney's group (Kumar *et al.*, 2004) argued that *E. coli* NDP kinase lacks the uracil-processing DNA repair nuclease activity and Postel's NDP kinase preparation might be contaminated with uracil-DNA glycosylase (UDG). A recent publication from Postel's group demonstrated that recombinant *E. coli* NDP kinase contains significant UDG activity that is not intrinsic, but rather, is a consequence of a direct physical and functional interaction between Ung (*E. coli* gene *ung* product that encodes the enzyme with UDG activity) and NDP kinase (Goswami *et al.*, 2006). Besides the argument above, like its human homologue NM23-H2/PuF/NDP kinase B, *E. coli* NDP kinase is capable of DNA binding and cleavage, and these activities are suggested to play an essential role in NDP kinase function *in vivo* (Levit *et al.*, 2002).

Apart from its metabolic role, eukaryotic NDP kinases are also involved in a variety of functions, such as the regulation of tumor metastasis (Kimura *et al.*, 2000; Hartsough and Steeg, 2000; Lacombe *et al.*, 2000; Ouatas *et al.*, 2003), endocytosis (Narayanan and Ramaswami, 2003), cell growth and differentiation (Kimura *et al.*, 2000; Timmons and

Shearn, 2000; Lombardi and Mileo, 2003), cell adhesion and migration (Fournier *et al.*, 2002), signal transduction (Kimura *et al.*, 2003), and cell motility (MacDonald *et al.*, 1996) in mammals, and light signal transduction for photosynthesis in plants and fungi (Hasunuma *et al.*, 2003) as well.

### **1.10 New Approaches to Study Protein-Protein Interactions**

Although the approaches mentioned in the above sections have produced useful results, they have some drawbacks. For example, protein affinity chromatography requires large amounts of purified proteins to immobilize on the column, which may create a big challenge for protein purification. It also can not distinguish the direct interaction from indirect interaction if a cell extract is applied. All the above methods can not quantitatively determine the dissociation constants of protein-protein interactions. Dissociation constants represent the strength of association, which is very useful for comparison. In this research we applied several other techniques to study the interactions, such as optical biosensor, fluorescence and analytical ultracentrifugation, to study the direct or indirect interactions between proteins in the complex using purified proteins.

### 1.10.1 IAsys Optical Biosensor

Optical biosensor technique began its research applications in early 1990's. The first optical biosensor, Biacore, originally developed by Pharmacia Biosensor AB (later became Biacore AB), revolutionized the study of macromolecular interactions in biology. It is able to monitor the protein-protein and ligand-ligand interactions by using changes in surface plasmon resonance (SPR) measured in real time (Szabo *et al.*, 1995; Lakey and Raggett, 1998; Fivash *et al.*, 1998; Hall, 2002).

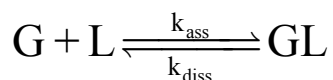
The IAsys instrument (Affinity Sensors, Inc.) is based on the resonant mirror (RM) technology (Cush *et al.*, 1993; IAsys, 1996a; IAsys, 1996c; IAsys, 1996d; Hall, 2001), which is very similar to SPR technology. The operating principles and structure of the sensor are shown in Figure 1.8. IAsys uses a small cuvette and the ligand is immobilized on the surface of the cuvette bottom, the hydrogel layer, which is exactly the sensing layer. Stirring is applied to quickly make the ligand solution homogeneous. Laser light is directed at the prism over a range of angles (only one angle is shown for clarity). Because the prism is made from material with high refractive index, when incident angle is larger than some value, total internal reflection (TIR) occurs when light goes from the interface between the prism and the coupling layer of low refractive index. That means, light is 100% reflected by the interface and no light gets into the coupling layer. At one unique angle in the range where TIR occurs, the resonant angle  $\phi$ , light tunnels through the coupling layer and propagates in the resonant layer of high refractive index. The resonant

mirror technique is dependent on the detection of refractive index changes in the evanescent field, which starts from the interface between the sensing layer (hydrogel) to about 1000 nm into the sample solution. The intensity of the evanescent field decays exponentially and is reduced to one third of its intensity at the surface within about several hundred nanometers where the ligand is immobilized and allows the ligate to bind or dissociate. The rapidly decaying envelope of the field intensity ensures that only interactions between immobilized species and ligate are monitored. The evanescent field of the light propagating within the resonant layer monitors the binding/dissociating events at the sensor surface. Molecules entering the evanescent field from the sample will alter the refractive index profile close to the surface of the device, changing the resonance angle. The change in position of the intensity peak can be precisely monitored with sampling interval of as fast as 0.3 second. The signal change is directly proportional to the amount of protein in the solution associated with the protein immobilized on the surface that alters the refractive index occurring at the surface of the cuvette (IASys, 1996a). A typical biosensing experiment is shown in Figure 1.9 where association and dissociation events are monitored by an IAsys optical biosensor instrument.

IASys is particularly sensitive to very small changes of refractive index occurring within the evanescent field. All biological molecules are virtually capable of being detected by IAsys when they get into this field. IAsys has several advantages over non-stirred optical biosensor systems, such as Biacore, and other techniques for detecting protein-protein interactions: i) using much smaller amount of sample; ii) quantitative and kinetic,

enabling determination of both steady-state and dynamic parameters of interaction; iii) real time monitoring of protein-protein interactions; iv) without the use of labeled molecules; v) sensitive to minute changes of refractive index occurring on the evanescent field. In addition, once one protein is immobilized, other binding partners do not need to be labeled, and might come from an impure solution (IASys, 1996a).

Dissociation equilibrium constants can be determined from IASys data (IASys, 1996c). The classical Langmuirian model for interaction in free solution is used to elucidate the data interpretation here. The simplest binding event is that a single molecule G (ligand) binds the other molecule L (ligate). Their interaction can be represented as follows:



where  $k_{\text{ass}}$  and  $k_{\text{diss}}$  are the association rate constant and dissociation rate constant, with units of  $M^{-1}s^{-1}$  and  $s^{-1}$ , respectively. This equation can be used to predict a monophasic association shown in Figure 1.10. At equilibrium,

$$k_{\text{ass}}[G][L] = k_{\text{diss}}[GL]$$

This can be rearranged as follows:

$$\frac{[G][L]}{[GL]} = \frac{k_{\text{diss}}}{k_{\text{ass}}} = K_D$$

where  $K_D$  is termed the dissociation equilibrium constant, and has units of M. The lower the value of  $K_D$ , the stronger the interaction. The association equilibrium constant  $K_A$ , with units of  $M^{-1}$ , is the reciprocal of  $K_D$ .

The amount of complex formed in time  $t$ , namely  $[GL]_t$ , is given by:

$$[GL]_t = [GL]_{eq} [1 - \exp(-k_{on} t)]$$

Where  $[GL]_{eq}$  is the concentration of complex at equilibrium, and  $k_{on}$  is a first-order apparent on-rate for the interaction with unit of  $s^{-1}$ , given by:

$$k_{on} = k_{ass} [L] + k_{diss}$$

The rate of complex (GL) formation is given by:

$$\frac{d[GL]}{dt} = k_{ass} [G][L] - k_{diss} [GL] \quad [1]$$

Experimentally, the concentration of ligate L is always in excess over that of ligand G and is considered as constant. Therefore, the concentration of free ligand can be calculated as:

$$[G]_{free} = [G]_{total} - [G]_{bound}$$

The total concentration of ligand G is given by the maximal binding of ligate ( $R_{max}$ ) obtained by IAsys instrument during the experiment, and the concentration of ligand G bound to ligate is given by  $R_t$ . Then, equation [1] can be rewritten as:

$$\frac{dR}{dt} = k_{ass} [L](R_{max} - R_t) - k_{diss} R_t$$

At equilibrium,  $dR/dt = 0$  and  $R_t = R_{eq}$ , the above equation will be:

$$R_{eq} = \frac{R_{max} [L]}{K_D + [L]}$$

Then  $R_{eq}$  is plotted against the ligate concentration,  $[L]$ , would give the binding curve shown in Figure 1.11.  $K_D$  can be obtained directly from the curve when the ligate concentration ( $[L]$ ) is equal to half of  $R_{max}$ .

### 1.10.2 Fluorescence Spectroscopy

Fluorescence technique is widely used for protein-protein interaction studies (Phizicky and Fields, 1995). Fluorescence spectroscopy is a highly sensitive method for detecting proteins through their tryptophan (Trp) residues, which can allow detection at concentrations in the order of nM. Fluorescence spectroscopy on the study of protein-protein interactions was first introduced by Anderson lab (Malencik *et al.*, 1982), which measures the Trp fluorescence since it is sensitive to the environment. Usually, excitation at 290 nm minimizes the contribution of tyrosine fluorescence. There are usually changes in intrinsic fluorescence that occur when protein molecules associate in that the fluorophore (mainly tryptophan) in the proteins could expose more or bury more during the association when mixing two proteins. Changes in the fluorescence emission spectrum on protein-protein interaction can occur either by a shift in the wavelength of maximum fluorescence emission or by a shift in fluorescence intensity caused by the mixing of two proteins. Blue shifts support decreased solvent exposure or a change from mobile environment to one that is more rigid. Quantum yield of Trp is influenced by amino acid side chains that are in contact with the side chain of Trp.

### 1.10.3 Analytical Ultracentrifugation

Analytical ultracentrifugation is one of the classical and extremely versatile and powerful techniques for the study of the solution behavior of macromolecules. Recent instrumental and computational developments have significantly enhanced this methodology (Cole and Hansen, 1999). There are two modes of analytical ultracentrifugation: sedimentation velocity and sedimentation equilibrium. Sedimentation velocity methods are much more rapid while sedimentation equilibrium methods are more accurate for the study of protein-protein interactions and protein self-association. In sedimentation velocity, the speed of sedimentation is determined by the rate of movement of the sedimenting boundary, which is usually represented in  $s$ , the sedimentation coefficient. In sedimentation equilibrium, the centrifuge speed is relatively low so that the sedimentation and the diffusion are balanced. Then a concentration gradient is formed along the centrifuge tube. Since the concentration distribution is exponentially dependent on the buoyant mass of the protein, the molecular weight (or molecular mass) can be calculated using the concentration of gradient and tube distance (Lebowitz *et al.*, 2002; Scott *et al.*, 2006), which is shown in the following equation.

$$c_r = c_0 \exp\left(\frac{\omega^2}{2RT} M(1 - \bar{v}\rho)(r^2 - r_0^2)\right)$$

where,  $c_r$  = concentration at radius  $r$

$c_0$  = concentration at reference radius  $r$

$\omega$  = angular velocity

$R$  = gas constant (J/mol·K)

$T$  = temperature in Kelvin

$M$  = molecular weight

$\bar{v}$  = partial specific volume of the solute  
 $\rho$  = density of solvent

If protein-protein interaction or protein self-association occurs, the molecular mass would be higher than that of unassociated counterparts.

### 1.11 Dissertation Aims

T4 dNTP synthetase complex is one of the best understood DNA precursor biosynthesis machines. It is believed that protein-protein interactions play key roles in this multi-enzyme complex. The overall aims in my thesis are to further characterize the T4 dNTP synthetase complex by biochemical and biophysical approaches using purified proteins. To sum up, there are four specific aims.

1. Identification of direct and indirect interactions between proteins in the T4 dNTP synthetase complex. Most of the evidence obtained by immobilized protein affinity chromatography can't distinguish direct protein-protein interaction from indirect association through a third (maybe fourth) component (Wheeler *et al.*, 1992; Wheeler *et al.*, 1996). With the help of IAsys optical biosensor, we can observe the real-time protein-protein interactions and further quantitatively the strength of the interactions by determining the dissociation equilibrium constants. We can not only observe the qualitative data, but conduct the analysis.

2. Analysis of effects of small molecules (substrates, products, allosteric modifiers) on protein-protein interactions. Eric Hanson (1994) in our laboratory observed that 1 mM ATP or 1 mM dATP enhances the phage T4 ribonucleotide reductase subunits R1·R2 interaction. He also found that in the presence of 1 mM ATP the immobilized RNR affinity column retains more proteins as well as the amount of proteins (Wheeler *et al.*, 1996). We would ask if the allosteric modifiers, such as ATP and dATP for T4 ribonucleotide reductase, could also enhance the associations between T4 RNR and other proteins in the complex.

3. Kinetic coupling was observed from the careful analysis using the rapidly sedimenting fraction of cell lysate (Reddy *et al.*, 1977; Allen *et al.*, 1980; Allen *et al.*, 1983; Thylén and Mathews, 1989). Kinetic analysis of partially reconstituted complexes will explore the nature of kinetic coupling. We would like to define effects of protein-protein interactions upon kinetic behavior of individual enzymes and linked multi-step reaction pathways by investigating whether kinetic coupling or channeling behavior can be reconstituted from purified proteins.

4. A mutant form of the hexameric Dictyostelium NDP kinase was reported to exist as homodimer in the absence of ATP. However, 0.5 mM ATP promotes the formation of native homohexamer (Mesnildrey *et al.*, 1998). We wonder if the tetrameric prokaryotic NDP kinase from *E. coli* also exhibits similar oligomeric properties in the presence of

ATP. We also would ask if tetramerization of NDP kinase would affect its interactions with other T4 proteins.

**Table 1.1.** Enzymes in the *de novo* synthesis of dNTP precursors of T4 DNA.

Enzyme	Gene	Native State	Subunit (kDa)	Holoenzyme (kDa)	References
dCMP hydroxymethylase	<i>42</i>	Dimer	28.5	59	Lamm <i>et al.</i> , 1988; Thylén, 1988
Thymidylate synthase	<i>td</i>	Dimer	33	66	Belfort <i>et al.</i> , 1983; Purohit and Mathews, 1984
Dihydrofolate reductase	<i>frd</i>	Dimer	21	42	Purohit and Mathews, 1984
dNMP kinase	<i>1</i>	Dimer	27	54	Sakiyama and Buchanan, 1971
dCTPase/dUTPase	<i>56</i>	Tetramer	20.4	82	Price and Warner, 1969
dCMP deaminase	<i>cd</i>	Hexamer	20	120	Maley <i>et al.</i> , 1990
Aerobic ribonucleotide reductase	<i>nrdAB</i>	$\alpha_2\beta_2$ / R1·R2	86, 45	262	Sjöberg <i>et al.</i> , 1986; Tseng <i>et al.</i> , 1988
Thymidine kinase	<i>tk</i>	Trimer	28	84	Iwatsuki, 1977
Anaerobic ribonucleotide reductase	<i>nrdDG</i>	$\alpha_2\beta_2$ / R1·R2	68, 18	172	Sun <i>et al.</i> , 1993; Young <i>et al.</i> , 1994a; Young <i>et al.</i> , 1994b
<i>E. coli</i> NDP kinase	Host <i>ndk</i>	Tetramer	15.5	62	Ohtsuki <i>et al.</i> , 1984; Hama <i>et al.</i> , 1991a; Hama <i>et al.</i> , 1991b
<i>E. coli</i> adenylate kinase	Host <i>adk</i>	Monomer	23.5	23.5	Brune <i>et al.</i> , 1985

**Table 1.2.** Overview of the characteristics of the ribonucleotide reductase classes<sup>a</sup>. (From Jordan and Reichard, 1998)

	Class Ia	Class Ib	Class II	Class III
Oxygen dependence	Aerobic	Aerobic	Aerobic/anaerobic	Anaerobic
Structure	$\alpha_2\beta_2$	$\alpha_2\beta_2$	$\alpha(\alpha_2)$	$\alpha_2\beta_2$
Genes	<i>nrdAB</i>	<i>nrdEF</i>	— <sup>b</sup>	<i>nrdDG</i>
Radical	Tyr... Cys	Tyr... Cys	AdB12... Cys	AdoMet... Gly... Cys?
Metal site	Fe-O-Fe	Fe-O-Fe	Co	Fe-S
Substrate	NDP	NDP	NDP/NTP	NTP
Reductant	Thioredoxin Glutaredoxin	NrdH-redoxin Glutaredoxin	Thioredoxin	Formate
Allosteric sites/ polypeptide chain	2	1	1	2
dATP inhibition	Yes	No	No	Yes
Occurrence	Eukaryotes Eubacteria Bacteriophages Viruses	Eubacteria	Archaeobacteria Eubacteria Bacteriophages	Archaeobacteria Eubacteria Bacteriophages
Prototype	<i>E. coli</i> Mouse	<i>S. typhimurium</i> <i>C. ammoniagenes</i>	<i>L. leishmannii</i>	<i>E. coli</i>

<sup>a</sup>Class I has been divided into two subclasses (Ia and Ib) based on differences in allosteric regulation and auxiliary proteins.

<sup>b</sup>The gene encoding the class II prototype from *L. leishmannii* has never been named.

**Table 1.3.** Regulation of T4 ribonucleotide reductase activity.

<b>Nucleotide bound in</b>		<b>Activates reduction of</b>	<b>Inhibits reduction of</b>
<b>Activity site</b>	<b>Specificity site</b>		
ATP	ATP or dATP	CDP, UDP	
ATP	dTTP	GDP	CDP, UDP
ATP	dGTP	ADP	CDP, UDP
dATP	Any effector		weak on GDP
hm-dCTP <sup>a</sup>	hm-dCTP <sup>a</sup>	UDP, CDP	

<sup>a</sup>It was not identified whether hm-dCTP binds to activity site or specificity site.

**Table 1.4.** Proteins retained on protein affinity columns where dCMP hydroxymethylase was immobilized.

Gene	Gene Product	Function	Phage Strain		
			T4D*	T432 <sup>am**</sup>	T4td <sup>am**</sup>
<i>42</i>	dCMP hydroxymethylase	dNTP synthesis	+	+	+
<i>td</i>	dTMP synthase	dNTP synthesis	+	±	-
<i>frd</i>	dihydrofolate reductase	dNTP synthesis	+	±	+
<i>56</i>	dCTPase/dUTPase	dNTP synthesis	+	+	±
<i>nrdA</i>	ribonucleotide reductase R1	dNTP synthesis	+	-	-
<i>nrdB</i>	ribonucleotide reductase R2	dNTP synthesis	+	-	-
<i>32</i>	ssDNA binding	DNA replication	+	-	-
<i>43</i>	DNA polymerase	DNA replication	±	±	±
<i>44</i>	Clamp loader	DNA replication	-	+	+
<i>45</i>	Sliding clamp	DNA replication	+	±	±
<i>61</i>	Primase	DNA replication	-	+	+
<i>62</i>	Clamp loader	DNA replication	-	+	+
<i>46</i>	Nuclease	Recombination	+	+	+
<i>uvvX</i>	RecA analog	DNA repair	+	-	-
<i>uvvY</i>	Repair protein	DNA repair	+	-	-
<i>pseT</i>	DNA Phosphatase/kinase	Unknown	+	+	+
<i>βgt/RNase H</i>	Glc-transferase/RNase H	DNA modification	-	+	+

\* T4D is the wild type phage.

\*\* T4 phage with *amber* mutant thymidylate synthase or single-stranded DNA binding protein (gp32). (Modified from Wheeler *et al.*, 1992)

**Table 1.5.** Proteins retained on protein affinity columns.

Gene	Gene product	Retained by immobilized							
		gp42	TS	gp56	CD	NDPK	DHFR	gp1	RNR
<i>td</i>	dTMP synthase	+	+	+	+		+		+
<i>frd</i>	DHF reductase	+	+	+	+	+	+		+
<i>56</i>	dCTPase/dUTPase	+			+			+	
<i>nrdA</i>	rNDP reductase R1	+				+	+		+
<i>nrdB</i>	rNDP reductase R2	+						+	+
<i>43</i>	DNA polymerase			+					+
<i>32</i>	ssDNA-binding protein	+	+	+	+	+	+	+	+
<i>45</i>	Sliding clamp	+	+		+	+	+	+	+
<i>61</i>	DNA primase	+	+		+	+	+	+	+
<i>uvrX</i>	RecA analog	+	+	+					
<i>uvrY</i>	Repair/Recombination	+	+	+	+	+	+	+	+
<i>βgt</i>	Glc-transferase		+	+	+		+		+
<i>pseT</i>	DNA kinase-phosphatase	+							
<i>regA</i>	Transcriptional control		+	+	+	+		+	+

**Note:** Each identified association results from detection of the indicated protein among those proteins retained at 0.2 M NaCl and eluted at 0.6 M NaCl and not retained by immobilized bovine serum albumin or phage lysozyme (From Wheeler *et al.*, 1996). gp42, dCMP hydroxymethylase; TS, dTMP synthase; gp56, dCTPase/dUTPase; CD, dCMP deaminase; NDPK, *E. coli* NDP kinase; DHFR, DHF reductase; gp1, dNMP kinase; RNR, rNDP reductase or ribonucleotide reductase.

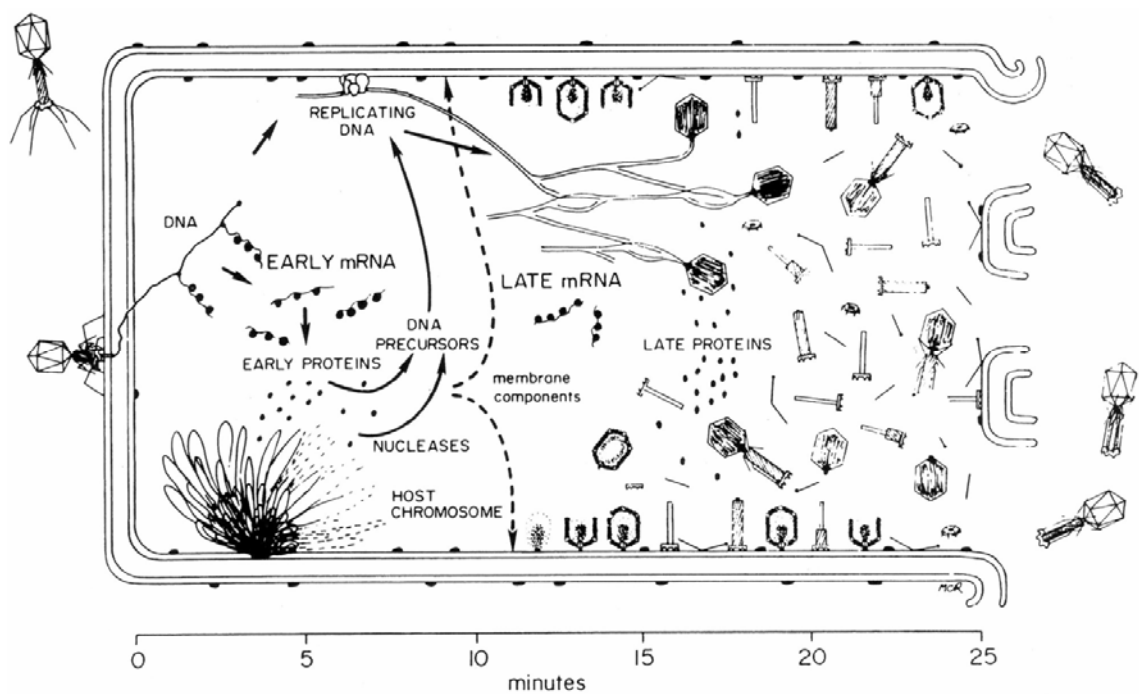


**Figure 1.1.** Overview of T4 developmental program. (From Mathews, 1994)

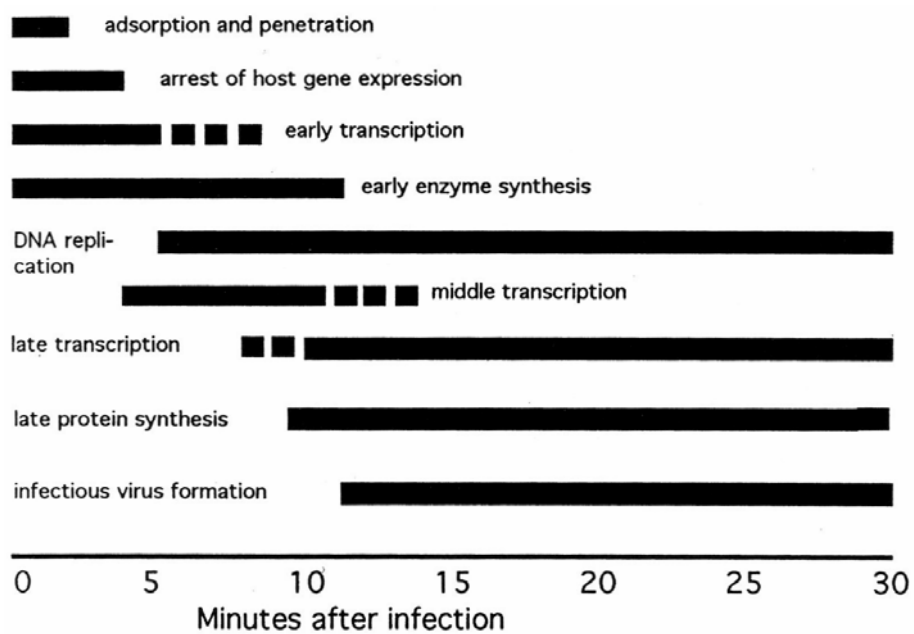


**Figure 1.2.** A chronology of major events in the T4 infective life. The precise times within which each of the major classes of transcripts are formed vary for individual genes within each temporal class. (From Mathews, 1994)

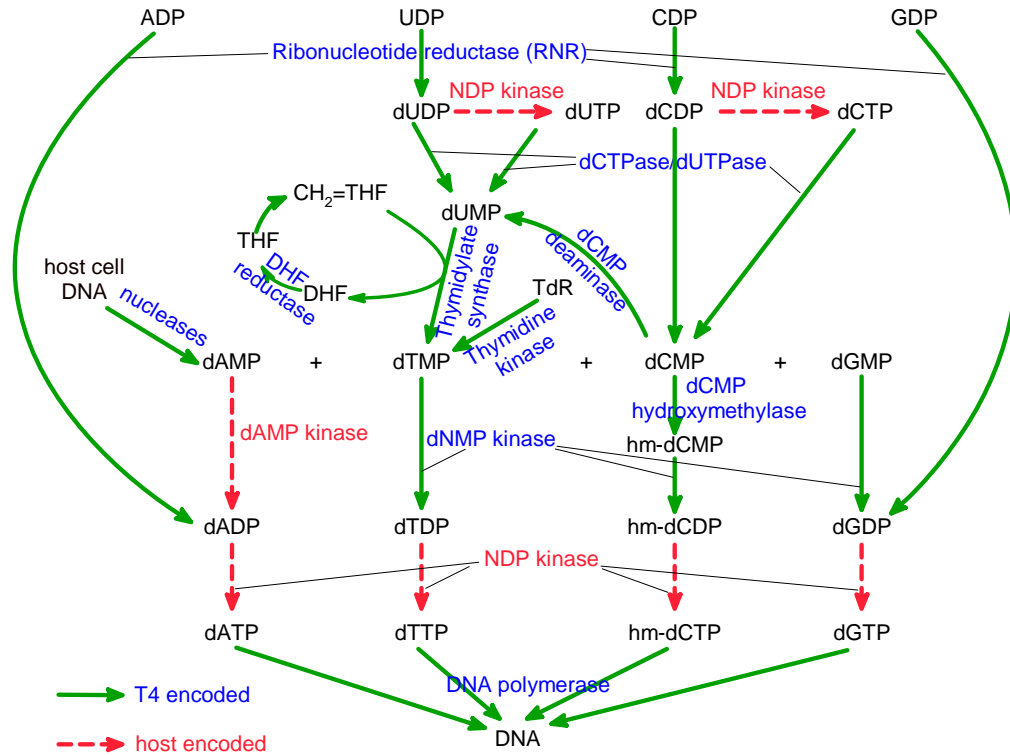


**Figure 1.3.** dNTP biosynthesis pathways in T4 phage-infected *E. coli* host. Solid green arrows represent reactions catalyzed by phage T4-coded enzymes; dashed red arrows stand for reactions catalyzed by host-coded enzymes (Modified from Mathews and Allen, 1983). T4 ribonucleotide reductase, thymidylate synthase, dihydrofolate reductase have host cell counterparts.

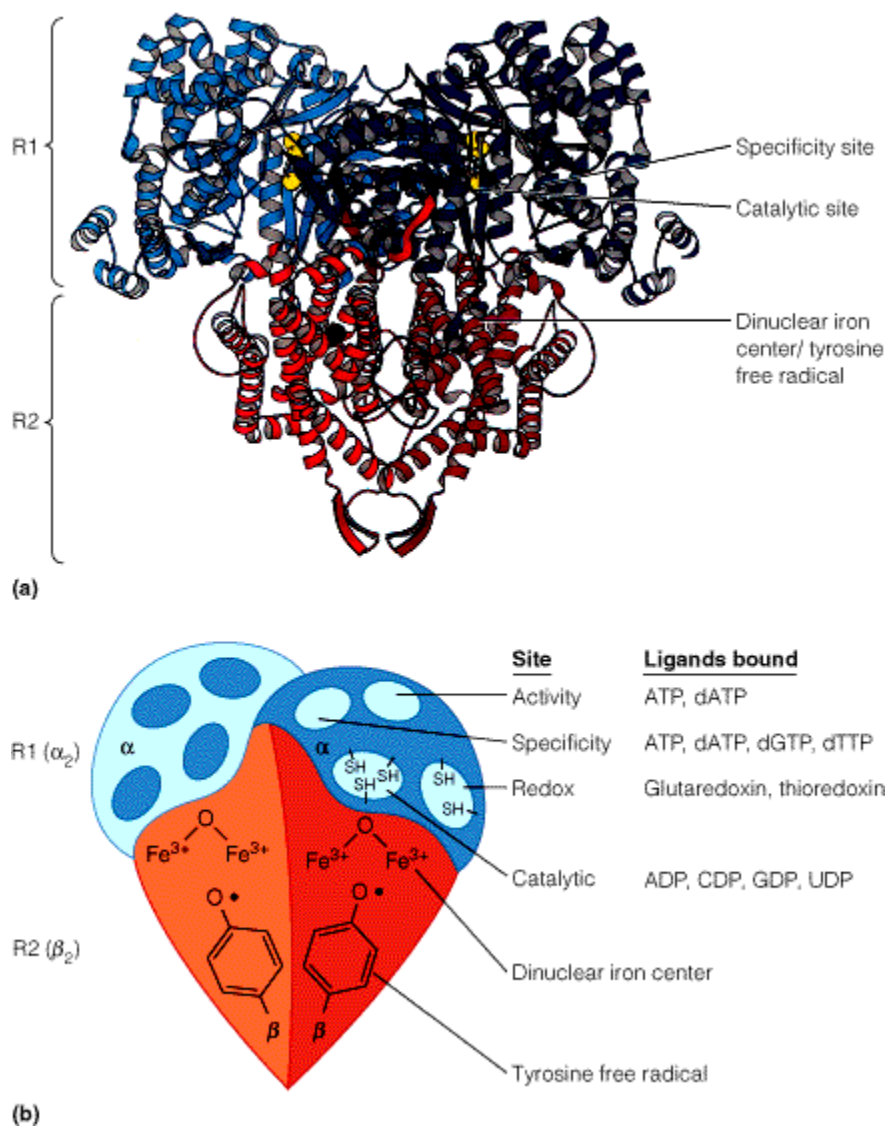


**Figure 1.4.** Structure of *E. coli* ribonucleoside diphosphate reductase. (From Uhlin and Eklund, 1994; Mathews *et al.*, 2000)

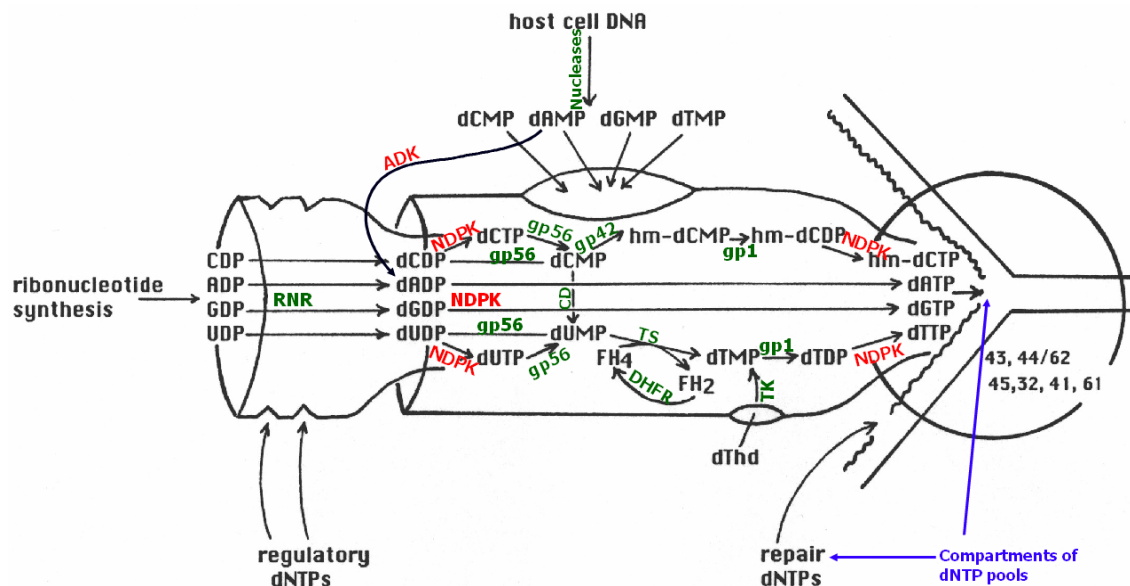


**Figure 1.5.** A “funnel” model of dNTP biosynthesis in T4 infection where T4 dNTP synthetase complex is juxtaposed with the DNA replication apparatus. RNR, ribonucleotide reductase; gp56, dCTPase/dUTPase; gp42, dCMP hydroxymethylase; CD, dCMP deaminase; TS, thymidylate synthase; DHFR, dihydrofolate reductase; gp1, dNMP kinase; TK, thymidine kinase; NDPK, NDP kinase; ADK, adenylate kinase. T4 encoded enzymes are in green, host-encoded in red. The numbers inside the circle at the right end represent T4 DNA replisome proteins. The *in situ* dNTP pools at the replication fork represent the small dNTP pool while repair dNTPs represent the large pool. (Modified from Mathews, 1993a)

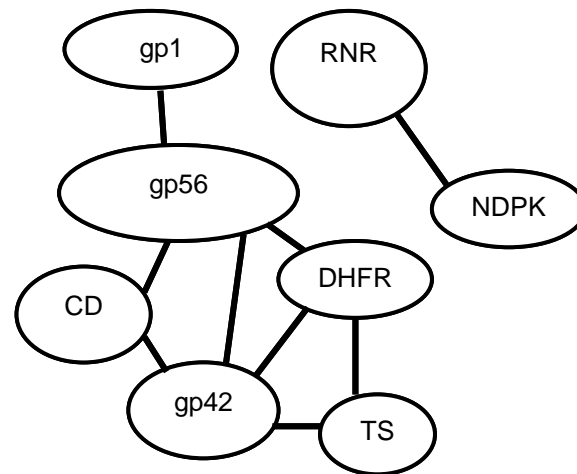


**Figure 1.6.** Protein-protein interaction model identified within the T4 dNTP synthetase complex as of 2000. RNR, ribonucleotide reductase; NDPK, nucleoside diphosphate kinase; gp56, dCTPase/dUTP ase; CD, dCMP deaminase; gp42, dCMP hydroxymethylase; TS, thymidylate synthase; DHFR, dihydrofolate reductase. (Modified from Mathews, 1993b)

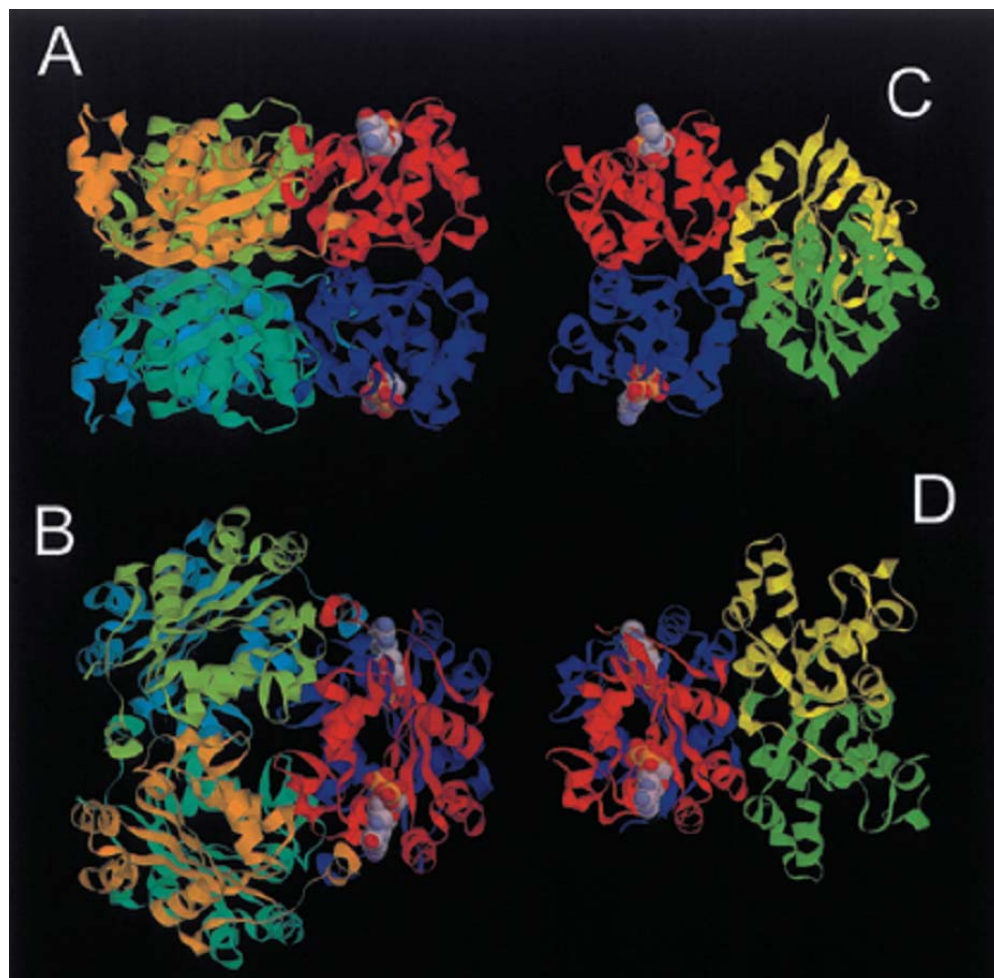


**Figure 1.7.** Comparison of subunit assembly of the NDP kinases of human NDP kinase B (A, B; PDB file 1NUE) and *Myxococcus* (C, D; PDB file 1NLK). The subunits colored in red and blue are similar orientation in A and C and B and D, respectively. The nucleotide bound to the active site is shown in space filling, but not in all subunits, for the sake of clarity. (Courtesy of Lascu *et al.*, 2000)

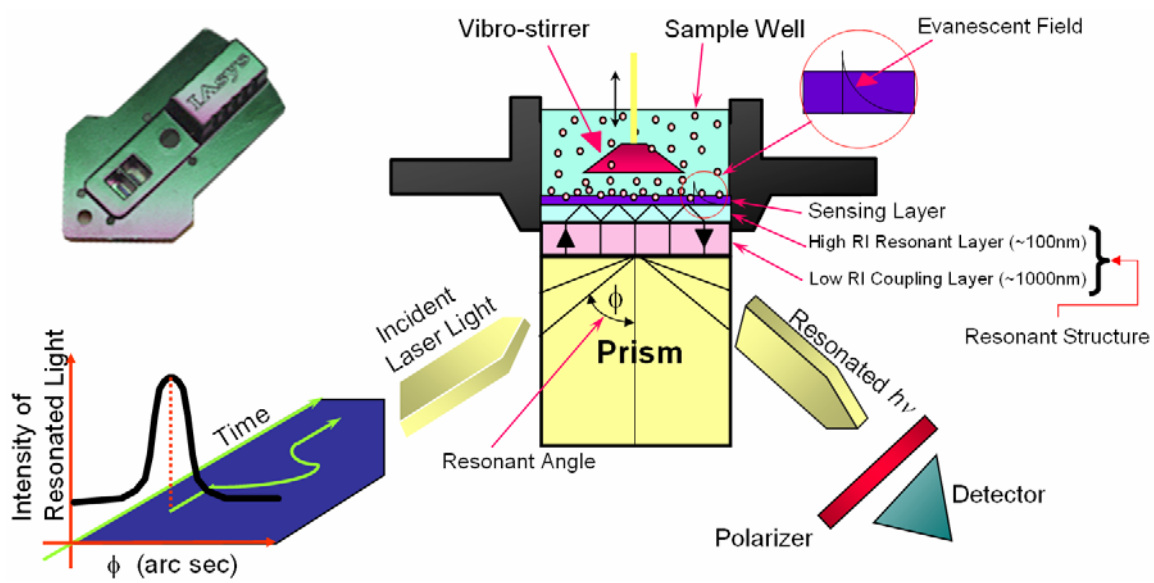


**Figure 1.8.** Configuration of the IAsys optical biosensor device and principles of Resonant Mirror technology. (IAsys, 1996b; IAsys, 1996c)

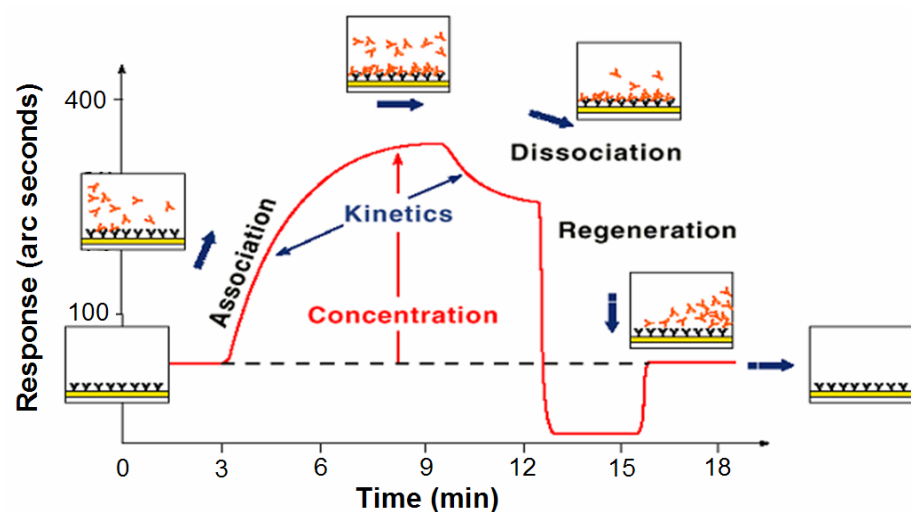


**Figure 1.9.** A typical biosensing experiment. The black “Y” is the ligand immobilized on the surface and the red “Y” is the ligate added to the solution. At time 0-3 min, a baseline is obtained with running buffer. At 3 min, the ligate is added to solution and association event occurs. At about 10 min, the solution containing the ligate is replaced by running buffer and dissociation event occurs. At about 12.5 min, the surface is regenerated with a sequence of reagents. (Modified from Campbell, <http://www.cpac.washington.edu/~campbell/projects/plasmon.pdf>)

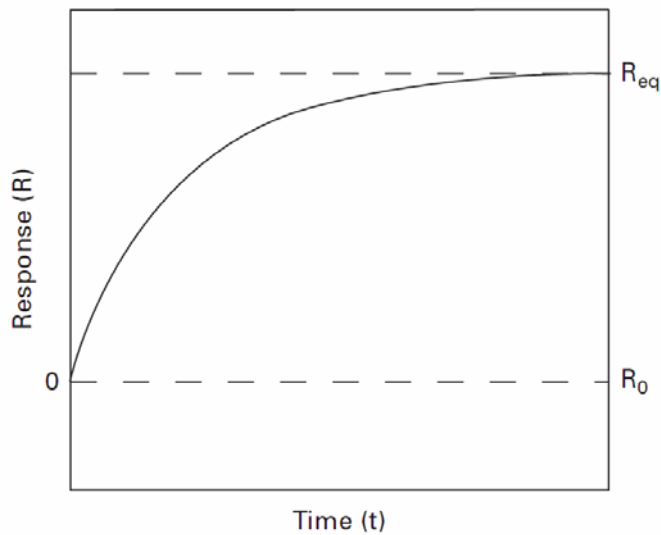


**Figure 1.10.** Monophasic association (theoretical).  $[L]$  is the concentration of ligate (IASys, 1996b).

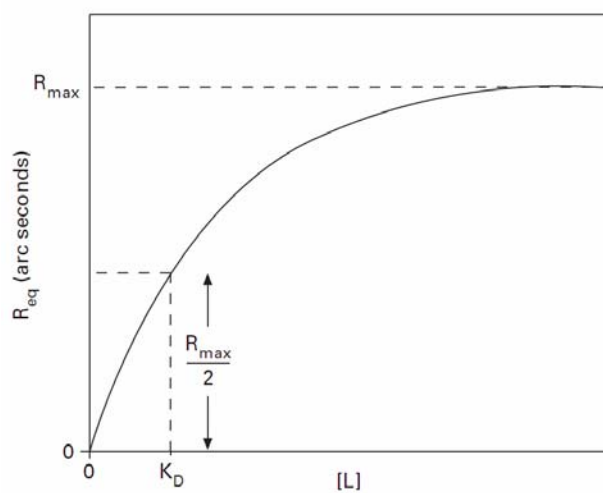


**Figure 1.11.** Typical binding curve analysis (theoretical).  $[L]$  is the concentration of ligate (IASys, 1996b).

## Chapter 2

### Materials and Methods

#### 2.1 Overview of Recombinant Proteins and Their Expression Systems

All of the purified or partially purified proteins in this thesis research were over-expressed from recombinant genes inserted into plasmids and cloned in their corresponding expressing *E. coli* hosts, shown in Table 2.1.

#### 2.2 Overexpression and Purification of T4 Aerobic Ribonucleotide Reductase (RNR)

Host *E. coli* strain MV1304 contains plasmid pnrdAB, where tandem *nrdA* and *nrdB* genes were inserted (Tseng *et al.*, 1992). The *nrdA* and *nrdB* encode the large and small subunits of T4 aerobic ribonucleotide reductase, namely  $\alpha$  and  $\beta$ , respectively. The pnrdAB clone was grown at 37°C in Luria-Bertani (LB) medium (1% (w/v) tryptone, 0.5% (w/v) yeast extract, 1% (w/v) NaCl, pH 7.5) plus 1% (v/v) glycerol and 100  $\mu$ g/ml ampicillin. When OD<sub>600</sub> of the culture reached 0.8-1.0, 400  $\mu$ M isopropyl- $\beta$ -D-thiogalactoside (IPTG) and 10  $\mu$ M ferrous ammonium sulfate (Fe(NH<sub>4</sub>)<sub>2</sub>(SO<sub>4</sub>)<sub>2</sub>) were added to induce the overexpression of the recombinant protein. In the meantime, the temperature was reduced to 30°C. After 4-6 hours of induction at 30°C, cells were harvested by centrifugation in a Sorvall GSA rotor at 6,000 rpm for 20 minutes. Cell

pellet was frozen at  $-80^{\circ}\text{C}$ . The induction of both  $\sim 86$  and  $\sim 43$  kDa proteins was checked by sodium dodecyl sulfate-polyacrylamide gel electrophoresis (SDS-PAGE) (Wheeler *et al.*, 1996).

Cell pellet was resuspend in 3 volumes of buffer A (50 mM Tris, pH 9.0, 20 mM NaCl, 5 mM  $\text{MgCl}_2$ , 10% (v/v) glycerol, 1 mM phenylmethanesulfonyl fluoride (PMSF), 1 mM dithiothreitol (DTT), and 1 mM ferrous ammonium sulfate in 2 mM ascorbic acid which were added just before sonic oscillation). All the steps were carried out either on ice or in a refrigerated chamber ( $0-4^{\circ}\text{C}$ ). Cells were then disrupted by sonic oscillation at 7-10 watts for 8 x 1 min with intervals of 1 min. The lysate was centrifuged in a Sorvall SS34 rotor at 10,000 rpm for 20 min to remove cell debris. To the supernatant, 1% streptomycin sulfate was added to precipitate nucleic acids. The mixture was centrifuged in an SS34 rotor at 10,000 rpm for 20 min to eliminate precipitated nucleic acid. To the supernatant, ammonium sulfate was slowly added to 40% saturation on ice. Stirring was continued for another 1 hour. Centrifugation was followed in an SS34 rotor at 10,000 rpm for 20 min. The precipitated protein was dissolved in buffer A and desalted by passing through a 10DG desalting column (Bio-Rad) equilibrated with buffer A. Chromatography was carried out on an anion exchange column (HiTrap Q HP (low sub, 1.0 ml bed volume), Amersham Pharmacia) on FPLC, which was equilibrated with buffer A. The loading speed was controlled at 1 ml/min. 30 ml of a gradient of 20 to 400 mM NaCl in buffer A (lacking PMSF) was used to elute. Two main peaks appeared. The first peak at about 100 mM NaCl contained R2. The second peak, which was larger than the first one,

contained R1 in the first fractions and R1·R2 in the remaining fractions. The fractions containing R1 were subjected to further purification by repeating the HiTrap Q HP column step (Hanson, 1994; Wheeler *et al.*, 1996). The purified proteins were concentrated in a CentriPrep YM-30 for storage if necessary. The protein was stored at -80°C in 50% (v/v) glycerol.

The T4 RNR R1·R2 holoenzyme was also purified by an affinity column. All the steps were carried out either on ice or in a cold box (0-4°C). Cell pellet was resuspended in 5 volumes of lysis buffer (50 mM HEPES, pH 8.4, 1 mM PMSF, 1 mM DTT). Cells were disrupted by sonic oscillation at 8 watts for 10 x 1 min with intervals of 1 min. The lysate was centrifuged in an SS34 rotor at 10,000 rpm for 20 min to remove cell debris. The supernatant was then filtered by 0.45 µm filter before being applied on to a dATP Sepharose affinity column (1.0 ml bed volume). The column was pre-equilibrated by washing to baseline with column buffer (50 mM HEPES, pH 8.4, 100 mM KCl, 1 mM DTT). All the flow rates of washing column, loading sample and eluting were controlled at 1 ml/min. R1·R2 complex was eluted with 5.0 ml column buffer containing 20 mM ATP. The purified protein was concentrated in a CentriPrep YM-30 for storage if necessary. The protein was stored at -80°C in 50% glycerol. The purified protein was checked with SDS-PAGE (Figure 2.1).

### 2.3 Preparation of $\gamma$ -PO<sub>4</sub>-Linked dATP Sepharose Column

Seven and a half grams of cyanogen bromide (CNBr)-activated Sepharose 4B (Pharmacia Biotech Ltd., Piscataway, NJ) was suspended in 2 mM HCl and washed on a sintered glass funnel with about 2 ml of 2 mM HCl over a 15-20 min period. The resin was then washed with about 500 ml of deionized water on a sintered glass funnel. The resin was further washed with about 100 ml of coupling buffer (0.1 M NaHCO<sub>3</sub>, pH 8.3, 0.5 M NaCl). 25 mg of 2'-deoxyadenosine-5'-( $\gamma$ -aminophenyl)-triphosphate (Nucleix Plus, USB Corporation, Cleveland, Ohio) was dissolved in 40 ml of coupling buffer. Right before coupling, 100  $\mu$ l of Nucleix Plus solution was taken for spectrum scanning. Ten-fold dilution was made by adding 900  $\mu$ l of coupling buffer. The UV spectrum was scanned from 190 nm to 350 nm. Resin was washed again with coupling buffer and then added to the Nucleix Plus solution in a 60-ml plastic tube. The tube was rotated on the rotating plate for 3 hours at room temperature. After coupling reaction, the coupled gel was allowed to settle. 100  $\mu$ l of supernatant was taken and added with 900  $\mu$ l of coupling buffer for spectrum scanning from 190 nm to 350 nm. The supernatant was decanted and the resin was resuspended in 0.1 M Tris-HCl buffer (pH 8.3), and rotated overnight in the cold box (4°C) to block unreacted active sites. The supernatant was kept at -20°C just in case the coupling failed. The resin was washed 3 times alternatively with buffer A (0.1 M sodium acetate buffer, pH 4.0) and buffer B (0.1 M Tris-HCl buffer (pH 8.3), 0.5 M NaCl). The resin was ready for packing into a column or storing in refrigerator (4°C) in

buffer C (0.1 M Tris-HCl buffer, pH 8.3, 0.5 M NaCl, and 0.02% NaN<sub>3</sub>). More detailed information are in Berglund and Eckstein (Berglund and Eckstein, 1972).

## **2.4 Overexpression and Purification of T4 Thymidylate Synthase (TS)**

Host *E. coli* strain, MB901, containing plasmid pKTd2 where T4 gene *td* coding for thymidylate synthase was inserted (Belfort *et al.*, 1983), was grown in LB medium at 37°C. When the absorbance at 600 nm (OD<sub>600</sub>) of the culture reached 0.5 (mid-log phase), nalidixic acid (2 mg/ml in 0.02M NaOH) was added to reach final concentration of 40 µg/ml. Incubation was continued at 37°C for 8 hr or overnight. Cells were harvested by centrifugation in a GSA rotor at 5,000 rpm for 20 min. Cell pellet was frozen at -20°C. The induction of a 33 kDa protein was checked on SDS-PAGE (Wheeler *et al.*, 1996).

Cell pellet was resuspended in 3 volumes of buffer A (50 mM Tris-HCl, pH 6.5, 25 mM KCl, 1mM EDTA, 10 mM β-mercaptoethanol (BME)). All the steps were carried out either on ice or in the cold (0-4°C). Cells were disrupted by sonic oscillation at 7-10 watts for 10 x 1min with intervals of 1 min. The lysate was centrifuged in an SS34 rotor at 10,000 rpm for 20 min. To the supernatant, ammonium sulfate was slowly added to 30% saturation on ice. Stirring was continued for another 1 hour. The precipitated proteins were removed by centrifugation in an SS34 rotor at 10,000 rpm for 20 min. To the

supernatant, ammonium sulfate was continued to be slowly added to reach 60% saturation on ice. Stirring was continued for another 1 hour. Centrifugation was followed in an SS34 rotor at 10,000 rpm for 20 min. The precipitated protein was dissolved in buffer A and further dialyzed against 1,500 ml cold buffer A for 12 hours or overnight. The buffer was changed in the next morning with another 1,500 ml buffer A. Dialysis was continued for at least 3 hours. The dialysate was centrifuged to remove some precipitation. The supernatant was ready for a cation exchange column. Ten grams carboxymethyl (CM) Sephadex resin was swelled in deionized water overnight and then packed into a column. The column was equilibrated with buffer A overnight at 0.5 ml/min controlled by a Pharmacia P3 pump. The dialysate was applied to CM Sephadex column at 0.5 ml/min. After all the sample was loaded, the column was washed with buffer A at 0.5 ml/min overnight. The protein retained on the column was eluted with a 500x500 ml salt and pH gradient of buffers CM-1 (50 mM Tris-HCl, pH 6.5, 50 mM KCl, 1 mM EDTA, 10 mM BME) and CM-2 (50 mM Tris-HCl, pH 7.7, 350 mM KCl, 1 mM EDTA, 10 mM BME). Fractions were collected with 5 ml per fraction. Fractions around peaks (or at 5-fraction intervals) were analyzed for thymidylate synthase activity (see next section). Fractions of high thymidylate synthase activity were combined and the rest were discarded. For all the following steps, the salt concentration was kept at least 250 mM to prevent the protein from precipitating. The pooled fractions were concentrated in CentriPrep YM-10. The concentrated protein was either mixed with glycerol to make final concentration of 20% glycerol for storage or directly passed to the next step – gel filtration on FPLC.

A Superose 6 FPLC column on FPLC was equilibrated with about 250 ml of buffer C (50 mM Tris, pH 7.4, 250 mM KCl, 1 mM EDTA, 10 mM BME). The concentrated protein from the previous step was applied on the column. The speed was controlled at 1 ml/min. Fractions were collected with 1 ml per fraction. Fractions around peaks were analyzed for thymidylate synthase activity. Fractions of high thymidylate synthase activity were combined and the rest were discarded. The pooled fractions were further concentrated in a CentriPrep YM-10. The concentrated protein was either mixed with glycerol to make final concentration of 20% glycerol for storage or directly applied in the experiments that thymidylate synthase was involved. The purified protein was checked with SDS-PAGE (Figure 2.1).

## **2.5 Thymidylate Synthase Activity Assay**

Thymidylate synthase activity was spectrophotometrically determined (Wahba and Friedkin, 1961). The method is based on the absorbance increase at 338 nm that occurs when 5,10-methylenetetrahydrofolate ( $\text{CH}_2=\text{THF}$ ) is converted to dihydrofolate (DHF) by thymidylate synthase. Formaldehyde (HCHO) and tetrahydrofolate (THF) can nonenzymatically yield  $\text{CH}_2=\text{THF}$ , which is stable for at least 1 hour at room temperature in the presence of an excess of formaldehyde and a high concentration of BME.

The reaction mixture contained 0.5 ml of THF solution (0.5 mM L-THF, 0.2 M BME, 30 mM formaldehyde, 0.2 M Tris-HCl, pH 7.4, 0.2 M KCl and 50 mM MgCl<sub>2</sub>, freshly made before use), 0.1 ml of 1.0 mM dUMP – deoxyuridine monophosphate – (for blank, H<sub>2</sub>O instead), 10-50 µl of TS protein sample, and H<sub>2</sub>O which was added to make 1.0 ml of total volume. The reaction was followed at OD<sub>338</sub> at room temperature by a Kinetic module of Beckman DU-65 UV/Vis spectrophotometer. The absorbance should increase due to the dUMP-dependent conversion of THF to DHF. The molar extinction coefficient is 0.0066 µMolar. The enzyme factor is 151.51.

## **2.6 Overexpression and Partial Purification of T4 dCMP Hydroxymethylase (gp42)**

Host *E. coli* strain, BL21(DE3), containing pT7-42 where T4 gene 42 coding for dCMP hydroxymethylase was inserted, was grown in LB medium plus 100 µg/ml ampicillin at 37°C (Wheeler *et al.*, 1992). When OD<sub>600</sub> value reached 0.5, 400 µg/ml of IPTG was added to induce the overexpression of dCMP hydroxymethylase. The induction was continued for 2 hours. Cells were harvested by centrifugation at 5,000 rpm in a GSA rotor for 20 minutes. Cell pellet was frozen at -20°C. The induction of a 28-kDa protein was checked on SDS-PAGE.

Cell pellet was resuspended in 3 volumes of buffer A (50 mM potassium phosphate, pH 6.5). All the steps were carried out either on ice or in a cold box (0-4°C). Cells were disrupted by sonic oscillation at 7-10 watts for 10 x 1min with intervals of 1 min. The

lysate was centrifuged in an SS34 rotor at 10,000 rpm for 20 min. To the supernatant, 2% protamine sulfate (pH 7.0) was added at 0.1 volume. The mixture was stirred for 1 hour on ice and then was centrifuged in an SS34 rotor at 10,000 rpm for 20 min. To the supernatant, ammonium sulfate was slowly added to 30% of saturation on ice. Stirring was continued for another 30 min. The precipitate was removed by centrifugation in an SS34 rotor at 10,000 rpm for 20 min. To the supernatant, ammonium sulfate was continued to be slowly added to 65% saturation. Stirring was continued for another 1 hour. Centrifugation was followed in an SS34 rotor at 10,000 rpm for 20 min. The precipitated protein was dissolved in buffer A and further dialyzed against 1,000 ml cold buffer B (0.2 M KPO<sub>4</sub>, pH 6.5, 10 mM BME) for 12 hours or overnight. The dialyzed partially purified protein was directly utilized for hm-dCTP synthesis.

## **2.7 Overexpression and Purification of T4 dCTPase/dUTPase (gp56)**

Host *E. coli* strain, M5219, containing plasmid pLAM71\* where T4 gene 56 for dCTPase/ dUTPase was inserted, was grown in LB medium plus 100 µg/ml ampicillin at 25°C (Wheeler *et al.*, 1996). Since the strain is heat sensitive, the temperature was always controlled at temperatures not higher than 25°C except for induction. When the OD<sub>600</sub> value of the culture at 25°C reached 0.5, induction was started by placing the culture in a 42°C water bath. Induction was continued for 30 minutes. The culture was chilled and

centrifuged to harvest the cells at 5,000 rpm in GSA rotor for 20 minutes. Cell pellet was frozen at -20°C. The induction of a 17-kDa protein was checked on SDS-PAGE.

Cell pellet was resuspended in 3 volumes of buffer A (50 mM Tris, pH 7.5, 10 mM EDTA, 10 mM BME). Cells were disrupted by sonic oscillation at 7-10 watts for 10 x 1 min with intervals of 1 min. Cellular debris was removed by centrifugation in an SS34 rotor at 10,000 rpm for 20 min. To the supernatant, 7% of streptomycin sulfate (0.3 volume of supernatant) was added to precipitate nucleic acids. This also brought down proteins bound to the nucleic acids, including gp56. The precipitated proteins were centrifuged in an SS34 rotor at 10,000 rpm for 20 min. The pellet was resuspended in buffer B (0.2 M potassium phosphate, pH 6.9, 2mM BME). The mixture was centrifuged again and the supernatant was saved.

A diethylaminoethyl (DEAE) cellulose weak anion exchange chromatography column was pre-equilibrated with buffer B. All the flow rates for washing column, loading sample and eluting were controlled at 0.5 ml/min. The supernatant was applied to a DEAE cellulose column. The column was then washed to baseline. The proteins retained on the column were eluted by a gradient from 0 to 5M NaCl in buffer B. Fractions were collected with 5 ml per fraction. Fractions around peaks (or at 5-fraction intervals) were analyzed for dUTPase activity. Fractions of high dUTPase activity were combined and the rest were discarded. The pooled fractions were concentrated in a CentriPrep YM-10.

The concentrated protein was either mixed with glycerol to make final concentration of 20% for storage or directly passed to the next step – gel filtration on FPLC.

A Superose 6 FPLC column was equilibrated with about 250 ml of buffer C (0.2 M KPO<sub>4</sub>, pH 6.9, 2 mM BME, 100 mM NaCl). The concentrated protein from the previous step was applied to the column. The speed was controlled at 1 ml/min. Fractions were collected with 1 ml per fraction. Fractions of high dUTPase activity were combined and the rest were discarded. The pooled fractions were concentrated in a CentriPrep YM-10. The concentrated protein was either mixed with glycerol to make final concentration of 20% for storage or directly passed to the next step – gel filtration on FPLC.

A HiTrap Phenyl FF FPLC hydrophobic column (low sub, 1.0 ml bed volume) was pre-equilibrated with buffer C. The speed was controlled at 1 ml/min. Fractions were collected with 1 ml per fraction. The concentrated protein from the previous step was mixed with buffer C plus 5 M NaCl at 1:1 ratio. The mixture was then applied to the column. A 30 ml gradient from high salt (buffer C plus 2.5 M NaCl) to low salt (buffer C) buffer was employed to elute the bound protein. Fractions of high dUTPase activity were combined and the rest were discarded. The pooled fractions were concentrated in a CentriPrep YM-10. The concentrated protein was either mixed with glycerol to make final concentration of 20% for storage or directly applied to experiments where gp56 was involved. The purified protein was checked with SDS-PAGE (Figure 2.1).

## 2.8 dUTPase/dCTPase Activity Assay

The activity assay for gp56 is coupled with thymidylate synthase assay. The reaction schema is shown in Figure 2.2. All the steps were the same as TS assay except that only the reaction mixture was modified accordingly including the starting substrate and enzymes. The reaction mixture contained 0.5 ml of THF solution (see Section 2.5), 0.1 ml of 1.0 mM dUTP – deoxyuridine triphosphate – (for blank, H<sub>2</sub>O instead), 10 µl of purified and active TS protein, 10-40 µl of gp56 protein sample, and H<sub>2</sub>O which was added to make 1.0 ml of total volume.

## 2.9 Overexpression and Purification of T4 dCMP Deaminase (CD)

The approach described below was modified from Keefe *et al.* (Keefe *et al.*, 2000) and McGaughey *et al.* (McGaughey *et al.*, 1996). Host strain, B121 (DE3) plysS, containing plasmid pET3C+T4dCD where T4 *cd* genes for dCMP deaminase was inserted, was grown at 30°C in Tryptone-Phosphate medium plus 100 µg/ml ampicillin and 25 µg/ml chloramphenicol. When OD<sub>600</sub> value of the culture reached 0.4-0.6, 400 µM IPTG was added to induce the expression of dCMP deaminase. Cells were harvested after 3 hours of induction by centrifugation in a GSA rotor at 5,000 rpm for 20 minutes. Cells were washed with TNE (10 mM Tris-HCl, pH 7.5, 150 mM NaCl, 1 mM EDTA (pH 8.0)) and

stored in a -20°C freezer after centrifugation. The induction of a 20 kDa protein was checked by SDS-PAGE.

All purification steps were carried out at 0-4°C. 5-10 g of cells was thawed in a beaker on ice, to which 12 ml of lysis buffer (50 mM potassium phosphate, pH 7.5, 100 mM NaCl, 10% (v/v) ethylene glycol, 20 mM BME) per gram of cells was added. Cells were disrupted by sonic oscillation on an ice/ethanol bath at 7-10 watts for 10 x 1min with intervals of 1 min. Cellular debris was removed by centrifugation in an SS34 rotor at 10,000 rpm for 20 min. To the supernatant, ammonium sulfate was slowly added to 35% saturation on ice. Stirring was continued for at least 30 min. The precipitates were removed by centrifugation in an SS34 rotor at 10,000 rpm for 20 min. To the supernatant, ammonium sulfate was continued to be added slowly to 80% of saturation. Stirring was continued for another 1 hour. Centrifugation was followed in an SS34 rotor at 10,000 rpm for 20 min. The precipitated protein was stored at -80°C or used in the next step.

A DE52 cellulose anion exchange column (2.5 x 18 cm) was pre-equilibrated with buffer A (10 mM Tris-HCl, pH 8.5, 10% (v/v) ethylene glycol, 20 mM BME). The precipitated protein from the previous step was dissolved in buffer A and dialyzed against buffer A overnight in the cold room. The dialysate was sonicated for 2-3 min at 7-10 watts if it appeared opalescent. The dialysate was then loaded on a DE52 cellulose column with reduced speed. Fractions were collected with 5 ml per fraction. The column was washed with buffer A until OD<sub>280</sub> was greatly reduced. Step elution was applied. The column was

washed with about 100 ml buffer A plus 50 mM NaCl, and followed with buffer A plus 100 mM NaCl and then buffer A plus 200 mM NaCl, each about 200 ml. dCMP deaminase was eluted with 200 mM NaCl. Fractions containing the deaminase peak were pooled and concentrated in a CentriPrep YM-10. Ammonium sulfate was added to 80% saturation to precipitate the proteins. The precipitates were dissolved in buffer B (10 mM potassium phosphate, pH 7.1, 10% (v/v) ethylene glycol, 0.2 mM MgCl<sub>2</sub>, 0.1 mM EDTA, 2 mM DTT) and dialyzed against buffer B at 0-4°C overnight. The dialysate was sonicated for 2-3 min at 7-10 watts if it appeared opalescent. The dialysate was then applied to a cellulose phosphate cation exchange column pre-equilibrated with buffer B. The column was then washed with 3-5 column volumes of buffer B, followed by 4-5 column volumes of buffer B plus 50 mM potassium phosphate at pH 7.1 and buffer B plus 100 mM potassium phosphate at pH 7.1. Finally, dCMP deaminase was eluted with buffer B plus 200 mM potassium phosphate at pH 7.1. Fractions containing the deaminase peak were pooled and concentrated in a CentriPrep YM-10 at 0-4°C. For long term storage, the enzyme was precipitated with ammonium sulfate to 80% saturation and the centrifuged protein was frozen at -80°C for storage. The purified protein was checked with SDS-PAGE (Figure 2.1).

## **2.10 dCMP Deaminase Activity Assay**

The activity assay for dCMP deaminase is coupled with thymidylate synthase assay. The reaction schema is shown in Figure 2.3. All the steps were the same as TS assay except

that only the reaction mixture was modified accordingly, including the starting substrate and enzymes. The reaction mixture contained 0.5 ml of THF solution (see Section 2.5), 0.1 ml of 1.0 mM dCMP – deoxycytidine monophosphate – (for blank, H<sub>2</sub>O instead), 10 µl of 10 mM hm-dCTP, 10 µl of purified and active TS protein, 10-40 µl of dCMP deaminase protein sample, and H<sub>2</sub>O which was added to make 1.0 ml of total volume. Hm-dCTP was prepared as described in APPENDIX A.

### **2.11 Overexpression and Partial Purification of *E. coli* NDP Kinase**

*E. coli* DH5α cells, containing plasmid pKT8P3 where *E. coli ndk* gene for NDP kinase was inserted, were incubated at 37°C overnight in nutrient broth plus 100 mg/ml ampicillin (Wheeler *et al.*, 1996). NDP kinase was constitutively induced. Cells were harvested by centrifugation in a GSA rotor at 5,000 rpm for 20 min. Bacteria were resuspended in buffer A (20 mM Tris-HCl, pH 7.4, 10 mM MgCl<sub>2</sub>, 10 mM BME, 10% (v/v) glycerol) and disrupted by sonic oscillation at 7-10 watts for 10 x 1 min with intervals of 1 min. Cell debris was removed by centrifugation in an SS34 rotor at 10,000 rpm for 20 min. To the supernatant was added 0.3 volume of 8% streptomycin sulfate, and the precipitated nucleic acid was discarded by centrifugation. Fractionation with ammonium sulfate followed with enzyme precipitating between 45 and 60% of saturation. The precipitated protein was ready for hm-dCTP preparation or for storage at -80°C.

### **2.12 *E. coli* NDP Kinase Activity Assay**

NDP kinase activity was assayed with ATP as a phosphate donor and dTDP as an acceptor nucleotide, in a coupled pyruvate kinase-lactate dehydrogenase assay that measures ADP formation from ATP (Postel and Ferrone, 1994).

### **2.13 Overexpression and Purification of T4 dNMP kinase (gp1)**

Host *E. coli* strain, HB101, contains plasmid pBK5 where T4 gene 1 for dNMP kinase was inserted (Brush *et al.*, 1990). Bacteria were grown at 30°C in 20 ml of Nutrient Broth (NB) plus 100 µg/ml ampicillin overnight. The culture was added to 200 ml of SLBH medium plus 100 µg/ml ampicillin (1:10 dilution) and continued to grow at 30°C. When OD<sub>600</sub> of the culture doubled, the temperature was raised to 42°C and continued for 9 hours. During the cell growth, if OD<sub>600</sub> began to level off, additional 50% glucose solution was added. At 3 hr intervals additional ampicillin was added to maintain the selection of bacteria containing plasmids. Cells were harvested by centrifugation in a GSA rotor at 5,000 rpm for 20 minutes. Cell pellet was frozen at -20°C. The induction of a 25 kDa protein was checked by SDS-PAGE.

Cell pellet was resuspended in 3 volumes of buffer (50 mM Tris, pH 7.5, 10 mM BME, 10 mM EDTA, 1 mM PMSF). Cells were disrupted by sonic oscillation at 7-10 watts for 10 x 1 min with intervals of 1 min. Cell debris was removed by centrifugation in an SS34 rotor at 10,000 rpm for 20 min. Sonication was repeated once on cell debris. This supernatant was added to the first supernatant. To the combined supernatant, 0.1 volume of 2% protamine sulfate solution (neutralized with NaOH) was added. The mixture was set on ice for 2 hr and the precipitated nucleic acid was discarded by centrifugation. Fractionation with ammonium sulfate followed with enzyme precipitating between 30 and 70% of saturation. The precipitated protein was ready for hm-dCTP preparation or for storage at -80°C.

#### **2.14 T4 dNMP Kinase Activity Assay**

dNMP kinase activity was assayed with ATP as a phosphate donor and dTDP as an acceptor nucleotide, in a coupled pyruvate kinase-lactate dehydrogenase assay that measures ADP formation from ATP (Brush *et al.*, 1990).

### **2.15 Overexpression and Purification of T4 Anaerobic Ribonucleotide Reductase Subunit (NrdD)**

Host JM109(DE3) bacteria carrying the pET29+T4NrdD plasmid where T4 *nrdD* gene was inserted was a gift from Dr. Britt-Marie Sjöberg, Stockholm University (Olcott *et al.*, 1998; Andersson *et al.*, 2001). Cultures of JM109(DE3)/pET29+T4NrdD bacteria in LB medium supplemented with 30 mg/ml kanamycin were incubated at 37°C under aerobic conditions. When the cells reached an absorbance at 600 nm of 0.8, the overexpression of NrdD was induced by the addition of 200 mM IPTG. After 3-4 h of induction, the cells were harvested by centrifugation, and the pellet was stored in -20°C freezer.

Cell pellet was resuspended in 5 volumes of lysis buffer (20 mM Tris-HCl, pH 8.0, 5 mM DTT). Cells were disrupted by sonic oscillation at 7-10 watts for 5 x 1 min with 1 min intervals. Cell debris was removed by centrifugation in SS34 rotor at 10,000 rpm for 20min. While stirring on ice, to the supernatant, 1.0% streptomycin sulfate was added to precipitate nucleic acids. Stirring was continued for 40 min. The precipitated nucleic acids were removed by centrifugation in an SS34 rotor at 10,000 rpm for 20min. To the supernatant, while stirring on ice, ammonium sulfate was slowly added to 40% saturation. Stirring was continued for 1 hour. The precipitated proteins were collected by centrifugation in an SS34 rotor at 10,000 rpm for 20min. The pellet was resuspended in 20 mM Tris-HCl, pH 8.0, 5 mM DTT.

The final purification step was hydrophobic interaction chromatography (butyl Sepharose 4 Fast Flow medium from Amersham Pharmacia Biotech) on FPLC using a gradient of 0.5-0 M ammonium sulfate in 50 mM Tris-HCl, pH 7.6, 5 mM DTT. The speed was controlled at 0.5 ml/min. The NrdD-containing fractions were pooled and then dialyzed against and stored in 20 mM Tris-HCl, pH 7.6, 10 mM DTT. The protein was further concentrated with CentriPrep YM-30 and stored in -80°C freezer after 50% glycerol was added. The purified protein was checked with SDS-PAGE (Figure 2.1).

## 2.16 Other Proteins

Highly purified *E. coli* NDP kinase, *E. coli* adenylate kinase and *E. coli* CTP synthetase were gifts from Dr. Michael C. Olcott (Oregon State University, Corvallis, OR) in this laboratory. The corresponding cloning, overexpression and purification procedures are described in detail in Shen *et al.* (Shen *et al.*, 2004) and Kim *et al.* (Kim *et al.*, 2005a). Purified T4 gp32 was a gift from Dr. Kathleen M. McGaughey (Oregon State University, Corvallis, OR) in this laboratory. Purified T4 dihydrofolate reductase was also a gift from Keith Nylin (Oregon State University, Corvallis, OR) in this laboratory. *E. coli* thymidylate synthase (TS) is a gift from Dr. Frank Maley (Department of Health, State of New York) and further purified by Michael C. Olcott in this laboratory. Partially purified GST-gp42 – GST-fusion dCMP hydroxymethylase – was a gift from Dr. JuHyun Kim

(Oregon State University, Corvallis, OR) in this laboratory. Some purified proteins were checked with SDS-PAGE (Figure 2.1).

### **2.17 Kinetic Coupling Assay for dCTP→dCMP→dUMP→dTMP Pathway**

T4 dCTPase/dUTPase (gp56), dCMP deaminase (CD) and thymidylate synthase (TS) are assumed to sequentially catalyze the three-step pathway of dCTP→dCMP→dUMP→dTMP shown in Figure 2.4. The kinetic coupling was measured with a coupled TS activity assay. The starting substrate was changed to dCTP (substrate of gp56) and all three enzymes were added to the solution. Hm-dCTP (see APPENDIX A for preparation) was added to the reaction as an activator of dCMP deaminase. All three purified enzymes at 0.05 μM each were mixed at 1:1:1 molar ratio. The reaction mixture consisted of 0.1 mM dCTP (for blank, H<sub>2</sub>O instead), 0.1 mM hm-dCTP, 0.05 μM gp56, 0.05 μM CD, 0.05 μM TS in 500 μl THF solution (see Section 2.5) and H<sub>2</sub>O which was added to make 1.0 ml of total volume. The increase of absorbance at 338 nm when the formation of DHF from THF occurs, was measured by a Kinetic module of Beckman DU-65 UV/Vis spectrophotometer. Other proteins at 0.05 μM indicated in Result sections, which do not involve in the catalytic pathway, were also individually added to the reaction in order to investigate their effects on the substrate channeling.

## 2.18 Immobilization of Protein onto an IAsys Cuvette

Carboxymethyl dextran (CMD) or carboxylate cuvette was employed to carry out the real-time protein-protein interaction assays. Protein was immobilized onto the surface of cuvette *via* EDC/NHS chemistry shown in Figure 2.5. CMD or carboxylate cuvette was washed with PBS/T buffer (10 mM sodium phosphate, 2.7 mM potassium chloride, 138 mM sodium chloride and 0.05% (v/v) Tween 20) for 5-10 min until a buffer baseline was obtained on an IAsys *plus* optical biosensor (Affinity Sensors, Inc.). The running condition was at 25°C with stirring speed of 100 rpm and sample rate at 0.3-0.5 second. 1.15 g 1-ethyl-3-(3-dimethylaminopropyl) carbodiimide (EDC) was dissolved in 15ml of deionized H<sub>2</sub>O and 0.2 g N-hydroxysuccinimide (NHS) in 15ml of deionized H<sub>2</sub>O. Carboxyl groups on the cuvette were activated by EDC/NHS mixture of 1:1 (v/v) ratio for 7 min. The cuvette was washed with PBS/T buffer for 2 min to remove activation mixture. The immobilization buffer, e.g., 5 mM maleate (pH 6.0), was used to wash the cuvette for three times and was left for 2 min. The immobilization buffer was chosen according to the criteria provided by the instrument manufacturer (IAsys, 1996a; IAsys, 1996b; IAsys, 1996c). The ligand protein in immobilization buffer was added to make the final concentration of about 0.1 mg/ml for best electrostatic uptake and was allowed to immobilize for 5-10 min. Non-coupled protein was removed by washing with PBS/T buffer and leaving for 2 min. Non-coupled activated carboxyl groups were blocked by 1 M ethanolamine, pH 8.5 and left for 3 min. The cuvette was alternatively washed with

PBS/T buffer for 5 min and with 1 M formic acid for 2 min. Repeat the last step and immobilization was complete (IASys, 1996a; IASys, 1996b; IASys, 1996c).

### **2.19 Real-Time Interaction Measurement and Data Analysis on an IASys Optical Biosensor**

Immobilized cuvette was equilibrated with running buffer (PBS/T or KGMT (150 mM potassium glutamate, 4 mM magnesium acetate, 20 mM Tris-HCl, pH 7.4)) until a buffer baseline was reached. The ligate protein solution was added to a desired final concentration and allowed to interact with ligand immobilized on the cuvette surface for 3-15 min. Real-time refractive index data were recorded automatically by a computer program – IASys ver3.0 – at sampling rate of 0.3-0.5 second. Immobilized cuvette was regenerated as the last step during immobilization. Association and dissociation profiles from the IASys data were plotted by FASTplot (Affinity Sensors, Inc.). IASys data were analyzed and fitted by FASTfit (Affinity Sensors, Inc.).

### **2.20 Fluorescence Spectroscopy**

Fluorescence experiments were conducted in a Perkin Elmer Luminescence Spectrometer LS50 (Perkin Elmer Life Sciences, USA). All of the proteins were in KGMT buffer. 0.5  $\mu\text{M}$  of single protein or 0.25  $\mu\text{M}$  of each single protein in a two-protein mixture was

excited at wavelength 290 nm, which measures tryptophan (Trp) fluorescence since it is sensitive to environment. Meanwhile, excitation at 290 nm minimizes the contribution of tyrosine (Tyr) fluorescence. In addition, additivity and linearity of protein fluorescence is assumed at low concentration and low absorbance. Emission spectrum was monitored at the wavelength range from 290 to 450 nm.

## **2.21 Analytical Ultracentrifugation**

Sedimentation equilibrium experiments were performed in a Beckman Optima XL-A analytical ultracentrifuge. Buffer densities and viscosity corrections were made according to data published (Laue *et al.*, 1992). The partial specific volume, estimated from the protein sequence according to the method of (Perkins, 1986), was  $0.733 \text{ cm}^3/\text{g}$ . Buffers for the sedimentation velocity and equilibrium runs contained KGMT buffer.

Sedimentation equilibrium experiments were performed at  $20^\circ\text{C}$  according to procedures described (Ausio *et al.*, 1992). Typically, three 120- $\mu\text{l}$  samples of protein with different concentrations indicated in Results sections were sedimented to equilibrium at speeds ranging from 15,000 to 24,000 rpm depending upon the concentration. Scans were collected with absorbance optics at wavelengths between 230 and 280 nm. The radial step size was 0.001 cm, and each  $c$  versus  $r$  datapoint was the average of 15 independent measurements. Wavelengths were chosen so that no points exceeded an absorbance of 1.0. Equilibrium data spanning the concentration range were examined by global fitting

using UltraScan software (Demeler, 2005). Equilibrium data were fitted to multiple models using global fitting. The resulting dissociation constant was further employed for statistics of the fit generated by a Monte Carlo analysis. The most appropriate model was chosen based on the best statistics and on visual inspection of the residual run patterns (see APPENDIX B for raw data).

**Table 2.1.** Recombinant proteins and their expression systems.

<b>Protein</b>	<b>Gene</b>	<b>Plasmid</b>	<b>Host</b>	<b>Reference</b>
dCMP hydroxymethylase	<i>42</i>	pT7-42	BC21(DE3)	Young and Mathews, 1992
Thymidylate synthase	<i>td</i>	pKTd2	MB901	Belfort <i>et al.</i> , 1983
dNMP kinase	<i>l</i>	pBK5	HB101	Brush <i>et al.</i> , 1990
dCTPase/dUTPase	<i>56</i>	pLAM71	M5219	Wheeler <i>et al.</i> , 1996
dCMP deaminase	<i>cd</i>	pET3C+T4dC D	B121(DE3) plysS	Maley <i>et al.</i> , 1990
Aerobic ribonucleotide reductase	<i>nrdAB</i>	pnrdAB	MV1304	Tseng <i>et al.</i> , 1992
Anaerobic ribonucleotide reductase	<i>nrdD</i>	pET29- T4NrdD	JM109(DE3)	Andersson <i>et al.</i> , 2001
<i>E. coli</i> NDP kinase	<i>ndk</i>	pKT8P3	DH5 $\alpha$	Hama <i>et al.</i> , 1991a

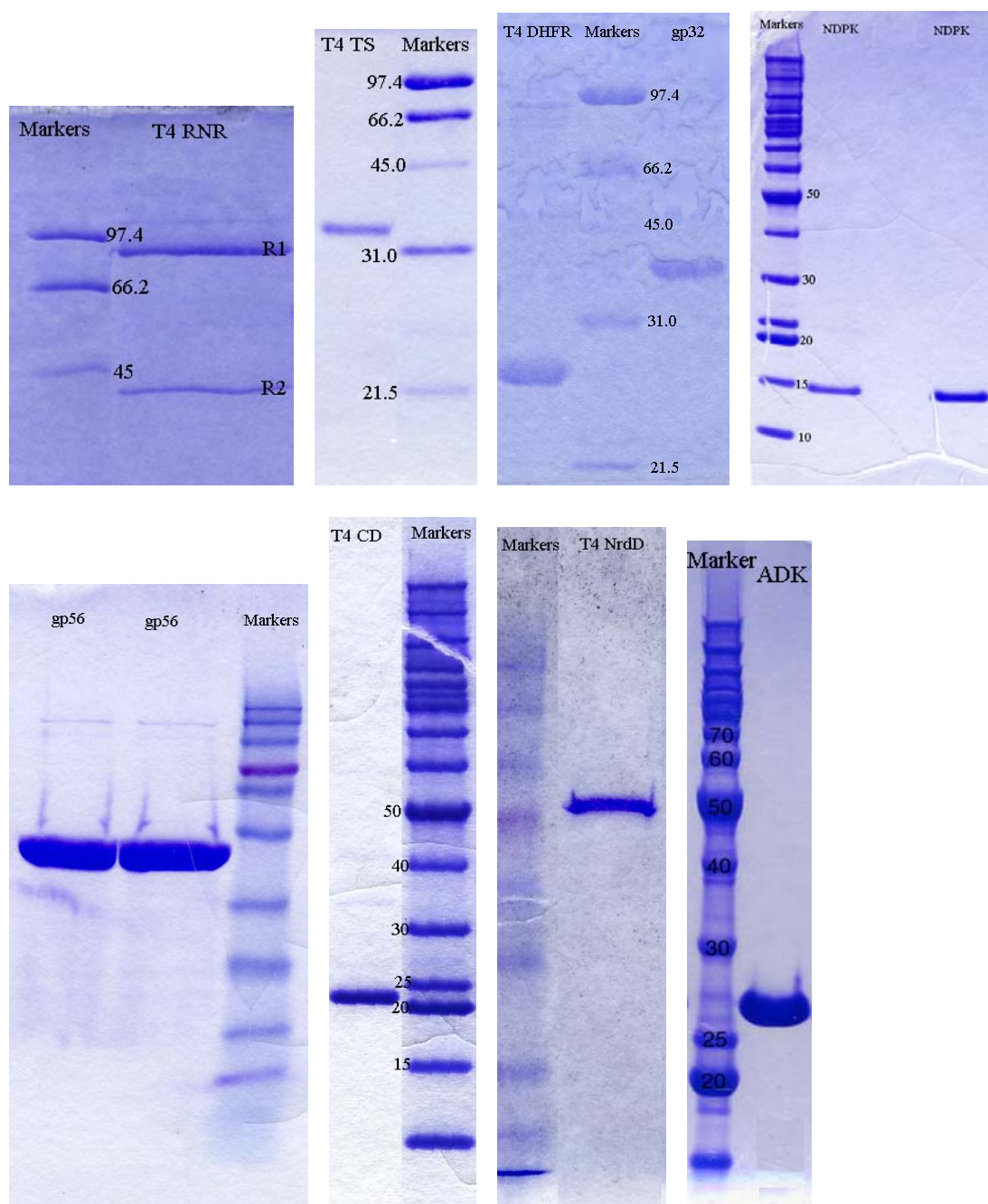


**Figure 2.1.** Highly purified proteins in SDS-PAGE.

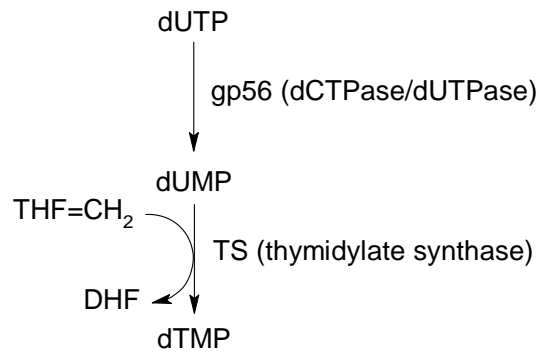


**Figure 2.2.** Activity assay for dUTPase/dCTPase (gp56) coupled with a TS assay.

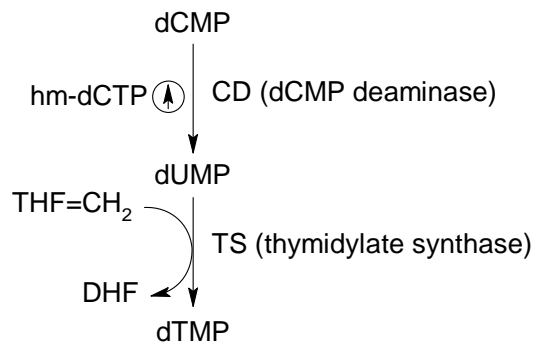


**Figure 2.3.** Activity assay for dCMP deaminase coupled with a TS assay.

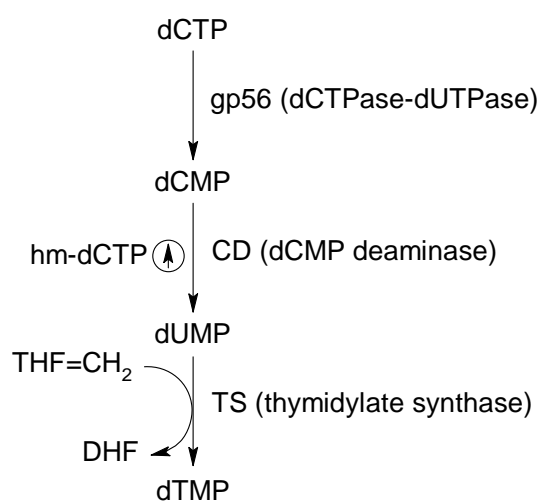


**Figure 2.4.** Kinetic coupling assay for dCTP → dCMP → dUMP → dTMP pathway.

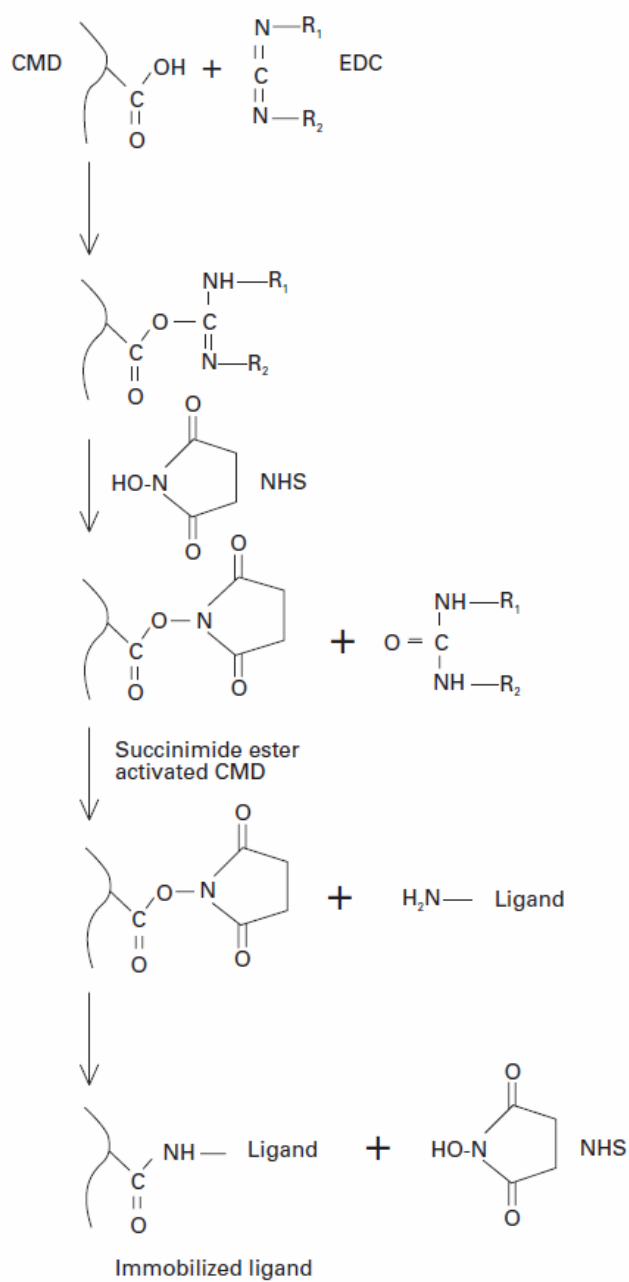


**Figure 2.5.** Chemistry for immobilization of proteins to CMD or carboxylate cuvette by EDC/NHS chemistry.

### Chapter 3

#### Direct Protein-Protein Interactions in the T4 dNTP Synthetase Complex

Previous data from this laboratory showing protein-protein interactions in the T4 dNTP synthetase complex were mainly from protein affinity columns (Wheeler *et al.*, 1992; Wheeler *et al.*, 1996). However, this approach can not distinguish direct interactions from secondary associations, in which two proteins are joined because of their common linkage to a third protein, if a cell extract is applied. Moreover, all the previous approaches lack the ability to quantitatively determine the strength of interaction. Study of direct protein-protein association helps explain how the dNTP synthetase complex is assembled and how it coordinates to function efficiently. With the advent of surface plasmon resonance (SPR) (Szabo *et al.*, 1995; Lakey and Raggett, 1998; Fivash *et al.*, 1998; Hall, 2001) and resonant mirror (RM) (Malmqvist and Karlsson, 1997; Hall, 2001) technologies, researchers can now not only qualitatively but quantitatively investigate the direct protein-protein interactions in real time. In this research, after carrying out extensive purification of the relevant enzymes as recombinant proteins, an IAsys optical biosensor instrument based on resonant mirror technology was used to characterize their interactions using purified proteins. In addition, fluorescence spectrophotometry was also employed to monitor the intrinsic fluorescence changes during protein-protein interactions.

### **3.1 Protein-Protein Interactions Involving T4 Phage-Encoded Proteins in Bacteriophage T4 dNTP Synthetase Complex**

In one of many protein affinity chromatography experiments where purified T4 aerobic ribonucleotide reductase (RNR) was immobilized on the column, T4 thymidylate synthase (TS) from a cell extract of *E. coli* cells infected with phage T4 was found to be retained in the column at NaCl concentrations up to 0.5 M, either in the absence or presence of 1 mM ATP (Wheeler *et al.*, 1996). However, by no means could we make a distinction whether column retention resulted from a direct or indirect interaction between T4 RNR and T4 TS. With the availability of an IAsys optical biosensor, we started with these two purified proteins for an investigation of direct protein-protein interaction. T4 thymidylate synthase was immobilized on an IAsys carboxylate cuvette. In order to verify whether the right protein was immobilized and the protein was in good shape, TS activity assay was conducted on the immobilized protein. The results confirm that the immobilized TS was active. Figure 3.1 shows that T4 RNR in the solution directly interacted with immobilized T4 TS on an IAsys carboxylate cuvette (Kim *et al.*, 2005b). In comparison, when T4 RNR was immobilized on a cuvette, T4 TS was also seen to directly interact with T4 RNR (Figure 3.2). These findings suggest that the association between T4 RNR and T4 TS has no preference or discrimination, no matter which protein is immobilized on the surface of a cuvette. In addition, their association was further confirmed by a fluorescence experiment. Figure 3.3 depicts that the fluorescence spectrum of an equimolar mixture of T4 RNR and T4 TS was observed to

have a quenching and a blueshift comparing with the calculated spectrum from their individual spectra, suggesting a direct interaction between them. Another experiment involving analytical ultracentrifugation reveals that some partial associations between T4 RNR and T4 TS were observed although some protein degradation happened due to the long run (24 – 48 hr) at 25°C (data not shown).

Figure 3.1 also shows a direct association between T4 single-strand DNA binding protein (gp32) and T4 TS immobilized on the cuvette (Kim *et al.*, 2005b). This confirms the finding in Wheeler *et al.* (1996) that purified gp32 was retained on an affinity column of immobilized T4 TS at up to 0.6 M NaCl. When T4 dihydrofolate reductase (DHFR) was immobilized on a column, T4 TS from a crude extract of T4-infected host cells was found to be retained in the column (Wheeler *et al.*, 1996). Here, Figure 3.1 shows that their interaction is a direct one. Another similar experiment shows a direct interaction between T4 dCTPase/dUTPase (gp56) and T4 TS from a fluorescence experiment as shown in Figure 3.4.

One of the features of the IAsys optical biosensor is that it can reveal the useful kinetic properties of dynamic protein-protein associations since it is able to monitor the real-time refractive index changes that are proportional to the amount of proteins bound to the surface occurring at the sensing layer (Figure 1.8). By applying varied concentrations of T4 RNR in the solution in the T4 TS-immobilized cuvette, the equilibrium dissociation constant ( $K_D$ ) was determined to be 0.5  $\mu\text{M}$ . T4 TS has been estimated to accumulate in a

T4-infected *E. coli* cell to about 2,000 molecules (Mathews, unpublished data). According to the average volume of a T4-infected bacterium (Mathews, 1972), the intracellular concentration of T4 TS can be estimated to be 3  $\mu\text{M}$ . The  $K_D$  value suggests that the association of these two proteins *in vivo* is significant although we do not have an estimate for the intracellular concentration of T4 RNR.

### **3.2 Protein-Protein Interactions Involving *E. coli* NDP Kinase**

Nucleoside diphosphate kinase occupies a distinctive location on metabolic charts at the interface between nucleotide biosynthesis and nucleotide polymerization, leading both to DNA and RNA. In bacteriophage T4 infection NDP kinase is even more distinctive, as one of very few enzymes in DNA metabolism that is not encoded by the virus; adenylate kinase also falls into this category (Allen *et al.*, 1983; Lu and Inouye, 1996). The earliest publications on the T4 dNTP synthetase complex from our laboratory suggested that *E. coli* NDP kinase is both physically and kinetically linked to phage-coded enzymes of dNTP biosynthesis (Reddy *et al.*, 1977; Allen *et al.*, 1983; Moen *et al.*, 1988). Later protein affinity chromatography with immobilized NDP kinase was carried out and results show that a column of this material retained several T4 enzymes of dNTP synthesis, including dihydrofolate reductase and ribonucleotide reductase large subunit; and several replication/recombination proteins, including products of genes 32, 45, 61, and *uvsY* (Wheeler *et al.*, 1996). Comparable experiments are described in a more recent

paper (Kim *et al.*, 2005b), where we identified several phage proteins that are coimmunoprecipitated by antiserum to *E. coli* NDP kinase in the presence and absence of the gene 32 single-strand DNA-binding protein. To better understand the linkage between host-encoded enzymes with virus-coded proteins, it is important to identify the direct protein-protein interactions.

Figure 3.6 presents data from IAsys optical biosensing experiments with immobilized *E. coli* NDP kinase and several T4 proteins, including T4 thymidylate synthase, aerobic ribonucleotide reductase, and the multifunctional dCTPase/dUTPase encoded by gene 56. All three of these enzymes have been assigned roles in the T4 dNTP synthetase complex, and all display significant affinity for NDP kinase, as judged by the rapid initial association rates. Significant association was seen also with T4 gp32. This is important, because we have proposed that gp32 plays a role in recruiting enzymes of the dNTP synthetase complex to replication sites (Wheeler *et al.*, 1996), and further evidence for our model is presented elsewhere (Kim *et al.*, 2005b). The Figure also shows two negative controls, one with purified *E. coli* CTP synthetase and, strikingly, one with purified *E. coli* thymidylate synthase. It is somewhat surprising that NDP kinase of the host cell interacts with thymidylate synthase of the phage destined to destroy that cell but not (by the criteria used here) with the host cell's own thymidylate synthase.

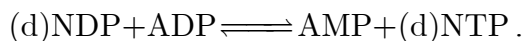
Figure 3.7 depicts experiments involving fluorescence spectroscopy. *E. coli* NDP kinase contains no tryptophans and hence is non-fluorescent. Figure 3.7A shows the

fluorescence of an equimolar mixture of NDP kinase and T4 aerobic ribonucleotide reductase to be enhanced relative to the fluorescence expected if the proteins do not interact. Figure 3.7B involves a similar experiment with NDP kinase and T4 thymidylate synthase; here an enhancement of fluorescence was also seen but smaller than that observed by mixing NDP kinase with T4 RNR. Figure 3.7C shows the quenching of fluorescence of an equimolar mixture of T4 gp56 and *E. coli* NDP kinase. All these results confirm the direct interactions between *E. coli* NDP kinase and T4 proteins observed in IAsys optical biosensor analysis. The interaction between NDP kinase and T4 RNR was also confirmed by JuHyun Kim in this laboratory, using a GST pulldown assay (Shen *et al.*, 2004; Kim, 2005). The assay also shows that only T4 RNR R2 (not R1) subunit interacts directly with NDP kinase.

Quantitative analysis was followed using the IAsys data from proteins in solution interacting with immobilized *E. coli* NDP kinase. From these data (Figure 3.8), the apparent equilibrium dissociation constants ( $K_D$ ) for T4 gp32 to NDP kinase, T4 CD to NDP kinase and T4 TS to NDP kinase were calculated as about 2  $\mu\text{M}$ , 1.6  $\mu\text{M}$  and 2.2  $\mu\text{M}$ , respectively. A similar calculation as T4 TS was applied for gp32, which is estimated to be about 10,000 molecules per T4-infected *E. coli* cell (Alberts and Frey, 1970); the intracellular concentration of gp32 was calculated to be about 15  $\mu\text{M}$ . The data suggest the associations of above protein pairs are significant.

### 3.3. Protein-Protein Interactions Involving *E. coli* Adenylate Kinase

Adenylate kinase catalyzes the reversible ATP-dependent phosphorylation of AMP to ADP. The reaction is involved in the *de novo* biosynthesis of adenine nucleotides, and it is also thought to participate in adjusting adenine nucleotide levels to meet the energy demands of a cell (Noda, 1973). Lu and Inouye (Lu and Inouye, 1996) reported a novel function for *E. coli* adenylate kinase when they found that the wild-type *adk* gene could complement a site-specific disruption of *ndk*, the structural gene for *E. coli* NDP kinase. Bernard *et al.* (2000) from our laboratory further showed that adenylate kinase could catalyze the conversion of nucleoside diphosphates to triphosphates as follows:



Apart from the fact mentioned in the previous section that *E. coli* NDP kinase takes part in the synthesis of dNTPs after T4 infection of *E. coli*, the host adenylate kinase (ADK) is also involved (Bello and Bessman, 1963b). T4 DNA contains a special nucleotide residue – hm-dCMP, which is produced from dCMP by T4 dCMP hydroxymethylase. Although, at the diphosphate level, *E. coli* NDP kinase acts on all the nucleoside diphosphates, including hm-dCDP (Bello and Bessman, 1963a), at the monophosphate level, a phage-coded enzyme is required since no host enzyme can phosphorylate hm-dCMP. This latter reaction is catalyzed by the unusual dNMP kinase (gp1), which also acts on dGMP and dTMP (Bello and Bessman, 1963a; Duckworth and Bessman, 1967), but not dAMP or dCMP. Hence, *E. coli* adenylate kinase plays an indispensable role to phosphorylate

dAMP, which is the product of host DNA degradation although it represents only 5-10% of total nucleotide of phage progenies (Mathews, 1966). Early study (Allen *et al.*, 1983) in our laboratory found that about 5% of the total ADK activity co-sedimented with the partially purified T4 dNTP synthetase complex. It is of great interest to investigate whether *E. coli* ADK directly interacts with other proteins in the complex.

Figure 3.9 depicts several protein-protein interactions involving *E. coli* adenylate kinase. Figure 3.9, *panel A* shows that *E. coli* adenylate kinase directly interacts with immobilized *E. coli* NDP kinase. JuHyun Kim (2005) in our laboratory reached the same conclusion using a GST pulldown assay. Figure 3.9, *panel B* shows that T4dCMP deaminase directly interacts with immobilized *E. coli* ADK. Figure 3.9, *panel C* shows that T4 thymidylate synthase directly interacts with immobilized *E. coli* ADK.

Figure 3.10 shows the results of two experiments that involve quantitative analysis of interactions involving ADK. *Panel A* depicts an analysis of the interaction between immobilized NDP kinase and adenylate kinase in solution. Determining the equilibrium binding of ADK at several concentrations permitted an estimate of 0.22  $\mu\text{M}$  for  $K_D$  for the interaction between NDP kinase and adenylate kinase. This result supports the qualitative result of the immunoprecipitation experiment (Kim *et al.*, 2005a). In *panel B*, adenylate kinase in solution was seen to interact with immobilized T4 thymidylate synthase, and analysis of the concentration dependence of binding yielded a  $K_D$  of 0.036  $\mu\text{M}$ , showing a close interaction between *E. coli* adenylate kinase and one of the T4

enzymes in the complex. Estimates of intracellular concentrations of T4-encoded enzymes, based upon activities in crude extracts and turnover numbers, suggest that these values lie in the low micromolar range. This estimate, plus the  $K_D$  data determined in Figure 3.10, suggests that the interacting proteins are indeed associated within the infected cell.

### **3.4 Protein-Protein Interactions Involving T4 Anaerobic Ribonucleotide Reductase Subunit (NrdD)**

Besides T4 aerobic ribonucleotide reductase (T4 RNR), T4 also encodes an anaerobic form of ribonucleotide reductase because aerobic T4 RNR is functional only in the presence of molecular oxygen. Under anaerobic conditions, phage T4 still can infect *E. coli* host with growth rate comparable to aerobic condition (Wheeler and Mathews, unpublished observation) because the T4 anaerobic ribonucleotide reductase (NrdD) replaces the function of aerobic T4 RNR. One difference between these two forms of ribonucleotide reductases is that T4 NrdD catalyzes the reduction on triphosphate substrates, i.e.,  $NTP \rightarrow dNTP$ , while T4 RNR converts  $NDP \rightarrow dNDP$ . We wonder whether, under anaerobic condition, the enzymes for dNTP biosynthesis also form a multi-enzyme complex similar to the aerobic T4 dNTP synthetase complex. Initial studies began with the investigation of direct protein-protein association involving T4 NrdD.

Fluorescence experiments (Figure 3.11) show that T4 NrdD interacts with T4 TS, T4 gp56 and *E. coli* NDPK, respectively. IAsys optical biosensor analysis confirms the direct interaction between T4 NrdD and *E. coli* NDP kinase, which is shown in Figure 3.12. The findings suggest that T4 NrdD might also interact with other proteins during dNTP biosynthesis.

We have applied several approaches, such as IAsys optical biosensor analysis and fluorescence spectroscopy, and a large number of direct protein-protein interactions were detected. We have employed the same approaches to investigate whether small molecules, such as nucleotides, would affect their interactions, which will be shown in the next chapter.

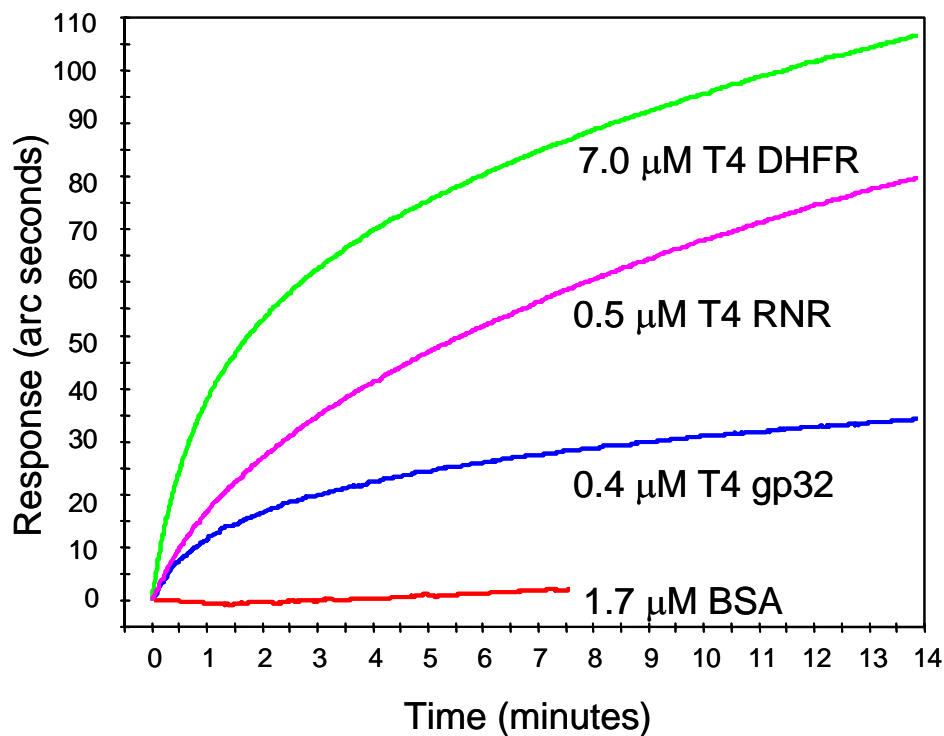


**Figure 3.1.** Interactions of T4 ribonucleotide reductase (RNR), T4 single-strand DNA binding protein (gp32), T4 dihydrofolate reductase (DHFR) with T4 thymidylate synthase (TS) that was immobilized on an IAsys carboxylate cuvette. Running buffer was PBS/T (138 mM NaCl, 2.7 mM KCl, 10 mM potassium phosphate, pH 7.4 and 0.05% Tween 20). The T4 proteins, at the final concentrations shown, were added individually to the cuvette. BSA depicts a negative control with bovine serum albumin. The figure was generated by using FASTplot program (Affinity Sensors).

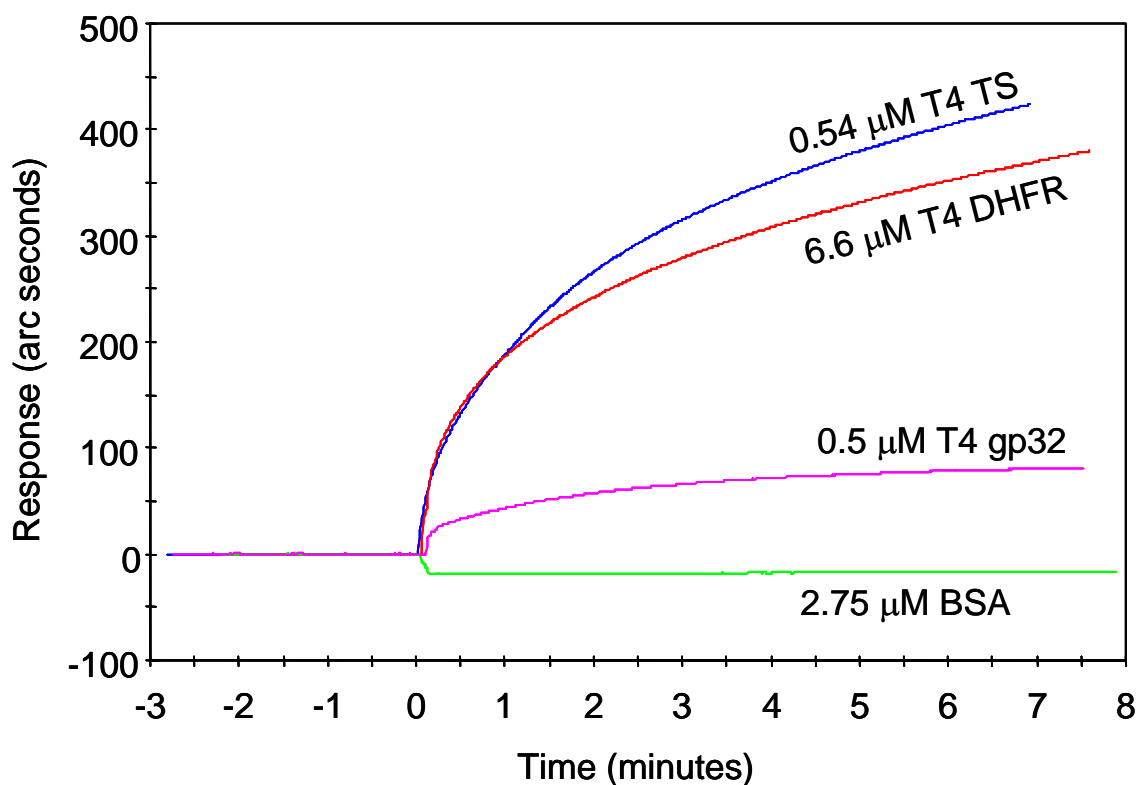


**Figure 3.2.** Interactions of T4 TS, T4 DHFR, T4 gp32 with T4 RNR that was immobilized on an IAsys carboxylate cuvette. Running buffer was PBS/T. The T4 proteins, at the final concentrations shown, were added individually to the cuvette. BSA depicts a negative control with bovine serum albumin. The figure was generated by using FASTplot program (Affinity Sensors).

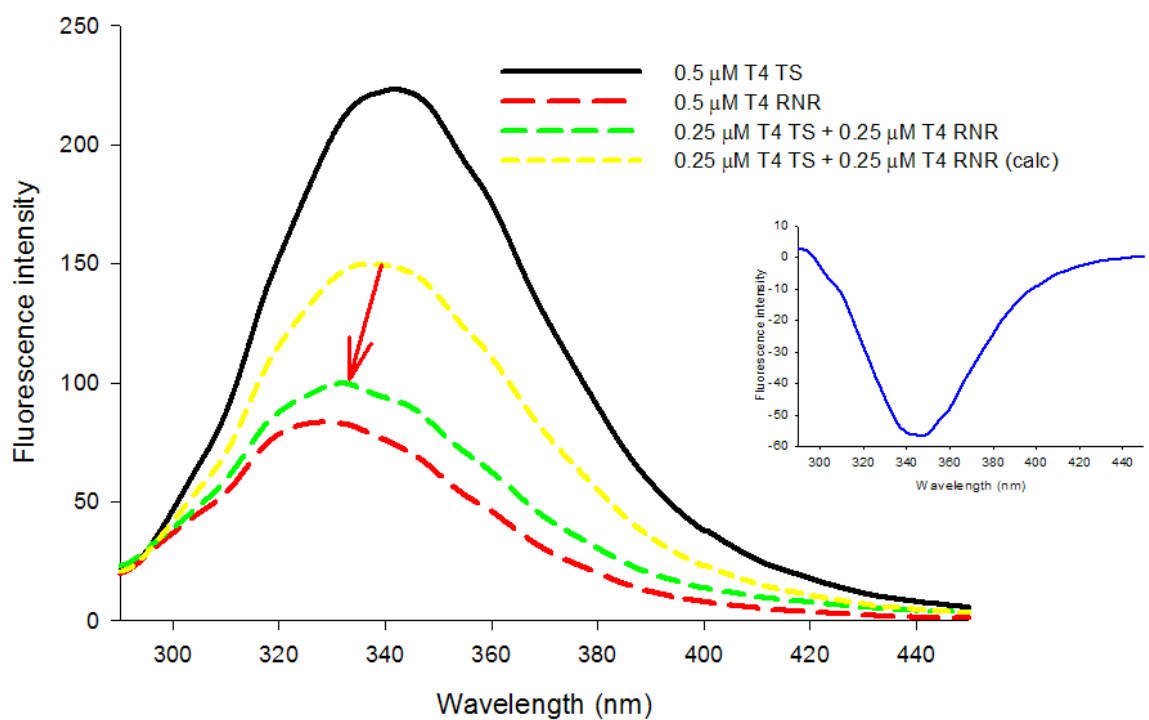


**Figure 3.3.** Fluorescence spectra of T4 RNR and T4 TS (excitation at 290 nm). The arrow shows that a quenching and a blue-shift occurred when mixing equimolar T4 RNR and T4 TS compared to the calculated spectrum (calc). The *inset* represents the fluorescence difference between the experimental and calculated spectra.

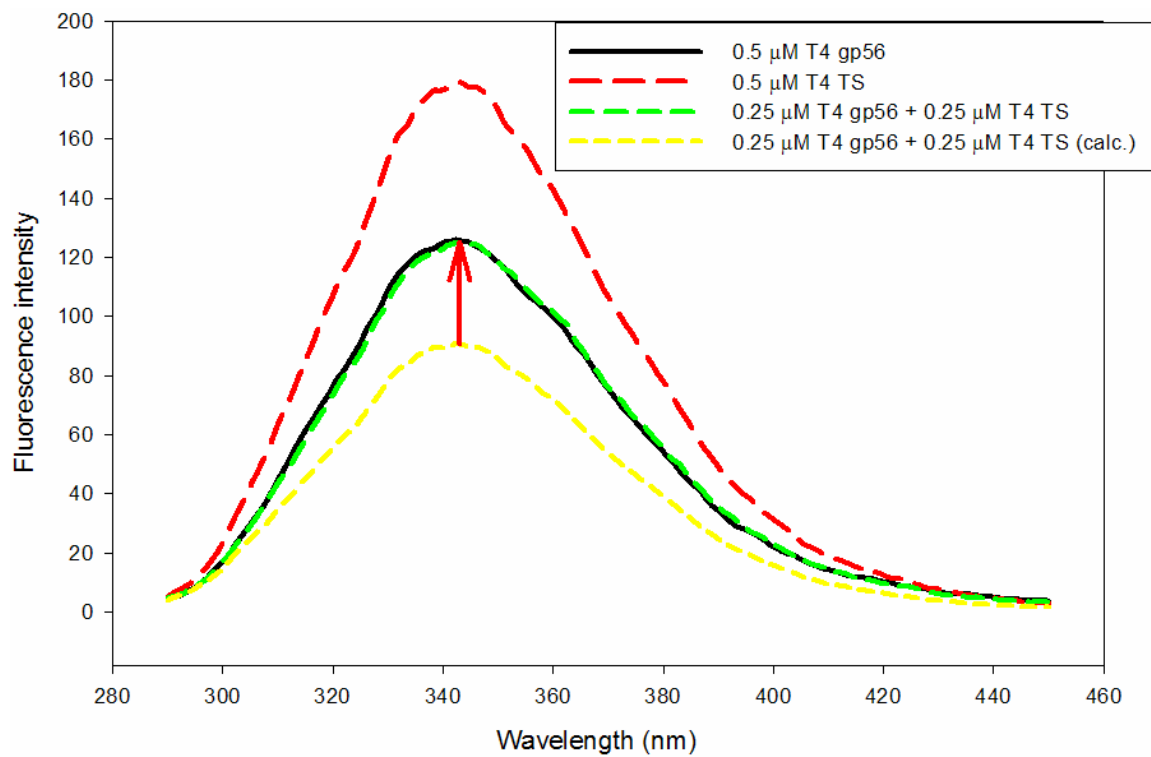


**Figure 3.4.** Fluorescence spectra of T4 gp56 and T4 TS (excitation at 290 nm). The arrow shows that a quenching and a blue-shift occurred when mixing T4 gp56 and T4 TS compared to the calculated spectrum (calc.).

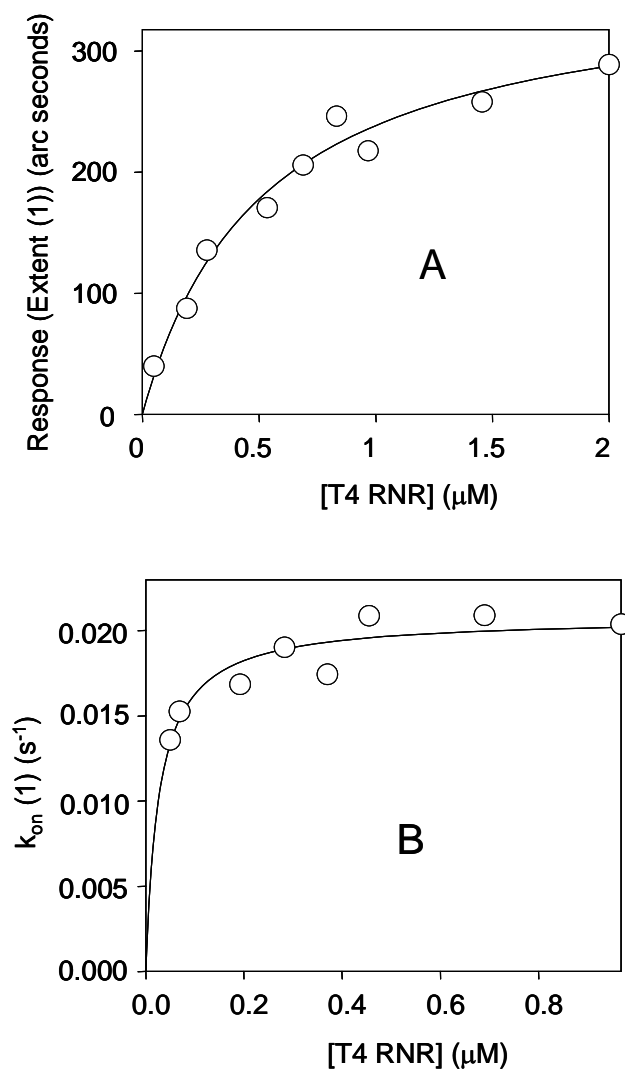


**Figure 3.5.** Binding curve of T4 RNR to T4 TS immobilized on IAsys carboxylate cuvette in the absence or presence of ATP. Running buffer was PBS/T. *Panel A*, no ATP; *panel B*, in the presence of 1 mM ATP. Data points (open circles) were calculated from the association and dissociation profiles under varied concentrations of T4 RNR. Curves were fitted from data points with FASTfit (Affinity Sensors). Extent (1) means the extended maximal response of the first phase in a biphasic association.  $k_{\text{on}}(1)$  means the apparent on-rate of the first phase in a biphasic association.

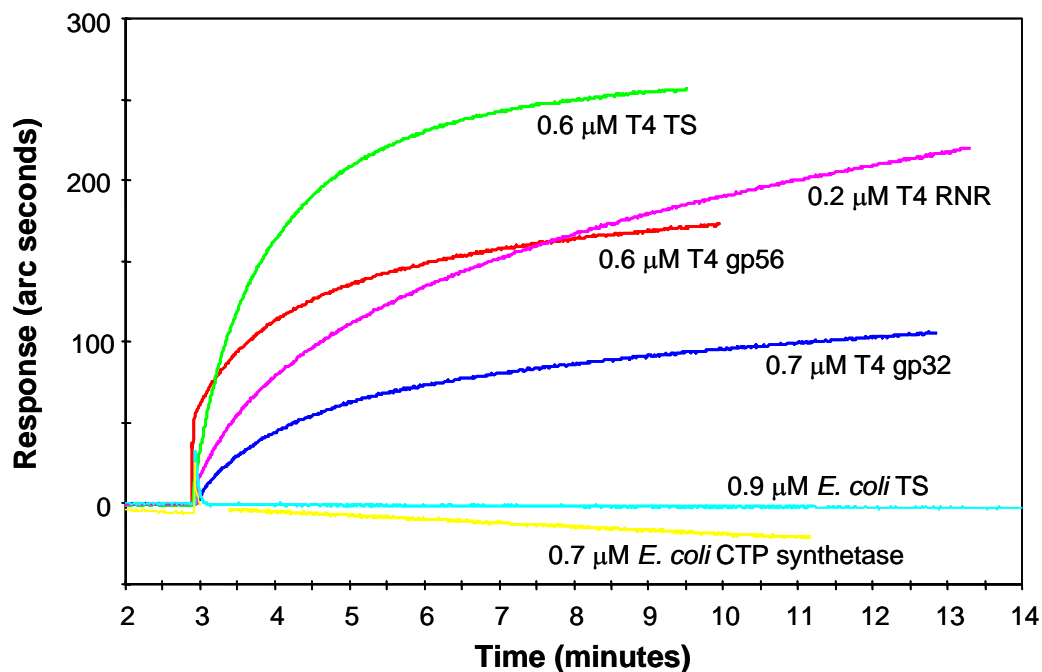
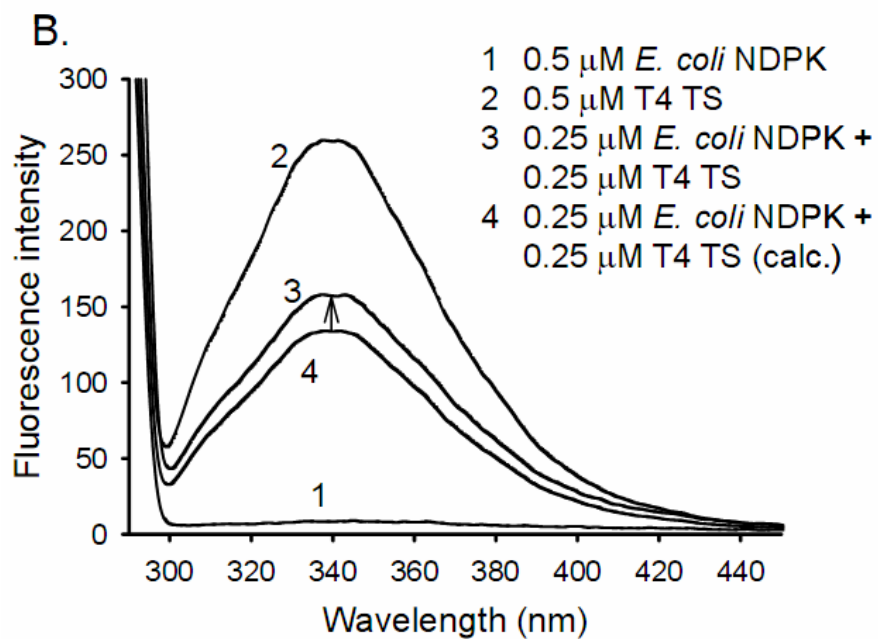
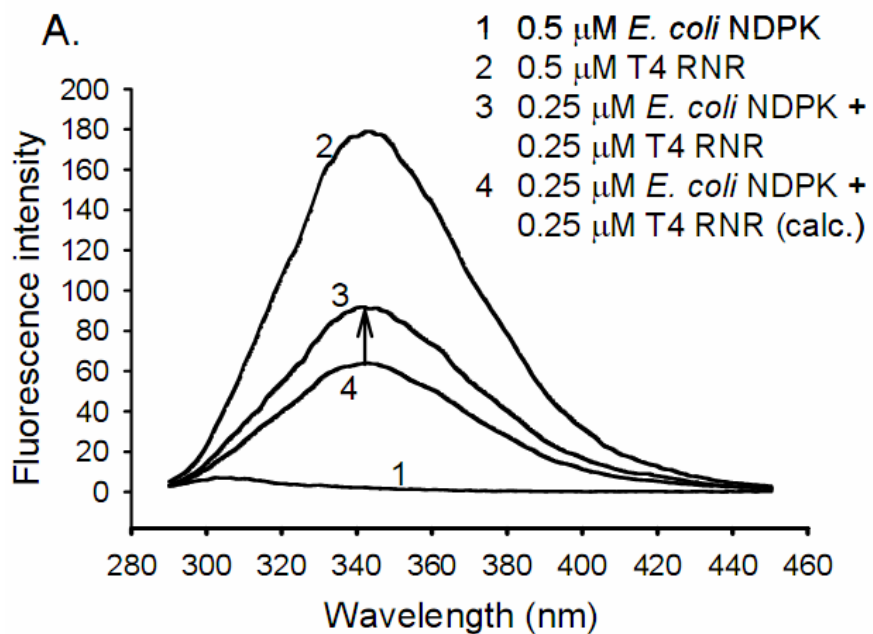


**Figure 3.6.** Interactions of T4 RNR, T4 TS, T4 gp32, T4 gp56 or *E. coli* TS, *E. coli* CTP synthetase with *E. coli* NDPK immobilized on an IAsys carboxylate cuvette. Running buffer was KGMT (150 mM potassium glutamate, 4 mM magnesium acetate, 20 mM Tris-HCl, pH 7.4). Protein concentrations were labeled by the association curves. The graph was generated by using FASTplot (Affinity Sensors).



(continued in next page)

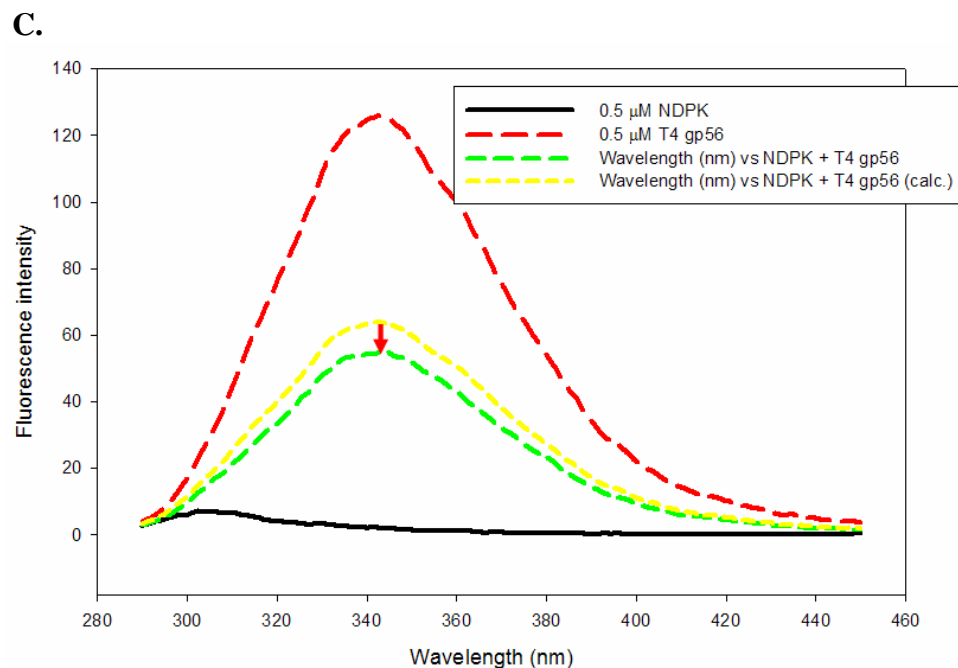
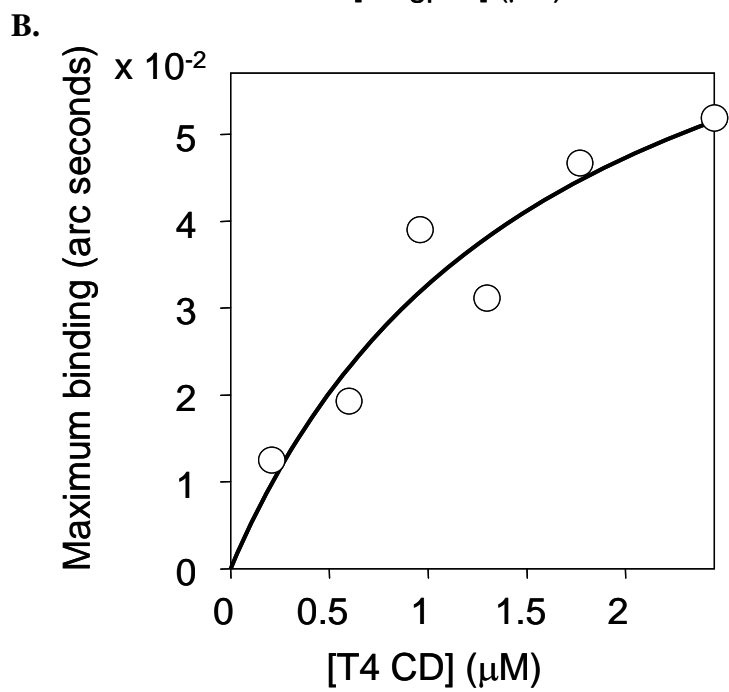
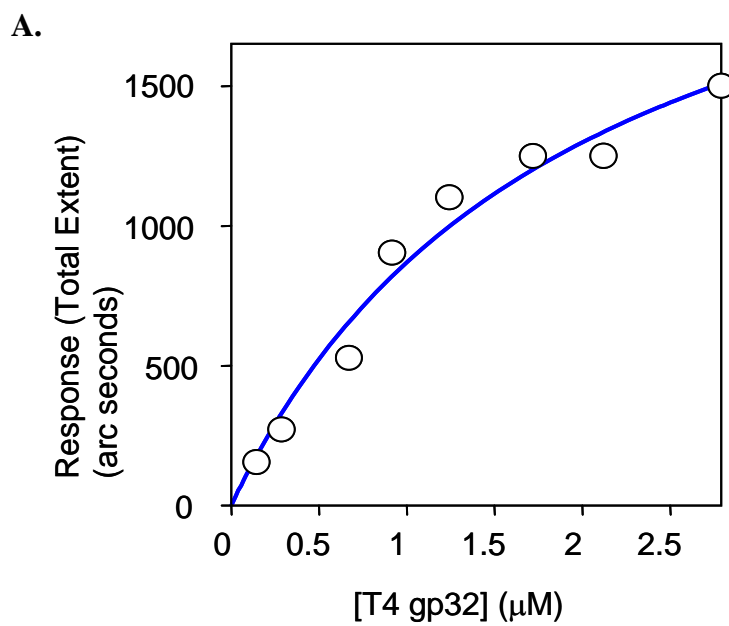


**Figure 3.7.** Protein-protein interactions as inferred by fluorescence enhancement. A, interaction of *E. coli* NDP kinase with T4 aerobic ribonucleotide reductase. B, interaction of *E. coli* NDP kinase with T4 thymidylate synthase. C, interaction of *E. coli* NDP kinase with T4 dUTPase/dCTPase (gp56). Excitation was at 290 nm. Fluorescence spectra were recorded for the proteins at the concentrations specified on the figure. For each panel the arrow identifies the enhancement of fluorescence, specifically, the difference between calculated and observed spectra for an equimolar mixture of the two enzymes being studied.



(continued in next page)

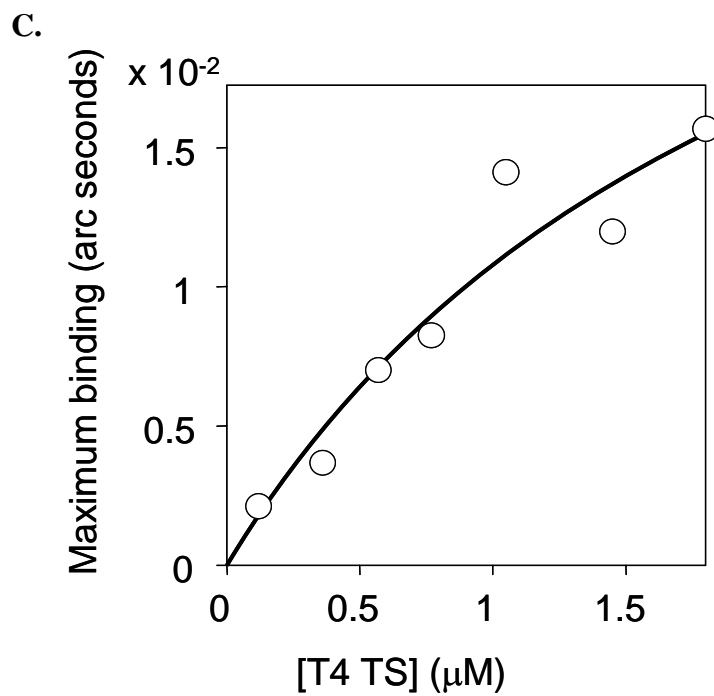
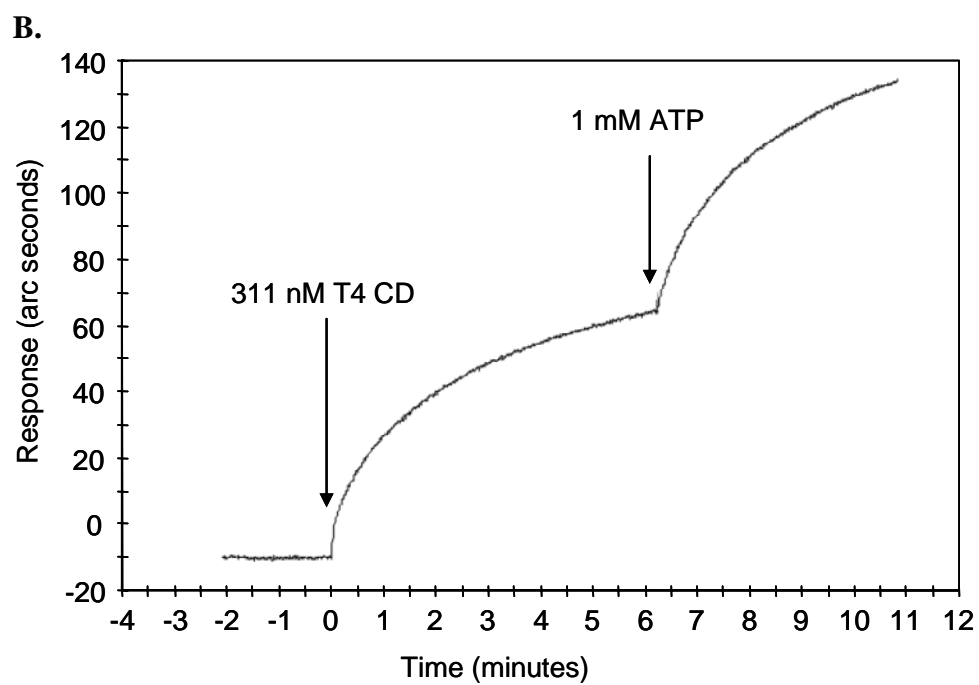
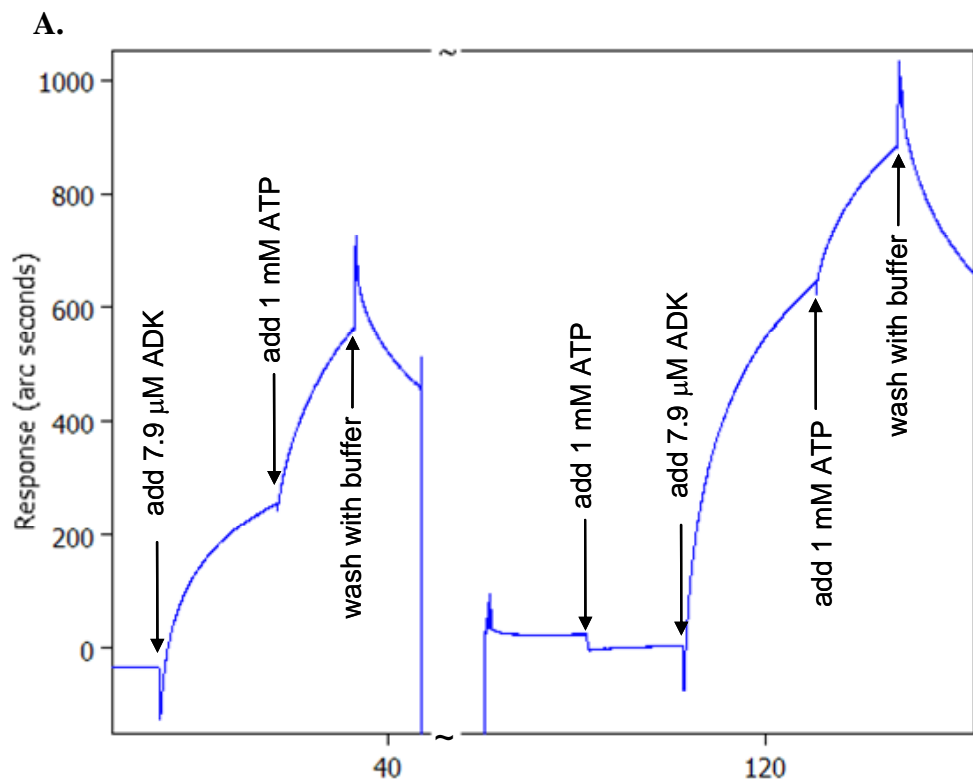


**Figure 3.8.** Quantitative analysis of the interaction of T4 gp32 (A), T4 dCMP deaminase (B), or T4 thymidylate synthase (C) in solution with immobilized *E. coli* NDP kinase on an IAsys carboxylate cuvette. All graphs were generated by using FASTfit (Affinity Sensors).



(continued in next page)

C.

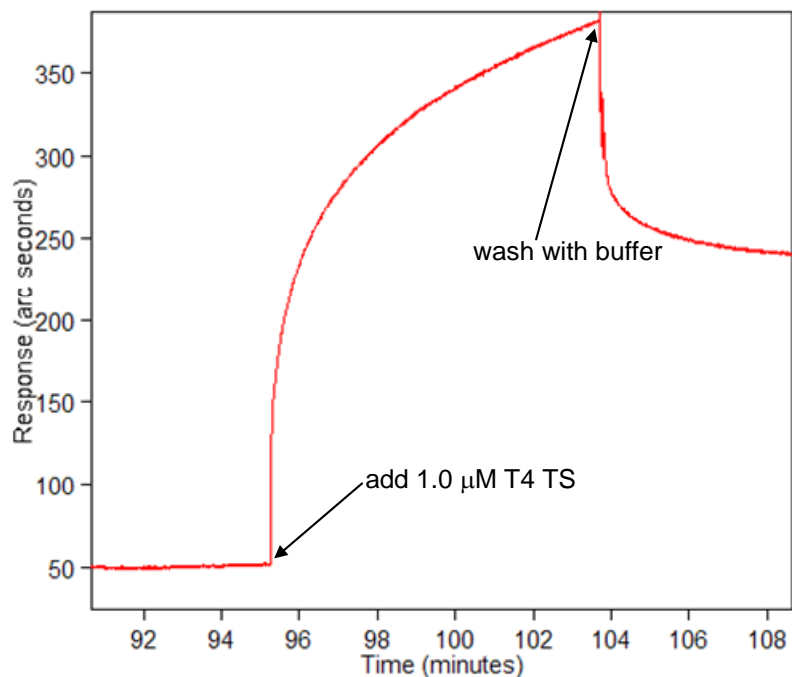


**Figure 3.9.** Protein-protein interactions involving *E. coli* adenylate kinase. A, interaction of *E. coli* ADK with *E. coli* NDPK immobilized on an IAsys carboxylate cuvette and ATP effect on their interaction. B, interaction of T4 dCMP deaminase with *E. coli* ADK immobilized on an IAsys carboxylate cuvette and ATP effect on their interaction. C, interaction of T4 TS with *E. coli* ADK immobilized on an IAsys carboxylate cuvette. Running buffer was KGMT.

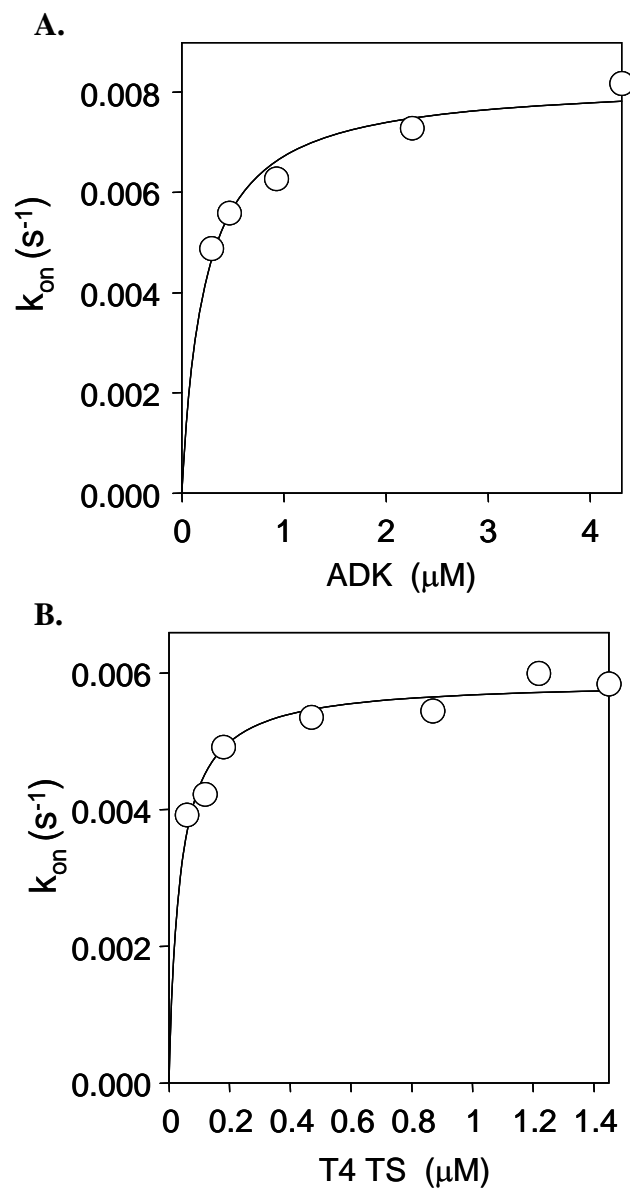
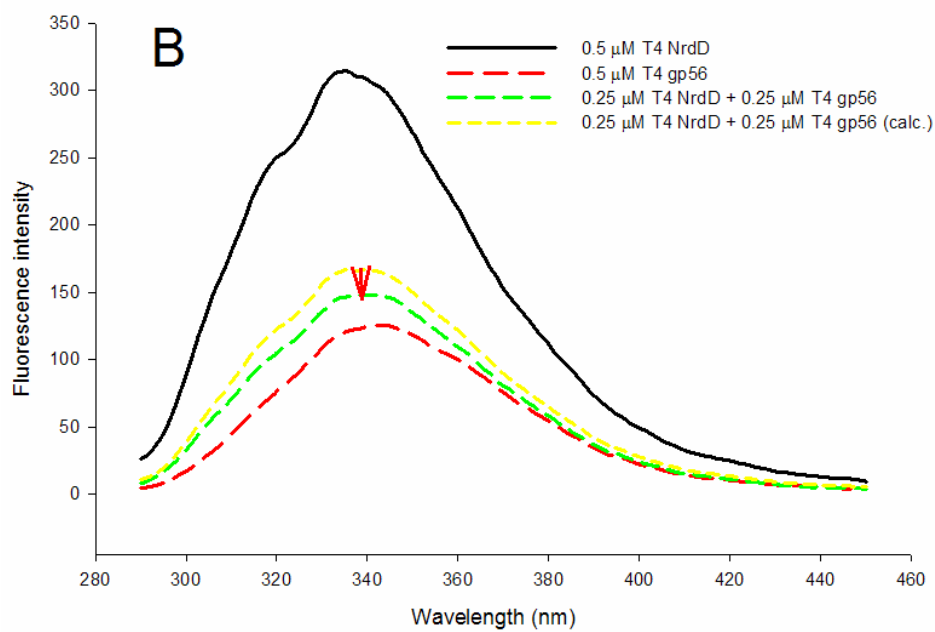
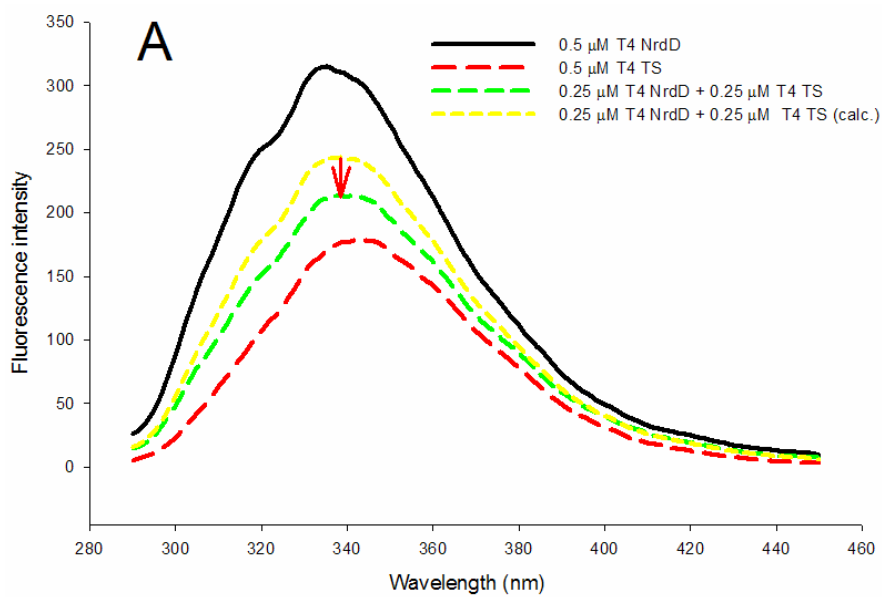


**Figure 3.10.** Quantitative analysis of protein-protein interactions. A. *E. coli* adenylate kinase (ADK) in solution with immobilized *E. coli* NDP kinase. B. T4 TS in solution with immobilized *E. coli* ADK. Both graphs were generated by using FASTfit (Affinity Sensors).



(continued in next page)

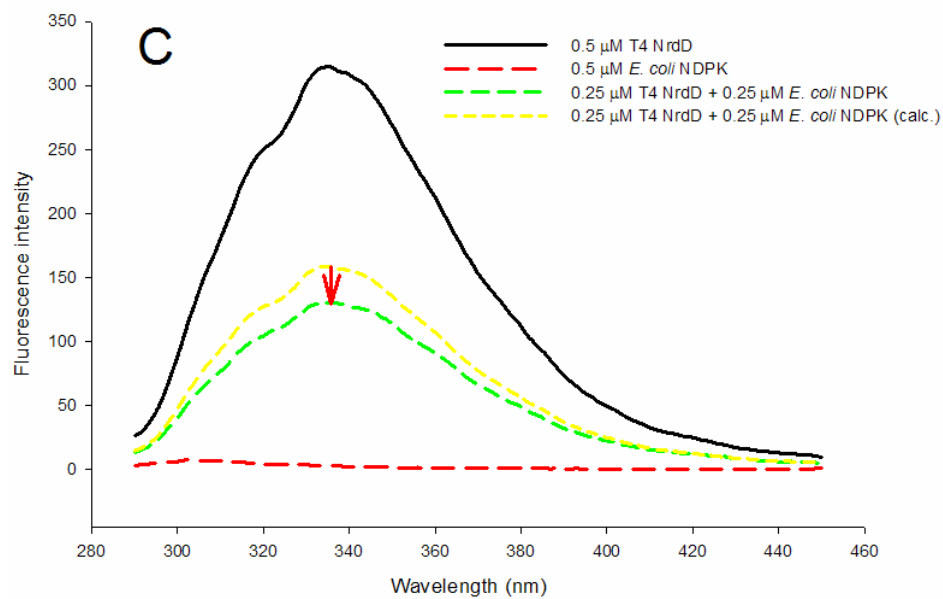


**Figure 3.11.** Fluorescence spectra of T4 NrdD with T4 TS (A), T4 gp56 (B) or *E. coli* NDPK (C) (excitation at 290 nm). Red arrows show that a quenching was observed when mixing T4 NrdD with corresponding proteins indicated in the legends.

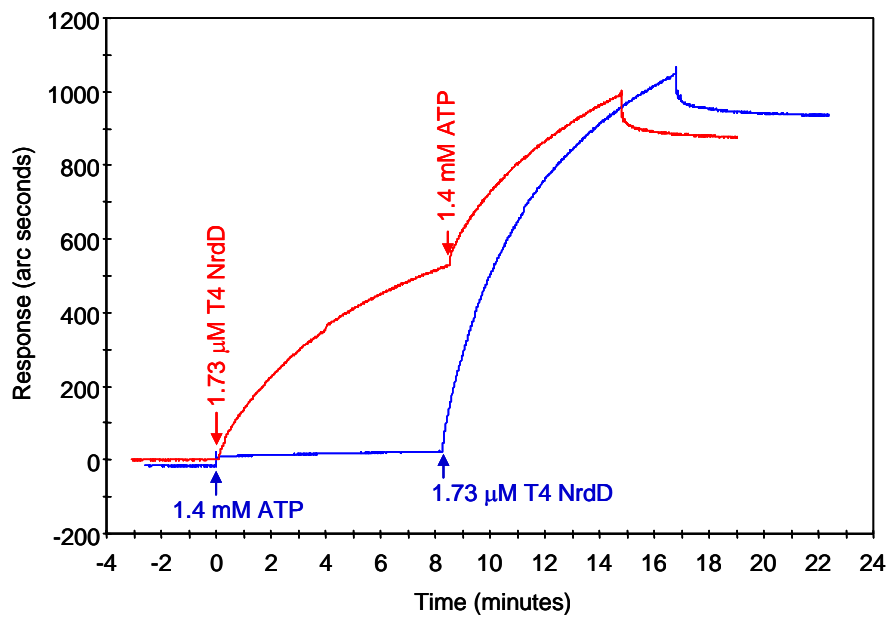


**Figure 3.12.** ATP effects on the association of T4 anaerobic ribonucleotide reductase (NrdD) to *E. coli* NDPK immobilized on an IAsys carboxylate cuvette. Running buffer was KGMT. The figure was generated by using FASTplot program (Affinity Sensors).

## Chapter 4

### Nucleotide Effects upon Protein-Protein Interactions

As mentioned in Chapter 1, the balance of dNTP pools of T4 phage-infected *E. coli* cells is mainly controlled by two T4-encoded enzymes, namely, ribonucleotide reductase and dCMP deaminase. First, the remarkable ribonucleotide reductase represents the branch point between RNA and DNA precursor biosynthesis. The enzyme is the point that is closely regulated to control the right ratio of four different dNDPs and downstream dNTPs. Table 1.3 shows that ATP, one of the allosteric effectors, binding to the activity site activates all the four NDP reductase activities. ATP or dATP was found to enhance the association between ribonucleotide reductase R1 and R2 subunits (Hanson and Mathews, 1994). Eric Hanson (Wheeler *et al.*, 1996) found that in the presence of 1 mM ATP, the number and the amounts of proteins retained in the immobilized ribonucleotide reductase affinity column were increased, suggesting that protein-protein interactions in the T4 dNTP synthetase complex are substantially mediated by low molecular weight substrates and regulatory molecules. Moreover, several other enzymes, e.g., *E. coli* NDP kinase, also require ATP as their substrates and energy provider. All these findings led us to investigate effects of nucleotides upon the protein-protein interactions in the T4 dNTP synthetase complex. Second, T4 dCMP deaminase activity is almost completely dependent on hm-dCTP *in vivo*. We wonder if upon the binding of hm-dCTP, dCMP

deaminase experiences some conformational changes and whether this affects the protein-protein interactions involving this enzyme.

#### **4.1 Nucleotide Effects upon Protein-Protein Interactions Involving T4-Encoded Proteins**

We first investigated whether ATP affects the interactions involving T4 aerobic ribonucleotide reductase (RNR). Figure 4.1 shows that in the presence of 1 mM ATP, comparable to physiological concentrations of ATP, enhanced the interaction between T4 RNR and T4 thymidylate synthase, whether T4 RNR was in solution bound or immobilized. ATP itself does not give considerable signal change when added to the solution. As expected, the activators – ATP and dATP – of T4 RNR enhanced the protein-protein interaction. Quantitative analysis from IAsys data shows that in the presence of 1 mM ATP, the apparent dissociation constant ( $K_D$ ) was determined to be about 0.03  $\mu\text{M}$  as shown in Figure 3.5, *panel B*. In the absence of ATP, however,  $K_D$  was about 0.5  $\mu\text{M}$  (Figure 3.5, *panel A*). This finding implies that the interaction between T4 RNR and T4 TS was strengthened by an order of magnitude. This effect might be explained by proposing that ATP helps form a tight T4 RNR R1·R2 holoenzyme, which further increases the binding to T4 TS. In addition, in Figure 4.1, *panel A*, in which duplicate association profiles were plotted, fairly high repetition was observed, implying IAsys optical biosensor analysis is a reliable approach for the study of protein-protein interaction.

More nucleotides belonging to the allosteric modifiers of T4 aerobic ribonucleotide reductase (RNR) were tested upon RNR – thymidylate synthase interaction. Some of the association profiles are shown in Figure 4.2. Full results are shown in Table 4.1. To our surprise, CTP, dCTP, ADP and dADP showed similar stimulatory effects while GTP, dGTP, UTP and dTTP showed negative effects that weakened the interaction to some extent, which are completely opposite to the results reported by Hanson and Mathews (1994), namely, that GTP and dTTP increased T4 RNR R1·R2 association. The discrepancies suggest that protein-protein interactions in the T4 dNTP synthetase complex might be dynamic depending on different metabolic conditions.

#### **4.2 Nucleotide Effects upon Protein-Protein Interactions Involving Host-Encoded Enzymes**

Since both *E. coli* NDP kinase and adenylate kinase utilize ATP as phosphate donor to phosphorylate their substrates, it is of great interest to investigate whether ATP affects the protein-protein interactions involving these two host enzymes. ATP was seen to enhance to interactions of *E. coli* adenylate kinase (Figure 3.9, *panel A*), T4 aerobic ribonucleotide reductase (Figure 4.3) and T4 dCTPase/dUTPase (Figure 4.4, *panel B*) in solution with immobilized NDP kinase. However, ATP had no effect between T4 thymidylate synthase in solution with immobilized NDP kinase. An interesting observation came from the interaction between T4 dCMP deaminase in solution and immobilized NDP kinase as

shown in Figure 4.5. One mM hm-dCTP decreased the signal of interaction by 70%. We suggest that T4 dCMP deaminase, upon hm-dCTP binding, experiences a conformational change that does not favor association with the *E. coli* NDP kinase. However, 1 mM ATP was seen to restore their interaction before hm-dCTP was added, suggesting that ATP promotes the tetramerization in NDP kinase, which will be discussed in detail in Chapter 5. Further addition of 1 mM hm-dCTP still weakened some newly established association promoted by ATP, but only by about 10-20% of total signal (Figure 4.5). This finding further supports our proposal of ATP enhancement on the tetramerization of NDP kinase. Although dCTP pool disappears and is replaced by hm-dCTP pool *in vivo* after T4 infection, dCTP is considerably more effective as an activator *in vitro* (Mathews and Allen, 1983). It is not surprised that dCTP behaves very similar to hm-dCTP on the interaction between *E. coli* NDP kinase and T4 dCMP deaminase (Figure 4.6).

A very similar observation was obtained between T4 dCMP deaminase in solution and immobilized adenylate kinase (Figure 4.7). Hm-dCTP again acted as an inhibitor of the interaction between these two enzymes. However, the interaction was restored followed by addition of 1 mM ATP. It is known that adenylate kinase undergoes large conformational change upon ATP binding (Schulz *et al.*, 1990; Berry *et al.*, 1994; Dahnke and Tsai, 1994; Sinev *et al.*, 1996). We suggest that the conformational change upon ATP binding results in the enhancement of the association between *E. coli* adenylate kinase and T4 dCMP deaminase.

### **4.3 Protein-Protein Interactions Involving T4 Anaerobic Ribonucleotide Reductase Subunit (NrdD)**

Since T4 NrdD, a Class III anaerobic ribonucleotide reductase, is also allosterically regulated by nucleotide modifiers, we wondered whether ATP also affects its interactions with other proteins. In agreement with the proposal, Figure 3.12 shows that ATP enhanced the interaction of T4 NrdD in solution and immobilized NDP kinase.

We have observed that small molecules, especially ATP, enhance the interactions between proteins in the T4 dNTP synthetase complex. The intracellular concentration of ATP was determined to be in millimolar range (Mathews, 1972), suggesting that *in vivo* the protein-protein associations are even more significant under physiological conditions. Moreover, Hansen and Mathews (1994) in this laboratory observed the stimulatory effect of ATP upon T4 aerobic ribonucleotide reductase R1·R2 interactions. However, it is not clear whether ATP enhances the protein-protein interactions, in which *E. coli* NDP kinase is involved, through promoting the tetramerization of NDP kinase. This will be discussed in the next chapter.

**Table 4.1.** Nucleotide effects on interaction of T4 RNR to T4 TS immobilized on an IA sys carboxymethyl dextran (CMD) cuvette.

ATP	GTP	CTP	UTP	ADP	dUMP
+	-	+	-	+	-
dATP	dGTP	dCTP	dTTP	dADP	dTMP
+	-	+	-	+	-

**Note:** +, positive effect; -, negative effect.

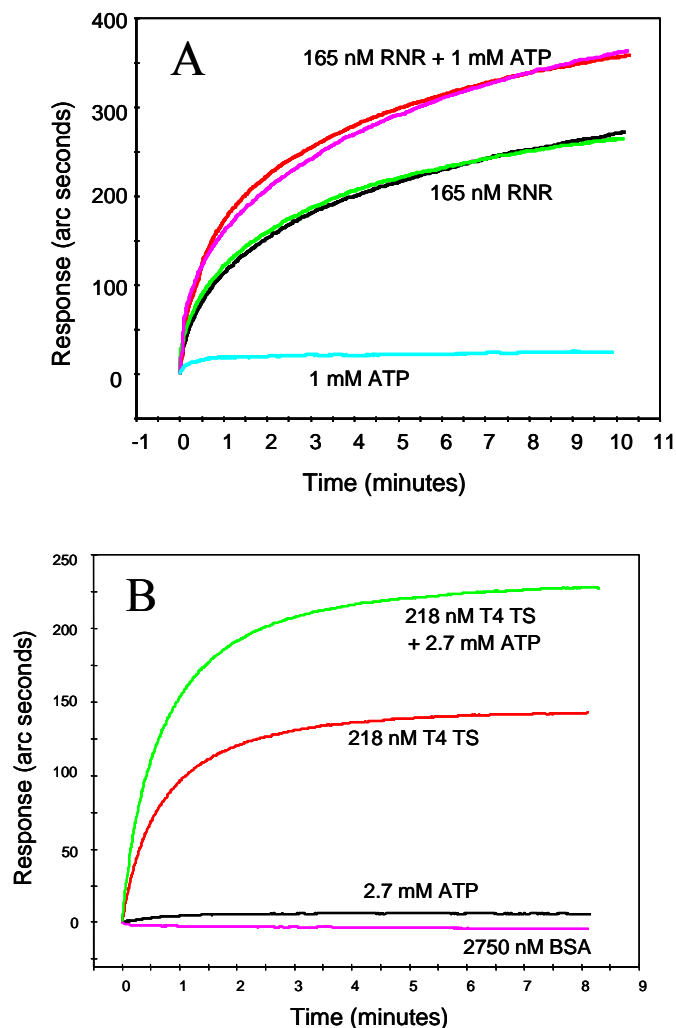


**Figure 4.1.** Interaction between T4 ribonucleotide reductase (RNR) and T4 thymidylate synthase (TS) and ATP effects on their interaction. **A**, T4 RNR in the solution interacts with immobilized T4 TS on an IAsys carboxylate cuvette. Note that duplicate binding profiles were plotted. Green and black curves show only T4 RNR was added into the solution; Red and purple curves show T4 RNR plus 1 mM ATP was added into the solution. **B**, T4 TS in the solution interacts with immobilized T4 RNR on an IAsys carboxylate cuvette. The concentrations of proteins and ATP are labeled by the curves. Running buffer was PBS/T. BSA depicts a negative control with bovine serum albumin. The figure was generated by using FASTplot program (Affinity Sensors).

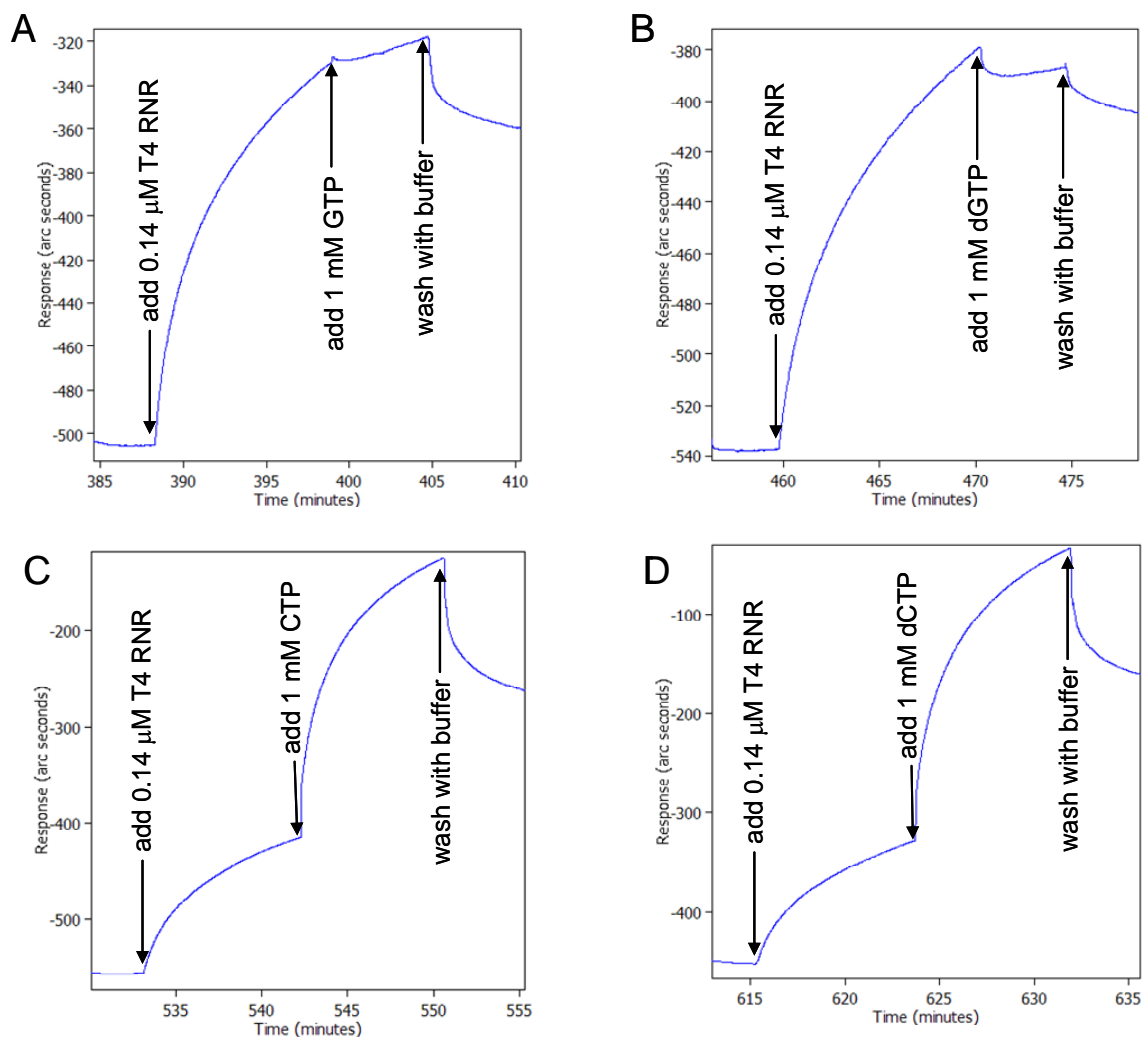


**Figure 4.2.** Nucleotide effects on interaction of T4 RNR to T4 TS immobilized on an IA sys carboxymethyl dextran (CMD) cuvette. A, GTP; B, dGTP; C, CTP; D, dCTP. All tested nucleotide effects are shown in Table 4.1.

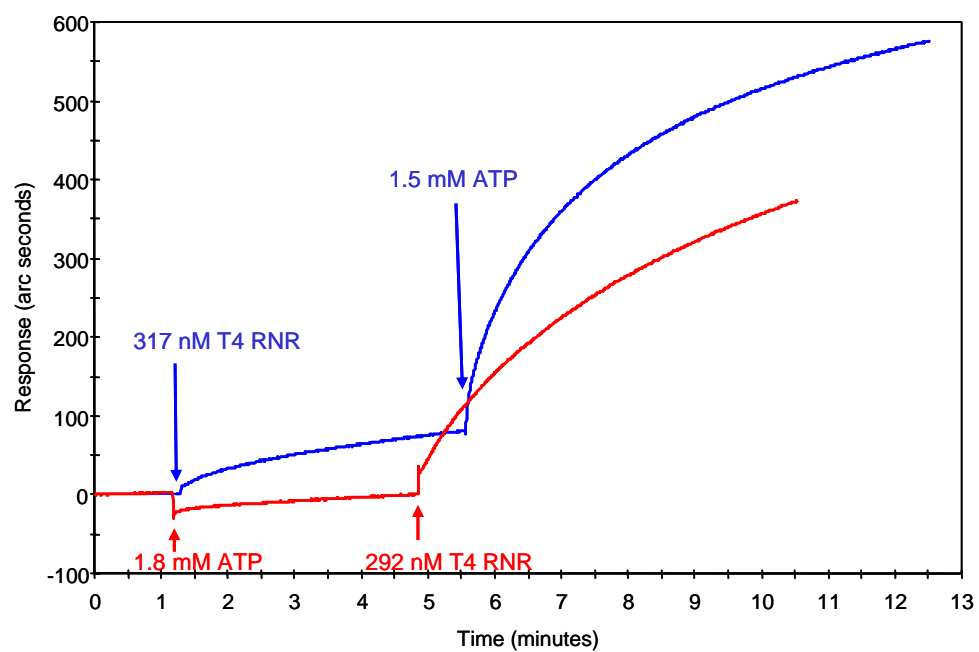


**Figure 4.3.** ATP enhances the association of T4 RNR to *E. coli* NDPK immobilized on IA sys carboxylate cuvette. Running buffer was KGMT.

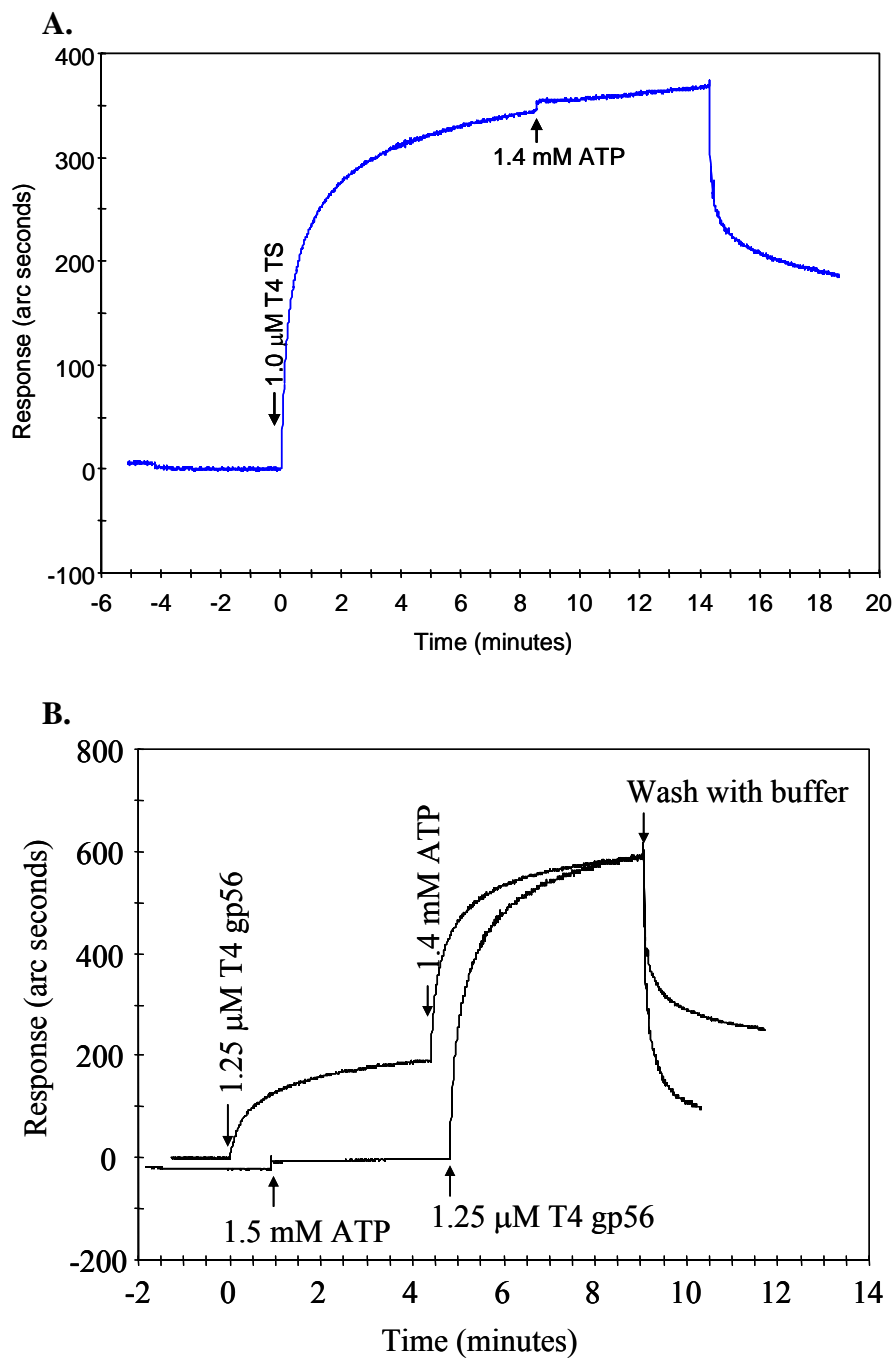


**Figure 4.4.** ATP effects on the association of T4 TS (A), or gp56 (B) to *E. coli* NDPK immobilized on an IAsys carboxylate cuvette. Running buffer was KGMT.

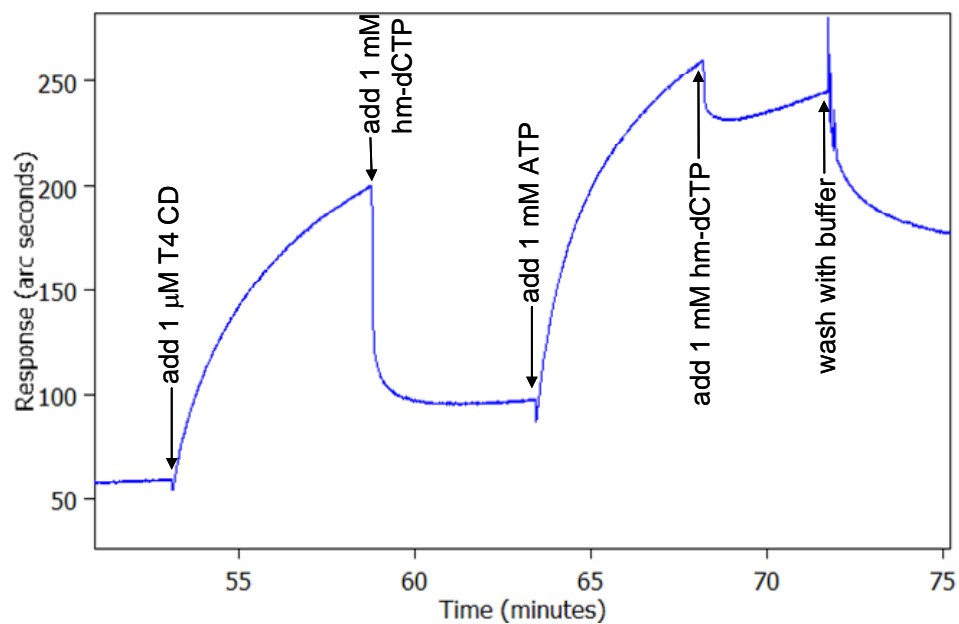


**Figure 4.5.** ATP and hm-dCTP effects on the association of T4 CD to *E. coli* NDPK immobilized on IAsys carboxylate cuvette. Running buffer was KGMT.

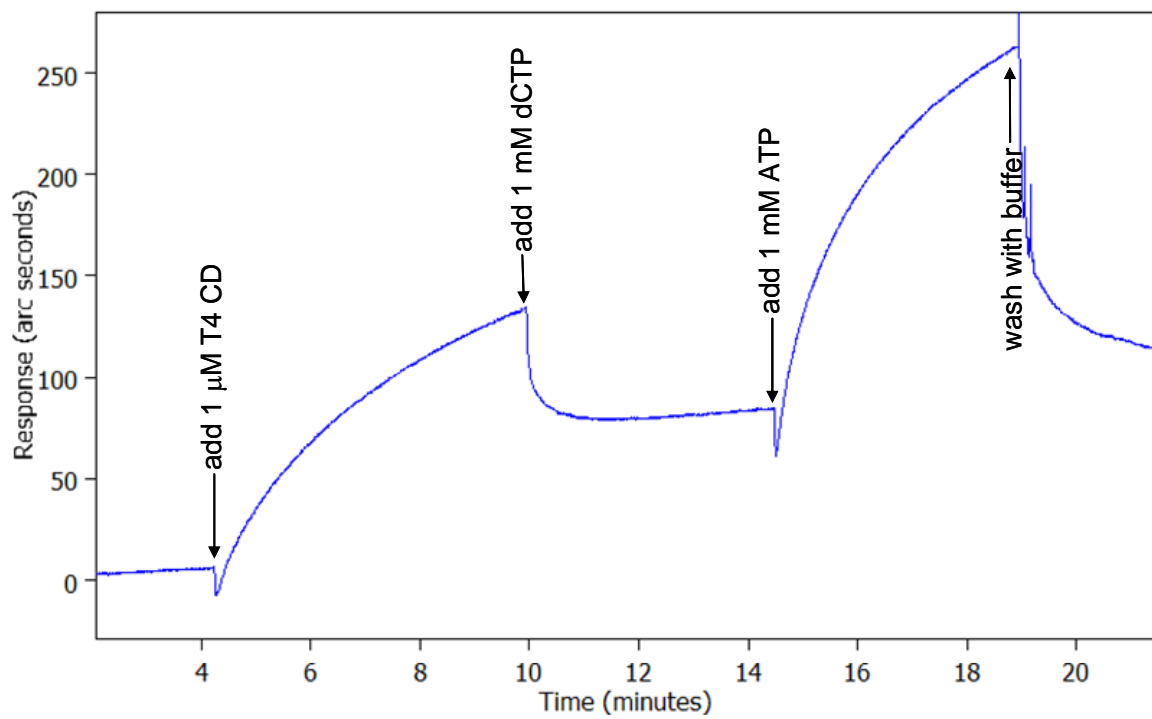


**Figure 4.6.** dCTP effect on the association of T4 CD to *E. coli* NDPK immobilized on IA sys carboxylate cuvette. Running buffer was KGMT.

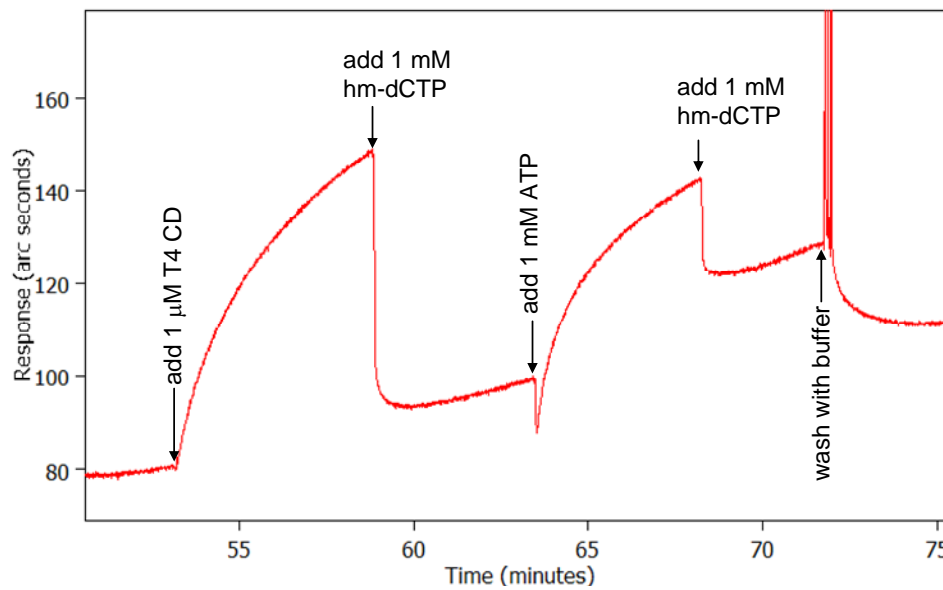


**Figure 4.7.** ATP and hm-dCTP effects on the association of T4 CD to *E. coli* ADK immobilized on IAsys carboxylate cuvette. Running buffer was KGMT.

## Chapter 5

### Tetramerization and Self-Association of *Escherichia coli* NDP Kinase

*E. coli* NDP kinase, catalyzing the last step of dNTP biosynthesis, is one of very few host-encoded enzymes involved in T4 dNTP or DNA synthesis. We have discovered that NDP kinase interacts with many of the proteins in the bacteriophage T4 dNTP synthetase complex (Wheeler *et al.*, 1996; Bernard *et al.*, 2000; Shen *et al.*, 2004; Kim, 2005; Kim *et al.*, 2005a; Kim *et al.*, 2005b; Shen *et al.*, 2006). Moreover, several of the protein-protein interactions are strengthened by nucleotides. Table 5.1 lists five T4 proteins and one *E. coli* protein whose affinity for NDP kinase is significantly strengthened by 1 to 1.5 mM ATP. There is some specificity to the effects we have observed; for example, 1 mM dADP strengthens the association between NDP kinase and T4 dihydrofolate reductase, while ATP has no evident effect upon this interaction (see Chapter 4) (Kim *et al.*, 2005a). These findings raised the possibility that intracellular nucleotides help to stabilize the dNTP synthetase complex *in vivo*, or to regulate its stability and hence, its ability to channel precursors to DNA. However, preliminary experiments involving sedimentation analysis of enzyme activities have not yet yielded evidence supporting this hypothesis. Moreover, in Chapter 4, in the study of interaction between *E. coli* NDP kinase and T4 dCMP deaminase, although hm-dCTP destroys their association first, the addition of 1 mM ATP later can “recover” the original interaction (Figure 4.5). I wondered, however, whether nucleotides might be exerting their effects through influence upon the quaternary structure of NDP kinase. The *E. coli* enzyme, like other microbial NDP kinases, is a

homotetramer with a subunit molecular mass of 15,332 Da, while the eukaryotic enzymes, with high levels of sequence and structure conservation, form homohexamers. In studies on the *Dictyostelium discoideum* enzyme, Mesnildrey *et al* (1998) reported that a mutant form of this enzyme, P100S, is a homodimer in the absence of ATP, but that 0.5 mM ATP drives formation of the familiar homohexamer. Giartosio *et al.* (1996) found that the tetrameric *E. coli* NDP kinase behaves more similar to the P105G mutant than to the wild-type NDP kinase from *Dictyostelium*, and that the thermostability of *E. coli* NDP kinase and the P105G mutant *Dictyostelium* enzyme was enhanced in the presence of 1 mM ADP. An attempt to test the ATP enhancement on self-association of *E. coli* NDP kinase was carried out in a non-denaturing gel electrophoresis experiment by JuHyun Kim in our laboratory. However, he reported that, in the presence of 1 mM ATP, 1 mM ADP or 1 mM AMP-PNP, only a trace amount of tetramer was detected by western blotting (Kim, 2005). In the study of this dissertation, three new approaches were used to determine whether ATP similarly promotes oligomerization of the *E. coli* enzyme.

### **5.1 Self-Association of *E. coli* NDP Kinase Detected by Optical Biosensing**

I first investigated *E. coli* NDP kinase – NDP kinase interaction on an IAsys optical biosensor. Figure 5.1 shows that 1 mM ATP was seen to dramatically promote the self-association of NDP kinase, no matter whether NDP kinase or ATP was added to the solution first. Although the interaction was enhanced substantially when ATP was added

following the addition of NDP kinase, the strength of enhancement – both the binding rate and the amount of NDP kinase bound to the surface – was lower than that in the opposite order of addition. This can be explained by proposing that NDP kinase immobilized on the surface makes some conformational changes upon ATP binding and thus facilitates the association with NDP kinase in the solution. Since the self-association of NDP kinase is strong, the entire surface mostly has already been covered by NDP kinase which is added first and it is difficult for ATP to bind to NDP kinase immobilized on the surface. Thus, mostly NDP kinase in the solution binds to ATP. Resonant Mirror technology has the characteristics that the closer and the greater amount of proteins that locate to the sensing layer, the higher the signal. Therefore, the protein density close to the sensing layer when ATP is added first is higher than that when NDP kinase is added first.

I further quantitatively investigated the strength of NDP kinase self-association in the absence or presence of ATP. Figure 5.2 shows the equilibrium dissociation constant ( $K_D$ ) determination in two experiments in which NDP kinase associates with itself. In Figure 5.2 *panel A*, in the absence of ATP, applying several different concentrations of NDP kinase in the solution,  $K_D$  was determined to be 0.1  $\mu\text{M}$ . In *panel B*, in the presence of 1 mM ATP,  $K_D$  yielded a value of 0.007  $\mu\text{M}$ , which is approximately one-fourteenth of the previous value in the absence of ATP. This finding implies that ATP can promote the self-association of NDP kinase by about an order of magnitude of affinity.

## 5.2 Tetramerization of *E. coli* NDP Kinase Detected by Analytical Ultracentrifugation

A quantitative analysis was then carried out by sedimentation equilibrium measurements. When 25  $\mu\text{M}$  NDP kinase was centrifuged to equilibrium at 16,500 rpm in the absence of added nucleotides, the profile showed an average molecular mass of 52,000 Da, suggesting a mixture of dimers (30,664 Da) and tetramers (61,328 Da). Further analysis with UltraScan software (Demeler, 2005) reveals that there were 29.3% of dimers and 70.7% of tetramer. When the run was carried out in the presence of 0.5 mM ATP or 0.5 mM ADP, the evident molecular weights were 62,260 and 62,010, respectively, suggesting that in the presence of nucleotide the enzyme was entirely in the tetrameric state.

To determine the dependence of protein oligomerization upon protein concentration, I carried out sedimentation equilibrium measurements at three different concentrations – 0.8  $\mu\text{M}$ , 4.65  $\mu\text{M}$ , and 32.6  $\mu\text{M}$ , based upon the tetramer – and at three different rotor speeds, namely, 15,000, 18,000 and 24,000 rpm. The data were analyzed with UltraScan software (Demeler, 2005) to determine the percent of total protein in dimeric and tetrameric forms at each concentration and rotor speed. Figure 5.3 was generated from a global fitting algorithm. The figure reveals that the protein is half dimer and half tetramer at 0.8  $\mu\text{M}$ , which therefore represents the equilibrium dissociation constant for tetramerization. The results at higher protein concentrations, i.e., 4.65  $\mu\text{M}$  and 32.6  $\mu\text{M}$ ,

verify that there is no association above the tetramer. Figure 5.4 was a statistics of the fit generated by a Monte Carlo algorithm using the above dissociation constant. The figure shows a typical Gaussian distribution of data points centered at the given value of dissociation constant, suggesting that the data obtained in the experiment are reliable and in good shape. As noted above, either ADP or ATP at 0.5 mM – within the physiological concentration range—drives the enzyme entirely into the tetrameric state. From the specific activity of NDP kinase in a crude *E. coli* extract and that of the highly purified enzyme (0.4 and 2400  $\mu\text{mol}/\text{min}/\text{mg}$  protein, respectively (Ray, 1992)), it can be estimated that an *E. coli* cell contains 800 molecules of the enzyme. From the volume of an *E. coli* cell (Mathews, 1972), the intracellular enzyme concentration can be estimated at 1.5–2  $\mu\text{M}$ . Thus, it is likely that the nucleotide concentration within the cell is a determinant of the enzyme's quaternary structure *in vivo*. Whether this parameter in turn regulates the intracellular interactions of the enzyme with other proteins remains to be seen.

### **5.3 Self-Association of *E. coli* NDP Kinase Detected by Fluorescence Spectroscopy**

As shown in Figure 5.5, the fluorescence properties of *E. coli* NDP kinase change upon nucleotide addition of increasing concentrations. This figure shows that the intrinsic fluorescence of NDP kinase decreases when the concentration of ATP added was increasing, suggesting that upon ATP binding fluorophore are buried more. This finding implies that the self-association property of NDP kinase is enhanced by ATP.

#### **5.4 Self-Association of Other Proteins in the T4 dNTP Synthetase Complex**

From IAsys data, *E. coli* adenylate kinase (Figure 5.6) and T4 aerobic ribonucleotide reductase (Figure 5.7) show self-association property. In Chapter 4, ATP was also observed to “recover” the interaction between *E. coli* adenylate kinase and T4 dCMP deaminase, which was decreased by hm-dCTP first. In agreement with the observation, ATP was seen to enhance the self-association of *E. coli* adenylate kinase (Figure 5.6).

In the next chapter, I describe a different method to study the protein-protein interactions by assaying the kinetic coupling of a partially reconstituted complex using purified proteins.

**Table 5.1.** Interactions involving *E. coli* NDP kinase and T4-encoded proteins plus *E. coli* adenylate kinase.

<b>Interacting protein</b>	<b>ATP stimulation</b>	<b>Interaction shown by</b>	<b>Reference</b>
DNA polymerase		NDE	(Bernard <i>et al.</i> , 2000)
Aerobic ribonucleotide reductase	Yes	NDE, FLU, BIO, GST, IP	(Bernard <i>et al.</i> , 2000; Shen <i>et al.</i> , 2004)
Anaerobic ribonucleotide reductase	Yes	BIO, FLU	(Shen <i>et al.</i> , 2004); This dissertation
Thymidylate synthase	No	FLU, BIO	(Shen <i>et al.</i> , 2004)
Dihydrofolate reductase	No	GST	(Kim <i>et al.</i> , 2005a)
dCTPase-dUTPase	Yes	BIO, FLU	(Shen <i>et al.</i> , 2004)
dCMP deaminase	Yes	BIO	This dissertation
dCMP hydroxymethylase		GST, IP	(Shen <i>et al.</i> , 2004)
ssDNA-binding protein (gp32)	Yes	BIO, GST	(Shen <i>et al.</i> , 2004; Kim <i>et al.</i> , 2005b)
<i>E. coli</i> adenylate kinase	Yes	BIO	This dissertation

Techniques used to demonstrate interactions include native gel electrophoresis (NDE), optical biosensor analysis (BIO), glutathione-S-transferase pulldown (GST), immunoprecipitation (IP), and fluorescence spectroscopy (FLU). Two interactions have been found not to be stimulated by ATP.

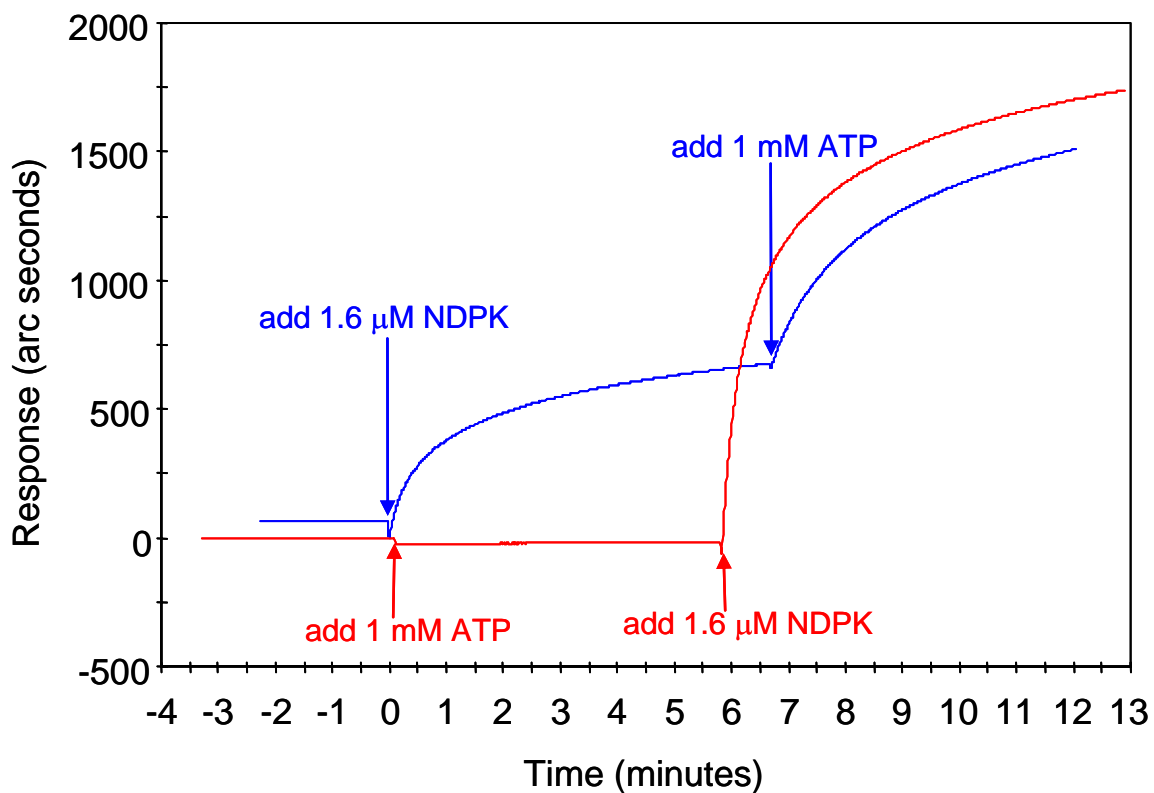


**Figure 5.1.** Association of *E. coli* NDPK to *E. coli* NDPK immobilized on an IAsys carboxylate cuvette. Approximately 7.2 ng of NDP kinase was immobilized on a carboxylate cuvette via EDC/NHS. Baseline was reached by KGMT buffer. In one experiment, as shown, 1.6  $\mu$ M NDP kinase was added at 52 min to buffer, followed 7 min later by addition of 1 mM ATP. In a following experiment, ATP was added first, followed several minutes later by NDP kinase. The graph was generated by using FASTplot (Affinity Sensors).

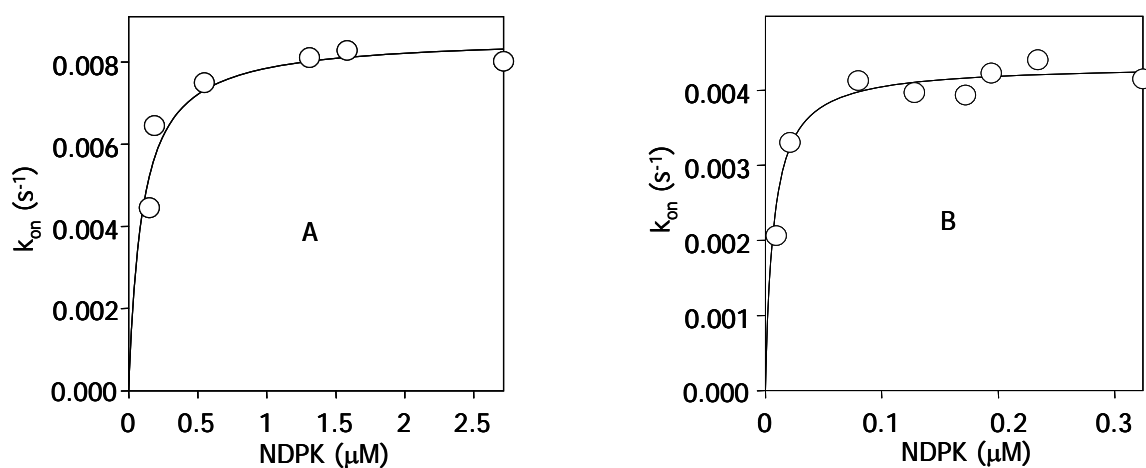


**Fig. 5.2.** Quantitative analysis of NDP kinase-NDP kinase interactions in the absence or presence of ATP. Baseline was reached by KGMT buffer. Binding reactions were conducted by adding NDP kinase at indicated concentrations to the cuvette in the absence of ATP (**A**) or in the presence of 1 mM ATP (**B**). For both experiments, apparent on-rate constants for binding ( $k_{on}$ ) were plotted against the concentration of the protein in solution.

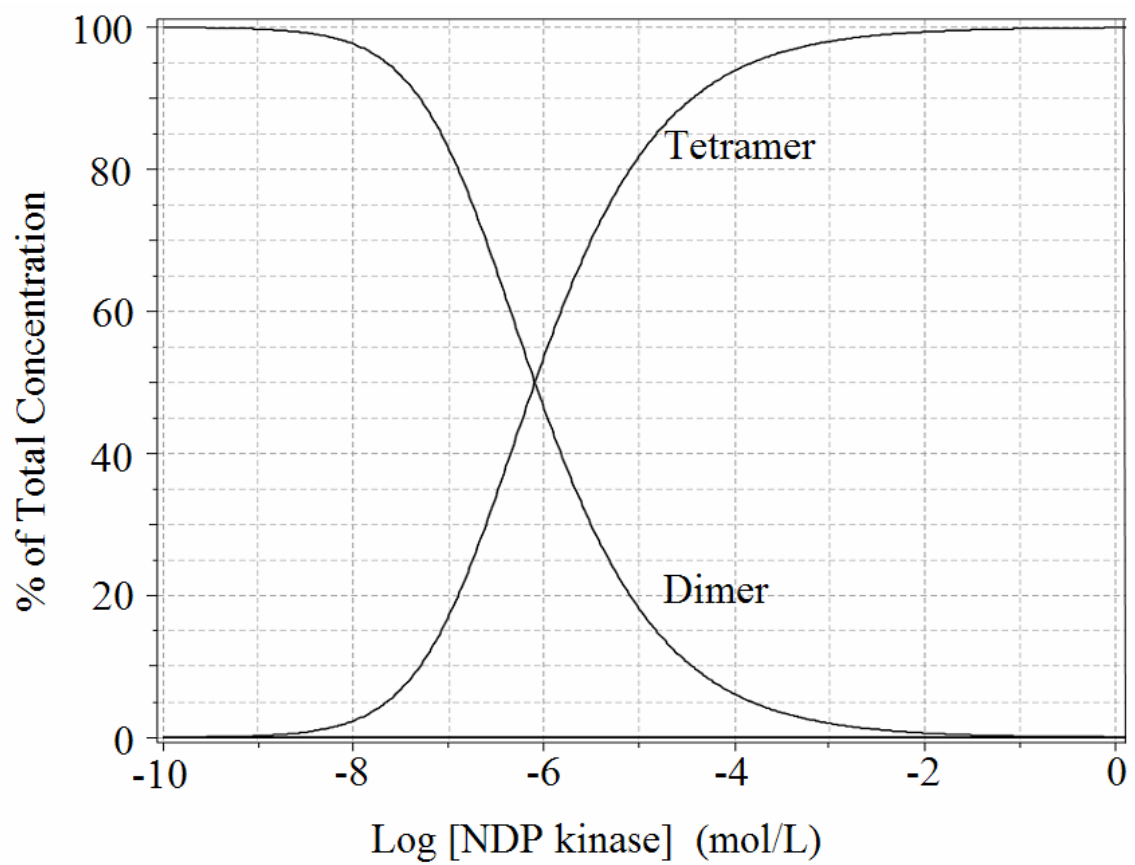


**Figure 5.3.** NDP kinase quaternary structure as a function of protein concentration generated by global fitting analysis.

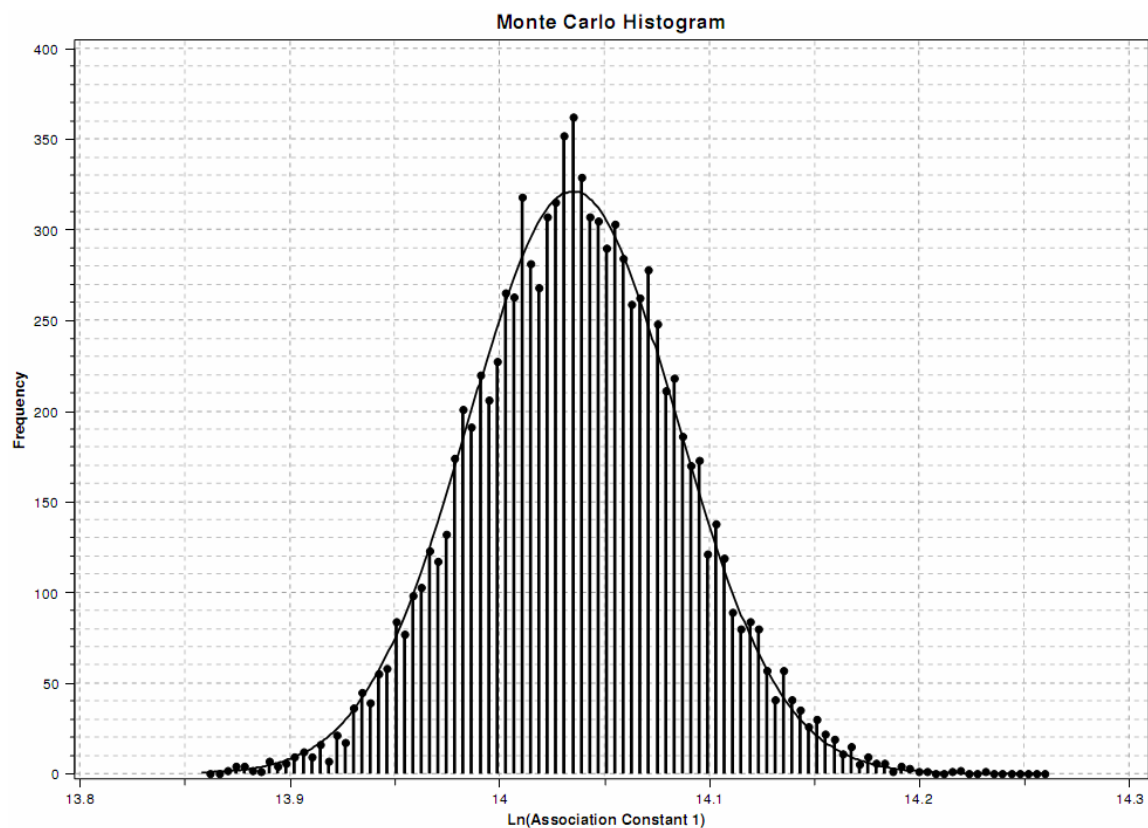


**Figure 5.4.** The apparent equilibrium association constant determination between dimer-tetramer species in *E. coli* NDP kinase generated by 10,000 iterations of Monte Carlo analysis.

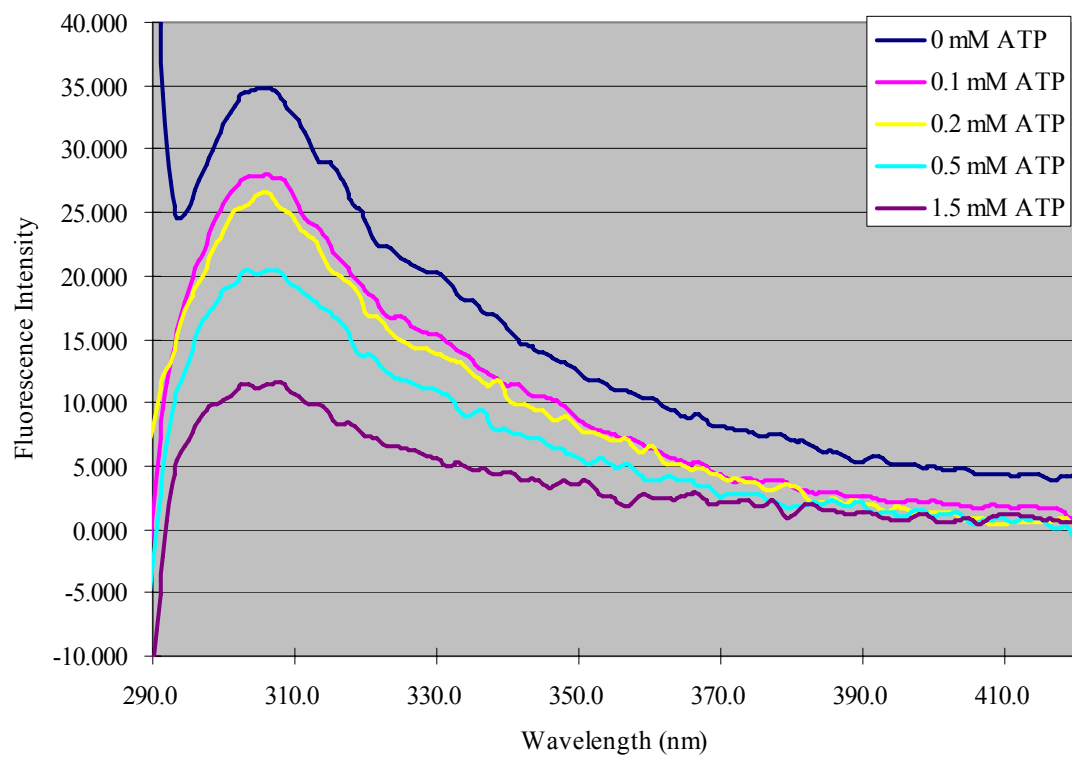


**Figure 5.5.** Effect of ATP titration to *E. coli* NDP kinase on fluorescence spectra. ATP at 0, 0.1, 0.2, 0.5 or 1.5 mM was mixed with NDP kinase at 0.5  $\mu$ M. Spectra were obtained with excitation at 285 nm. All the spectra were adjusted with the spectra of ATP alone at corresponding concentrations.

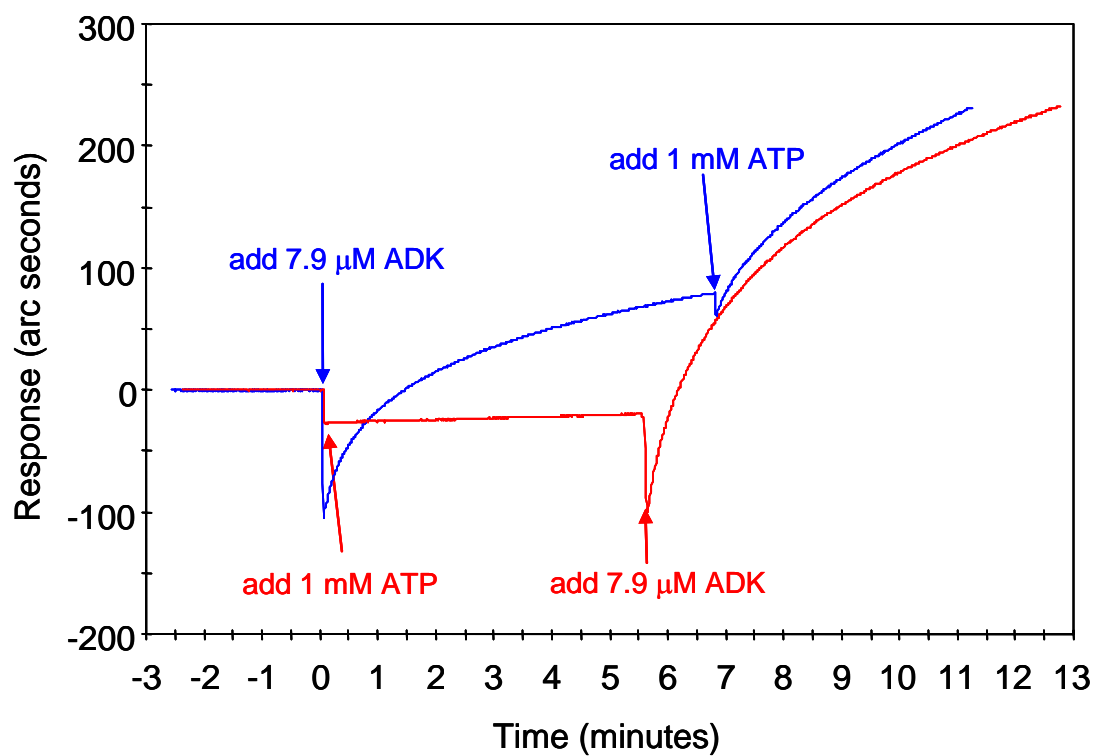


**Figure 5.6.** Self-association of *E. coli* adenylate kinase. Interaction of ADK in solution with immobilized ADK. The graph was generated by using FASTplot (Affinity Sensors). Note that the big drop of signal after ADK was added is because ADK was in low-salt buffer, which is also called bulk effect.

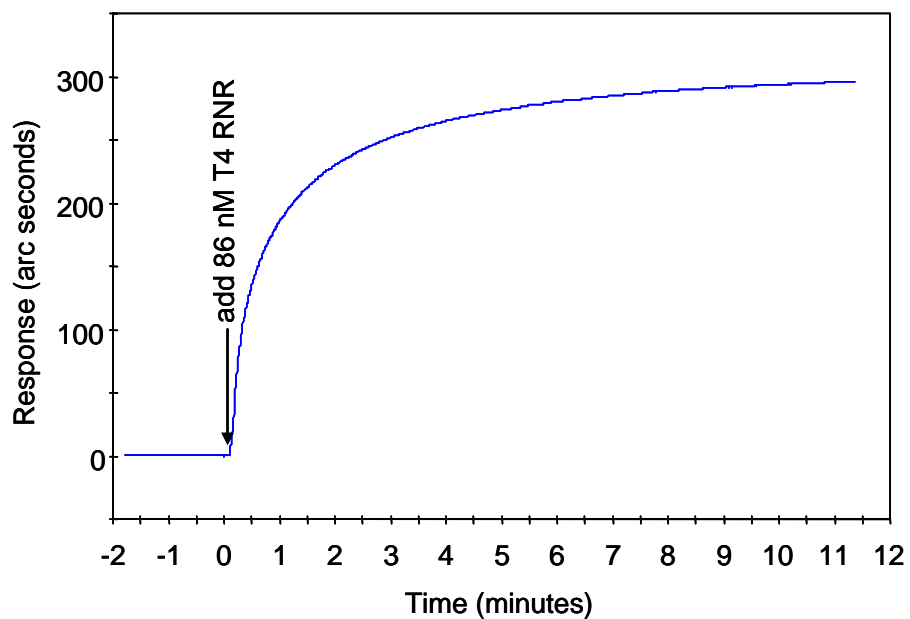


**Figure 5.7.** Self-association of T4 aerobic ribonucleotide reductase. Interaction of T4 RNR in solution with immobilized T4 RNR. The graph was generated by using FASTplot (Affinity Sensors).

## Chapter 6

### **Kinetic Coupling Assay for a Three-Step dCTP→dCMP→dUMP→dTMP Pathway**

Several lines of evidence supporting the T4 dNTP synthetase complex model had been obtained with kinetic coupling assays in our laboratory (Reddy *et al.*, 1977; Allen *et al.*, 1980; Thylén and Mathews, 1989). Kinetic coupling or substrate channeling was observed in a multi-step pathway through partially purified complex from *E. coli* cells infected with T4 phage. In the complex, enzymes are assumed to be kinetically coupled to one another and physically juxtaposed, kinetic coupling reduces the transient time for catalysis of a multi-step reaction pathway without diffusing intermediates into outside of the complex. Evidence cited above supported this assumption. Enzyme aggregation contributes to compartmentation of metabolites without physical barriers and greatly reduces the volume into which an intermediate can diffuse before reaching the next enzyme. That is, the product from the first enzyme can be channeled to the second enzyme site as its substrate, and obviously saturation is achieved at the second enzyme site. Therefore, time is significantly saved without the need to accumulate saturating levels of the substrate for the second enzyme throughout the bulk phase where enzymes are not complexed.

### **6.1 Kinetic Coupling Assay for a Three-Step dCTP→dCMP→dUMP→dTMP Pathway**

Previous kinetic coupling assays were conducted using a partially purified complex from an extract of *E. coli* cells infected with T4 phage. However, it would be interesting to investigate whether kinetic coupling or channeling behavior occurs through a partially reconstituted complex from purified proteins. The significance of this design is to seek the possibility of reconstituting the whole complex using purified enzymes and also to develop a system for analysis of channeling at the structural level.

A three-step pathway of dCTP→dCMP→ dUMP→dTMP was tested to measure the kinetic coupling. The particular pathway is sequentially catalyzed by T4 dCTPase-dUTPase (gp56), T4 dCMP deaminase (CD) and T4 thymidylate synthase (TS), respectively (Figure 2.3). All three purified enzymes at 0.05 μM each were mixed at 1:1:1 molar ratio. dCTP was the initial substrate for this pathway. Hm-dCTP, which acts as an essential activator for dCMP deaminase, was also added. The assay was readily monitored by the absorbance at 338 nm. In fact,  $A_{338}$  monitors the final reaction – thymidylate synthase – by quantitating oxidation of  $\text{CH}_2=\text{THF}$  to DHF. Figure 6.1 shows that dTMP production reached its highest rate within 15 seconds, at least no later than the time that the first data point detected by the spectrophotometer. In comparison, a computer program was carried out to simulate the three-step pathway sequentially catalyzed by three uncomplexed enzymes, where only substrate diffusion occurred without substrate channeling. All these three enzymes exhibit Michaelis-Menten kinetics

with respect to their deoxyribonucleotide substrates. The Michaelis constants ( $K_M$ ) for dCTPase and dCMP deaminase are 40  $\mu\text{M}$  and 80  $\mu\text{M}$ , respectively (Mathews, unpublished data).  $K_M$  for thymidylate synthase is 20  $\mu\text{M}$  (Reddy *et al.*, 1977). Values for  $V_{\max}$  were calculated from  $k_{cat}$  and enzyme concentrations. Values for  $k_{cat}$  were 7800  $\text{min}^{-1}$ , 466  $\text{s}^{-1}$  and 11.8  $\text{s}^{-1}$ , for gp56 (Price and Warner, 1969), CD (Keefe *et al.*, 2000) and TS (LaPat-Polasko *et al.*, 1990), respectively. The equations describing the unassociated system are as follows:

$$\begin{aligned}\frac{d[\text{dCTP}]}{dt} &= -\frac{V_{\max}^{\text{gp56}}[\text{dCTP}]}{K_M^{\text{gp56}} + [\text{dCTP}]} \\ \frac{d[\text{dCMP}]}{dt} &= \frac{V_{\max}^{\text{gp56}}[\text{dCTP}]}{K_M^{\text{gp56}} + [\text{dCTP}]} - \frac{V_{\max}^{\text{CD}}[\text{dCMP}]}{K_M^{\text{CD}} + [\text{dCMP}]} \\ \frac{d[\text{dUMP}]}{dt} &= \frac{V_{\max}^{\text{CD}}[\text{dCMP}]}{K_M^{\text{CD}} + [\text{dCMP}]} - \frac{V_{\max}^{\text{TS}}[\text{dUMP}]}{K_M^{\text{TS}} + [\text{dUMP}]} \\ \frac{d[\text{dTMP}]}{dt} &= \frac{V_{\max}^{\text{TS}}[\text{dUMP}]}{K_M^{\text{TS}} + [\text{dUMP}]}\end{aligned}$$

Figure 6.1 shows the simulated curves calculated by a program in Perl (see source code in APPENDIX C). The unassociated enzymes needed about 2 minutes to reach the maximal rate of dTMP production. Even when the first intermediate in this pathway, dCMP, was increased by 50-fold, the lag was almost not altered. Therefore, the partial complex reconstituted with purified enzymes apparently behaves *in vitro* as postulated for substrate channeling as *in vivo* of the T4 dNTP synthetase complex. This was realized by

saving time significantly without the need of accumulating the saturating levels of intermediates for the next enzyme in the sequence through the bulk phase.

## **6.2 Effects on Kinetic Coupling by Other Proteins That Are Not Catalytically Involved in the Pathway**

Thylén and Mathews (1989) in this laboratory assayed the same three-step  $dCTP \rightarrow dCMP \rightarrow dUMP \rightarrow dTMP$  pathway with a partially purified multiple-enzyme complex from an extract of *E. coli* cells infected by wild type or by gene 42 *amber* mutants of T4 phage, purified by a gel filtration chromatography. Although T4 dCMP hydroxymethylase (gp42) is not catalytically involved in this three-step pathway, the truncation of C-terminal region of gp42 abolished the kinetic coupling behavior and destabilized the complex such that the activities assayed no longer coeluted from a gel filtration column. Interestingly, the mutants of almost full length of gp42 gave normal kinetic coupling in this pathway. This observation may appear to be at variance with the findings of Thylén and Mathews (1989), who observed a requirement for gp42 in the partially isolated multienzyme complex, in order for kinetic coupling to be seen in that system. However, they did not assay the individual activities of these three enzymes. This evident discrepancy might be explained if the gene 42 *amber* mutation might have altered expression of one or several of these three enzymes and then cause disruption of the complex.

For the mixture of three purified enzymes described in section 6.1, a number of proteins were tested to investigate whether they affect the behavior of kinetic coupling for this particular pathway. Figure 6.2 shows that *E. coli* NDP kinase and T4 gp32 slightly increased the initial steady-state rate of dTMP production by 10-17%. ATP, however, did not alter the rate at all. This might be because ATP is not a substrate for any of these three enzymes, nor is it an allosteric effector for dCMP deaminase.

Although both NDP kinase and gp32 demonstrated positive effects on kinetic coupling for this pathway, we wondered whether adding enzymes more closely related to the sequence under study would yield more striking results, similar to the effect of gp42 on the assay in cell-free extract, in which highly truncated gp42 significantly reduced the kinetic coupling, implying that gp42 affects the kinetic behavior structurally but not functionally (Thylén and Mathews, 1989). We also wondered whether some other proteins besides gp42 would behave in a similar way in this assay. We then conducted a similar experiment shown in Figure 6.3, in which either GST-fusion T4 dCMP hydroxymethylase (gp42), T4 dihydrofolate reductase (DHF reductase or DHFR), T4 aerobic ribonucleotide reductase (RNR) or *E. coli* adenylate kinase (ADK) was added to the coupling assay reaction individually one at a time. Figure 6.3 shows that the steady-state rates of dTMP production were increased by 32%, 54% and 55% by the addition of ADK, RNR and gp42, respectively. Gp42's effect on the coupling agrees with Thylén and Mathews' findings (1989) and suggest that the effects seen in this *in vitro* system are biologically significant. The strongest effect observed resulted from the addition of DHF

reductase, which almost doubled the rate (increased by 92% relative to the original rate). This might be because DHF reductase is closely related to thymidylate synthase kinetically and functionally, and improves the supply of  $\text{CH}_2=\text{THF}$  for conversion from dUMP to dTMP by the enzyme. Although other proteins mentioned above are not functionally associated with these enzymes apparently, they might facilitate the formation of the partial complex or structurally form a bigger yet tighter partial complex. All these findings suggest that the proteins in the T4 dNTP synthetase complex positively cooperate to associate with each other and thus stabilize the complex. The possible interpretations are discussed further in Chapter 7.

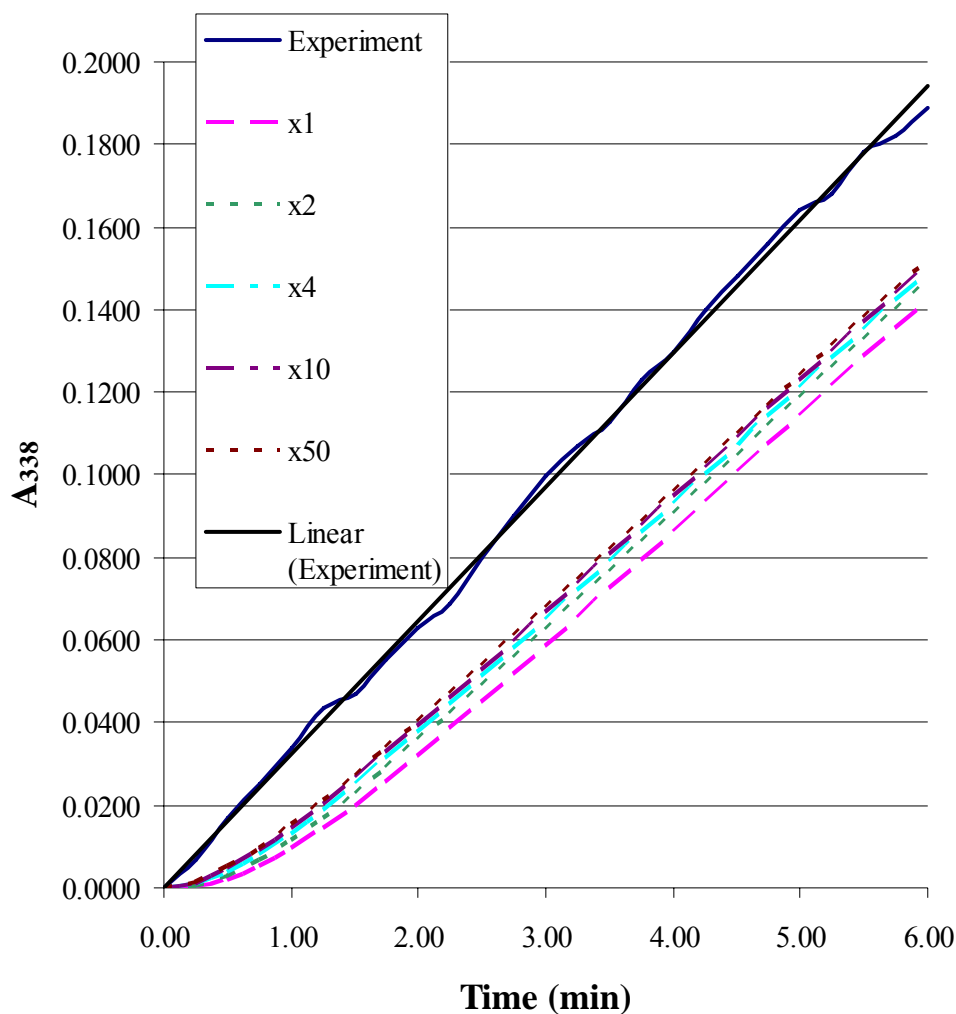


**Figure 6.1.** Kinetic coupling assay for the three-step  $dCTP \rightarrow dCMP \rightarrow dUMP \rightarrow dTMP$  pathway sequentially catalyzed by  $dCTPase/dUTPase$ ,  $dCMP$  deaminase and thymidylate synthase. Solid curve is plotted from the experimental data, along with which a linear regression line is also plotted. All the dashed curves are plotted from computer simulation data, which were calculated assuming that no substrate channeling occurred. The concentration of the first intermediate,  $dCMP$ , was increased by factors of 2, 4, 10 and 50 for the simulation, which indicated as x2, x4, x10 and x50 (x1 means no increase of  $dCMP$  concentration). The calculated concentrations of  $dCTP$ ,  $dCMP$ ,  $dUMP$  and  $dTMP$  are listed in Figure C.1 in Appendix C.

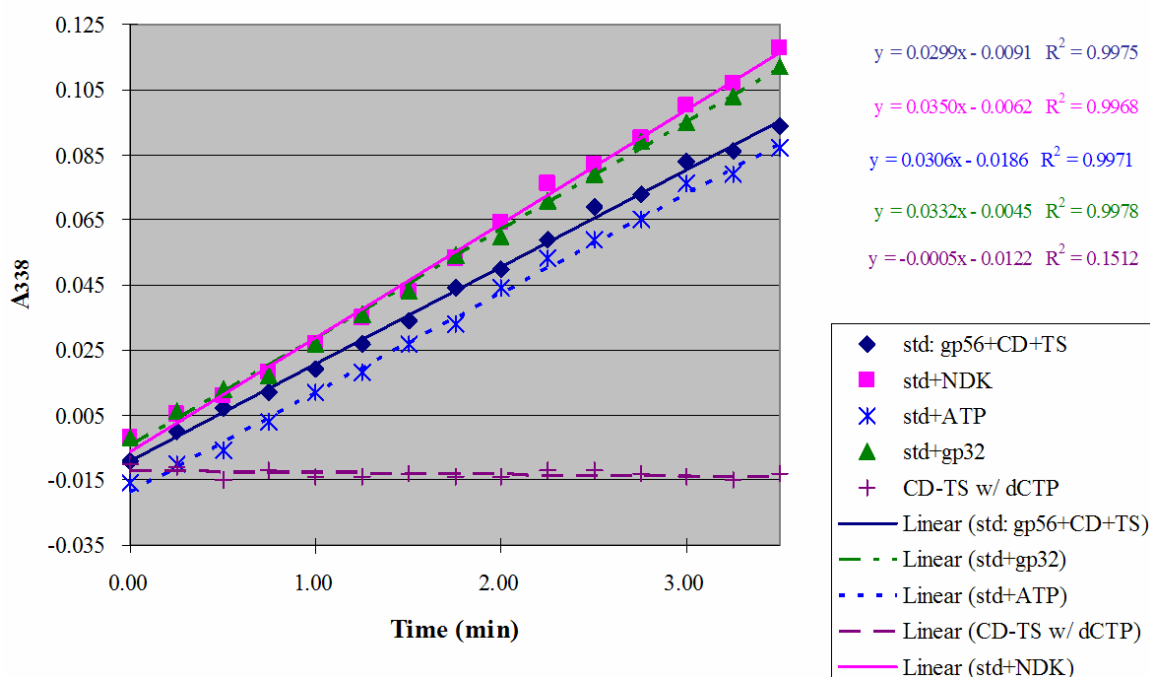


**Figure 6.2.** Effects on kinetic coupling by enzymes that do not catalytically participate in the three-step  $dCTP \rightarrow dCMP \rightarrow dUMP \rightarrow dTMP$  pathway – I. The standard reaction (std) sequentially catalyzed by dCTPase/dUTPase, dCMP deaminase and thymidylate synthase. NDK, *E. coli* NDP kinase; gp32, T4 ssDNA binding protein; CD-TS w/ dCTP, as a negative control, represents that only dCMP deaminase and thymidylate synthase were added to the reaction, but dCTP was still used as the initial substrate. Linear regression curves are plotted along with their corresponding data points.

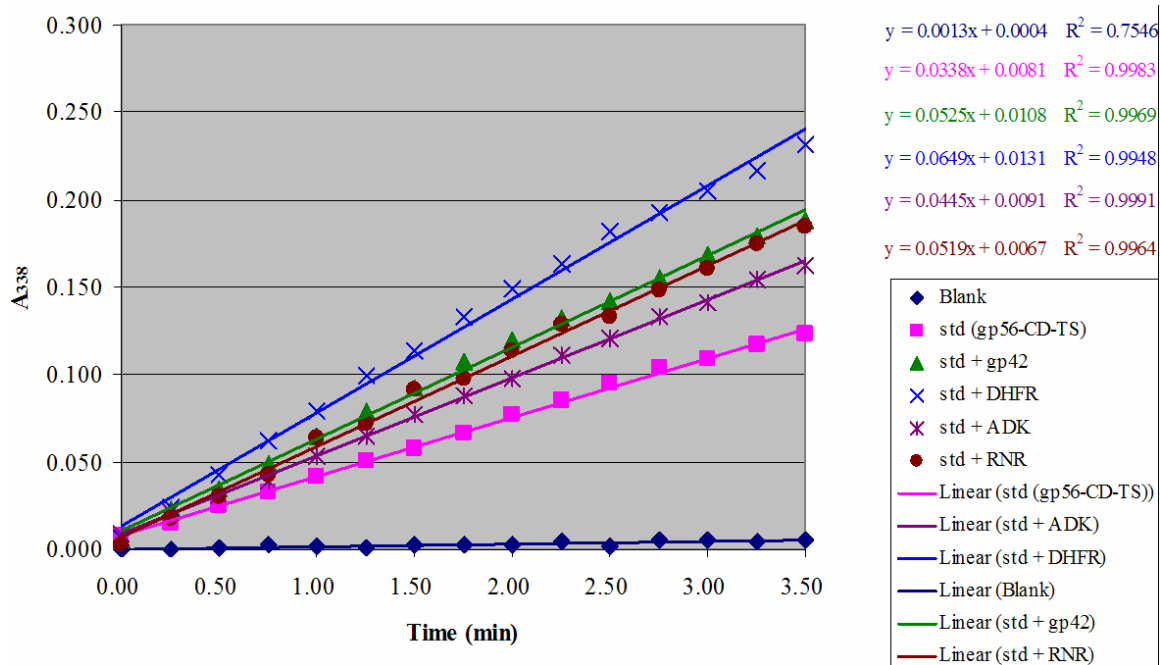


**Figure 6.3.** Effects on kinetic coupling by enzymes that do not catalytically participate in the three-step  $dCTP \rightarrow dCMP \rightarrow dUMP \rightarrow dTMP$  pathway – II. The standard reaction (std) sequentially catalyzed by dCTPase/dUTPase, dCMP deaminase and thymidylate synthase. RNR, T4 aerobic ribonucleotide reductase; gp42, a GST-fusion dCMP hydroxymethylase; DHFR, dihydrofolate reductase; ADK, *E. coli* adenylate kinase. Linear regression curves are plotted along with their corresponding data points. Blank, as a negative control, had the same reaction but no substrate – dCTP – was added.

## Chapter 7

### Discussion and Conclusions

The enzymes of dNTP biosynthesis in *E. coli* host cells infected by T4 phage associate to form a multienzyme complex, which is called the T4 dNTP synthetase complex (Tomich *et al.*, 1974; Reddy *et al.*, 1977; Mathews and Allen, 1983; Mathews *et al.*, 1993; Mathews, 1993a; Greenberg *et al.*, 1994). The complex facilitates the flow of precursors *en route* to dNTPs and their subsequent flow into DNA, to sustain the rapid DNA synthesis rate per infected cell that is up to 10-fold higher than that of the uninfected cell (Mathews, 1972; Mathews and Sinha, 1982; Mathews and Allen, 1983). Study of protein-protein interactions helps one to understand how the enzymes in the complex are organized and how they are coordinated to function efficiently. In this study, several new approaches, namely, IAsys optical biosensor analysis, fluorescence spectroscopy and analytical ultracentrifugation have been employed to investigate protein associations in the complex.

#### 7.1 Direct Protein-Protein Interactions in the T4 dNTP Synthesis Complex

By use of those new approaches, a number of direct protein-protein interactions among those enzymes in the complex were detected. The detailed direct associations are listed in Table 7.1 and an interactome (Figure 7.1) is concluded along with previous data from this

laboratory. In Table 7.1, previously demonstrated or indicated interactions by other methods are also listed for comparison, most of which represent indirect evidence, incapable of identifying direct associations. Those newly observed direct associations involved not only T4-encoded proteins, but also two host-encoded enzymes, namely, *E. coli* NDP kinase and *E. coli* adenylate kinase. Quantitative analysis of some of the above direct associations from IAsys data show that their apparent equilibrium dissociation constants fall into micromolar range as listed in Table 7.1 too. The intracellular concentrations of some proteins were estimated to be in the comparable concentrations, suggesting that those protein-protein interactions are significant *in vivo* (Shen *et al.*, 2004; Kim *et al.*, 2005a).

In addition, direct interactions between T4 single-strand DNA binding protein (gp32) and T4 aerobic ribonucleotide reductase, T4 thymidylate synthase or *E. coli* NDP kinase observed in this research suggest a linkage between the dNTP synthetase complex and DNA replication machinery. It is also in agreement with previous findings in this laboratory, supporting the model that gp32 acts as an organizing factor for the T4 dNTP synthetase complex at DNA replications sites (Wheeler *et al.*, 1996; Kim, 2005; Kim *et al.*, 2005b).

Although a large number of individual direct protein-protein interactions in pairs were detected in this study, some protein-protein pairs remain to be tested, especially associations involving T4 dCMP hydroxymethylase (gp42) and T4 dNMP kinase (gp1).

Fortunately, direct protein-protein interactions in the complex involving the above two enzymes were partially complemented by JuHyun Kim's work in this laboratory (Shen *et al.*, 2004; Kim, 2005; Kim *et al.*, 2005a; Kim *et al.*, 2005b). He found that *E. coli* NDP kinase directly interacts with T4 dCMP hydroxymethylase or T4 aerobic ribonucleotide reductase individually, by either coimmunoprecipitation or GST-pulldown assay (Shen *et al.*, 2004; Kim, 2005). He also found no evidence for direct association between gp32 and either DHF reductase, gp42 or gp1 (Kim, 2005; Kim *et al.*, 2005b).

Additional direct protein-protein interactions in the complex will be identified in the future. Apart from the current approaches that have generated useful results, some high-throughput methods should be considered. Among those, high-throughput yeast two-hybrid (HT-Y2H) assays (Walhout *et al.*, 2000) will be of great interest. It uses an automatable recombination cloning system to eliminate the need for gene-specific manipulations and then employs high-throughput protocols to transform yeast cells in up to 96-well plate format, the resulting transformants are spotted. The final complete protein-protein interactome is generated from a series of computer-aided analysis. By the advantage of high-throughput, we can study the protein-protein interaction network at whole genome or proteome scale in a fairly short time. Not only can it detect protein-protein associations in T4 phage early proteins involved in dNTP and DNA biosynthesis, but also it can discover interactions between early proteins and late proteins used for assembly of infectious virus, or between late-late proteins. However, according to our models of the T4 dNTP synthetase complex and gp32 as the recruiter for the complex

(Wheeler *et al.*, 1996; Kim, 2005; Kim *et al.*, 2005b), we may not expect many specific direct interactions between proteins of dNTP synthetase complex and proteins of DNA replisome since in this model gp32 acts as a connector between them, eliminating the need of those associations. However, these experiments would present an opportunity to test the gp32 connector model.

With the rapid improvement of computing technology and the development of advanced algorithms and mathematical and statistical models, protein structure prediction (Zhang and Skolnick, 2005; Shen, 2006; Nayeem *et al.*, 2006) and protein-protein interaction prediction (Pazos and Valencia, 2001; Tan *et al.*, 2004; Aytuna *et al.*, 2005; Ogmen *et al.*, 2005) provide promising perspectives. Protein-protein interactions can be predicted by inferring interactions between pairs of proteins based on their phylogenetic distances based on the rationale that interacting proteins are likely to co-evolve (Pazos and Valencia, 2001). Phylogenetic distances are generated from BLAST search, which is based on multi-sequence alignment. Other protein-protein interaction prediction methods include identification of homologous interacting pairs (Aloy and Russell, 2003) and identification of structural patterns (Aytuna *et al.*, 2005; Ogmen *et al.*, 2005). We could employ some of those available approaches to predict the associations in the T4 dNTP synthetase complex.

As listed in Table 7.2, four of the ten enzymes in the T4 dNTP synthetase complex, plus gp32 and anaerobic ribonucleotide reductase, have crystal structures available. Half of

the proteins in the table do not have crystal structures yet, which could be computationally predicted although it would require much computational power. The available crystal structures combined with predicted structures could be used to predict protein-protein complex by protein-protein docking methods, such as Monte Carlo methods (Gray *et al.*, 2003), the CAPRI assessment (Janin *et al.*, 2003). One demonstrated example is the interaction between dCMP hydroxymethylase and thymidylate synthase proposed by Song *et al.* (Song *et al.*, 1999), where the crystal structures of both enzymes were determined. They also suggested that the position of T4 DHF reductase associating with T4 thymidylate synthase is similar to that of the DHF reductase domain in the bifunctional dihydrofolate reductase-thymidylate synthase from *Leishmania major* (Knighton *et al.*, 1994).

In general, although protein-protein interaction prediction methods might be able to generate useful results, biological validation is still essential to verify them. All the biochemical and biophysical approaches mentioned in this thesis are useful.

## **7.2 Nucleotide Effects upon Protein-Protein Interactions**

Several observations over the years in our laboratory suggest that small molecules – such as substrates, coenzymes and allosteric modifiers – affect the protein-protein associations in the T4 dNTP synthetase complex (Hanson and Mathews, 1994; Wheeler *et al.*, 1996).

We found that ATP can enhance most of the tested protein-protein interactions (Table 7.1 and Figure 7.1) except *E. coli* NDP kinase-T4 thymidylate synthase, in which ATP had no effect. Quantitative analysis from IAsys data shows that, in the presence of about 1 mM ATP, the apparent equilibrium dissociation constants are an order of magnitude lower than that in the absence of ATP. The intracellular concentration of proteins in the complex was estimated in micromolar range (Shen *et al.*, 2006) and intracellular ATP concentration was determined to be in millimolar range (Mathews, 1972), suggesting that *in vivo* the associations are even more significant at physiological conditions and that ATP plays an important role in stabilizing the complex *in vivo*.

In future experiments one might add ATP in all buffers during the isolation of the T4 dNTP synthetase complex from an extract of T4 phage-infected *E. coli* cells so that an intact complex might be isolated by sucrose gradient centrifugation. Once an intact complex is available, proteomic approaches, such as mass spectrometry or protein microarray (Zhu *et al.*, 2003), could be applied to define protein composition and stoichiometry of the complex.

T4 anaerobic ribonucleotide reductase subunit (NrdD) was observed to interact with several proteins in the complex, such as *E. coli* NDP kinase, T4 thymidylate synthase and T4 dCTPase/dUTPase. In addition, the association between T4 NrdD and *E. coli* NDP kinase was also enhanced by ATP. It would be interesting to further investigate dNTP biosynthesis under anaerobic conditions. Once infected by T4 phage, host cells will be

grown in an anaerobic chamber. By use of procedures similar to those described above, ATP would be added during isolation of the intact complex if it exists. The isolated complex will be further analyzed using proteomic approaches.

### **7.3 Tetramerization and Self-Association of *Escherichia coli* NDP Kinase**

Since several interactions involving *E. coli* NDP kinase were observed to be enhanced by ATP, we wondered whether ATP might be exerting its effects through influence upon the quaternary structure of the tetrameric *E. coli* NDP kinase. Mesnildrey *et al.* (1998) reported that a mutant form of *Dictyostelium discoideum* NDP kinase is a homodimer in the absence of ATP, but that 0.5 mM ATP drives formation of the familiar homohexamer. In our study on *E. coli* NDP kinase, equilibrium sedimentation shows that in the absence of ATP or ADP, the dissociation constant between dimers and tetramers was determined to be 0.8  $\mu$ M (Figures 5.4 and 5.5). However, in the presence of 0.5 mM ATP or 0.5 mM ADP, all species of NDP kinase appeared to be tetramers. The estimated intracellular concentration of NDP kinase is in micromolar range and ATP is in millimolar range, suggesting that *in vivo* most of *E. coli* NDP kinase molecules are tetramers. The self-association property of *E. coli* NDP kinase was further confirmed by IAsys optical biosensor analysis (Figures 5.1 and 5.2) and fluorescence spectroscopy (Figure 5.6). In addition, T4 aerobic ribonucleotide reductase and *E. coli* adenylate kinase also exhibited self-association. ATP also enhanced self-association of *E. coli* adenylate kinase. Most

enzymes in the T4 dNTP synthetase complex are homo-multimers, except that both ribonucleotide reductases are hetero-tetramers and that *E. coli* adenylate kinase is monomer (Table 1.1), suggesting that self-association might be universal in the complex. To test this, IAsys optical biosensing or analytical ultracentrifugation would be useful and sufficient.

The effect of hm-dCTP on the interaction between T4 dCMP deaminase and *E. coli* NDP kinases is somewhat surprising in that it weakened the established association, suggesting that protein-protein interactions in the complex are dynamic depending on the local concentrations of metabolites and allosteric modifiers. It could be better understood if the crystal structure of T4 dCMP deaminase could be solved through appropriate collaboration, with or without hm-dCTP being co-crystallized. However, a predicted structure of dCMP deaminase might also be helpful. Moreover, we would ask whether hm-dCTP always weakens the interactions involving dCMP deaminase by analyzing more proteins from the complex, that is, whether the enhancement by hm-dCTP of interactions involving dCMP deaminase exists. It will be very useful to understand the enzyme organization in the complex. In addition, hm-dCTP is also an activator of T4 aerobic ribonucleotide reductase (Berglund, 1975). Therefore, it would be interesting to study the effect of hm-dCTP on protein-protein interactions involving T4 aerobic ribonucleotide reductase.

#### **7.4 Merits of IAsys Optical Biosensing on Protein-Protein Interaction Study**

Among those new approaches for the study of protein-protein interactions employed in this research, IAsys optical biosensor analysis is of special merit. It requires much smaller amounts of purified proteins than that of other methods, such as analytical ultracentrifugation, protein affinity chromatography and fluorescence spectroscopy; it is much faster than analytical ultracentrifugation, which typically requires more than 24 hours; it does not need the use of labeled molecules; it can monitor the protein-protein interactions in real-time; it can also quantitatively and kinetically determine both steady-state and dynamic parameters of interaction; it can distinguish direct interactions from indirect ones; and it is sensitive to minute changes of refractive index when protein association occurs on the surface of the cuvette. To sum up, IAsys optical biosensing is especially useful for the study of protein-protein interactions.

#### **7.5 Kinetic Coupling Assay for a Three-Step dCTP→dCMP→dUMP→dTMP Pathway**

Kinetic coupling assays for a mixture of purified T4 proteins were carried out. A three-step dCTP→dCMP→dUMP→dTMP pathway is sequentially catalyzed by dCTPase/dUTPase, dCMP deaminase and thymidylate synthase. Kinetic coupling through substrate channeling behavior was observed compared with computer simulation of uncoupled reactions, suggesting the association of the enzymes involved. Interestingly,

some other proteins in the T4 dNTP synthetase complex that do not participate in this three-step reaction sequence substantially enhanced the kinetic coupling. These findings further suggest positive cooperativity among interactions stabilizing the complex.

Although preliminary investigation on the kinetic coupling assay is promising, further study is necessary. With the availability of the crystal structure T4 thymidylate synthase, if the structures of T4 dCMP deaminase and T4 dCTPase/dUTPase is solved or predicted, we could further investigate the structural basis of mechanism of coupling by asking how those enzymes dock and how substrates are channeled from one active site to another, by a similar approach to that advanced by Song *et al.* (1999).

Following the success of kinetic coupling assay in the three-step pathway with purified proteins, we wonder whether we could reconstitute the whole complex using freshly purified proteins and ask whether the whole reconstituted complex has the kinetic coupling behavior. However, the requirement for ten or more purified and active enzymes, some of which are unstable to prolonged storage, would make this a substantial undertaking.

## **7.6 Merits of the T4 dNTP Synthetase Complex Model**

All the data obtained in this research support the model of the T4 dNTP synthetase complex. Although this model was proposed decades ago (Tomich *et al.*, 1974; Reddy *et*

*al.*, 1977; Mathews and Allen, 1983; Mathews *et al.*, 1993; Mathews, 1993a; Greenberg *et al.*, 1994), it is still a very useful model system for analysis of the metabolon concept. *In vivo*, metabolon is a complex of enzymes catalyzing related functions, which is stabilized by weak interactions between proteins (Srere, 1987). Study of protein-protein interactions is helpful to understand how metabolon is organized and coordinated to function *in vivo*. The T4 dNTP synthetase complex is a typical example of metabolon since T4 encodes almost all of its own enzymes and proteins for dNTP biosynthesis and those proteins coordinate to fulfill their functions. In addition, the T4 dNTP synthetase complex is also a powerful model for testing the concept of multi-enzyme complexes, in which multiple separate enzymes catalyzing sequential reactions associate with each other strongly enough to form a complex for efficient biosynthesis of dNTPs.

**Table 7.1.** Direct protein-protein interactions and ATP enhancement upon their interactions observed in this thesis comparing with previous results.

Protein-protein interaction in pairs	Previously demonstrated or indicated by	Shown or confirmed in this thesis by	ATP enhancement	$K_D^a$ ( $\mu\text{M}$ )	
				No ATP	ATP
TS-RNR	Affinity	IASys, Fluor	Yes	0.5	0.03
TS-gp32	Affinity	IASys			
TS-DHFR	Affinity, NDE	IASys			
TS-gp56	Affinity	Fluor			
RNR-DHFR	Affinity	IASys			
RNR-gp32	Affinity, GST	IASys		2.0	
NDPK-TS		IASys, Fluor	No	2.2	
NDPK-RNR	NDE, GST, IP	IASys, Fluor	Yes		
NDPK-gp56		IASys, Fluor	Yes		
NDPK-gp32	Affinity, GST	IASys	No		
NDPK-ADK		IASys		0.22	
NDPK-CD		IASys	Yes	1.6	
NDPK-NrdD		IASys, Fluor	Yes		
NrdD-TS		Fluor			
NrdD-gp56		Fluor			
ADK-TS		IASys	No	0.04	
ADK-CD		IASys	Yes		
NDPK-NDPK		IASys, Fluor, AUC	Yes	0.1, 0.8 <sup>b</sup>	0.007
ADK-ADK		IASys	Yes		
RNR-RNR	Affinity, IP	IASys			

<sup>a</sup>  $K_D$ 's were determined by IASys optical biosensor unless noted otherwise.

<sup>b</sup> determined by analytical ultracentrifugation.

Abbreviations for proteins are: TS, T4 thymidylate synthase; RNR, T4 aerobic ribonucleotide reductase; gp32, T4 single-strand DNA binding protein; DHFR, T4 dihydrofolate reductase; gp56, T4 dCTPase/dUTPase; NDPK, *E. coli* NDP kinase; ADK, *E. coli* adenylate kinase; NrdD, T4 anaerobic ribonucleotide reductase subunit. Abbreviations for approaches are: Affinity, protein affinity chromatography; NDE, non-denaturing gel electrophoresis; GST, glutathione-S-transferase pulldown; IP, immunoprecipitation; IASys, IASys optical biosensor analysis; Fluor, fluorescence spectroscopy; AUC, analytical ultracentrifugation.

**Table 7.2.** Proteins in the T4 dNTP synthetase complex and their available crystal structure information. (Modified from Mathews, unpublished manuscript)

<b>Protein name</b>	<b>Gene</b>	<b>Crystal structure</b>
dCMP hydroxymethylase	42	Yes (Song <i>et al.</i> , 1999)
Thymidylate synthase	<i>td</i>	Yes (Finer-Moore <i>et al.</i> , 1994)
dCTPase/dUTPase	56	No
Aerobic ribonucleotide reductase	<i>nrdA, nrdB</i>	No
Anaerobic ribonucleotide reductase	<i>nrdD, nrdG</i>	Yes (Logan <i>et al.</i> , 1999)
dCMP deaminase	<i>cd</i>	No
Dihydrofolate reductase	<i>frd</i>	No
dNMP kinase	1	Yes (Teplyakov <i>et al.</i> , 1996)
<i>E. coli</i> NDP kinase	<i>E. coli ndk</i>	No
<i>E. coli</i> adenylate kinase	<i>E. coli adk</i>	Yes (Müller and Schulz, 1992)
Single-strand DNA binding protein	32	Yes (Shamoo <i>et al.</i> , 1995a)

**Note:** gp32 and anaerobic ribonucleotide reductase are also included in this table although they are currently not included in the complex of our model.

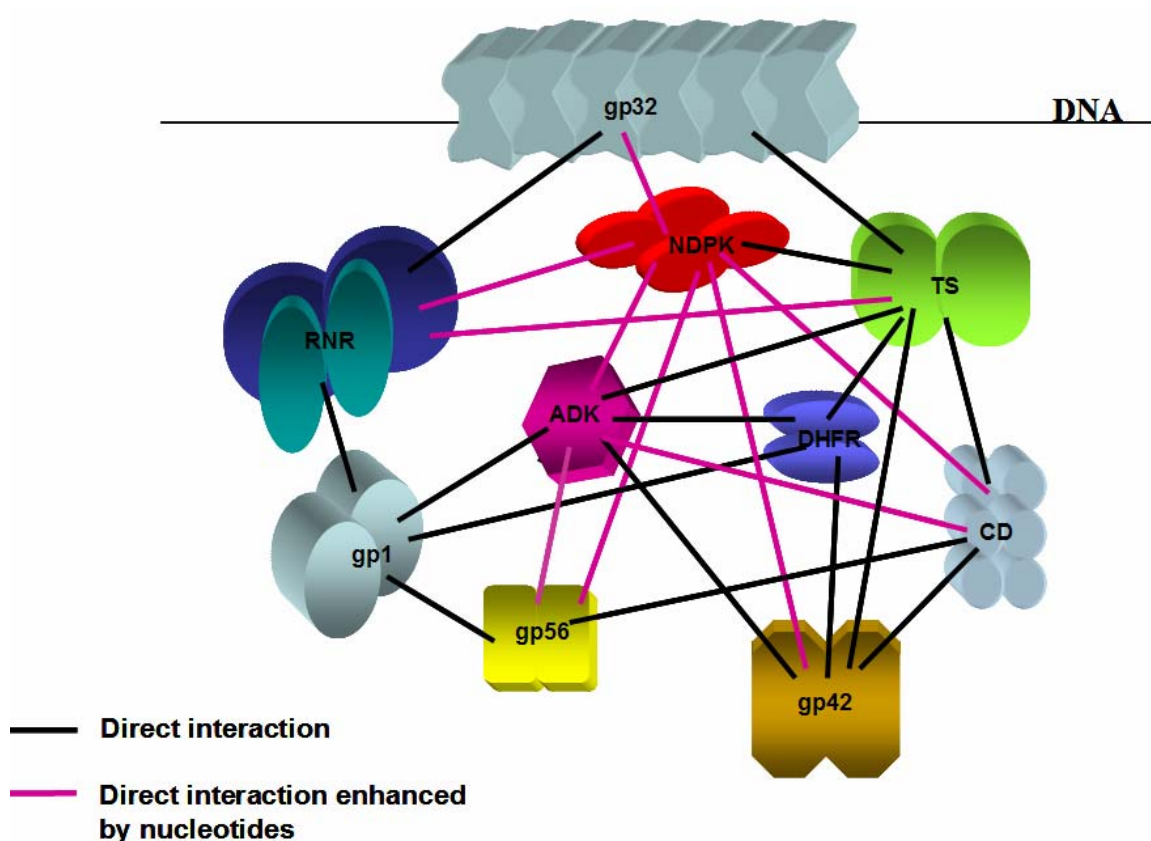


**Figure 7.1.** An interactome model for the organization of the T4 dNTP synthetase complex around DNA. Black lines represent the direct protein-protein interactions. Red lines stand for the direct interactions enhanced by nucleotides. gp32, T4 single-strand DNA binding protein; NDPK, *E. coli* NDP kinase; RNR, T4 aerobic ribonucleotide reductase; TS, T4 thymidylate synthase; ADK, *E. coli* adenylate kinase; DHFR, T4 dihydrofolate reductase; gp1, dNMP kinase; CD, T4 dCMP deaminase; gp56, T4 dCTPase/dUTPase; gp42, T4 dCMP hydroxymethylase.

## Bibliography

1. Alberts, B. M., and Frey, L. (1970). T4 bacteriophage gene 32: a structural protein in the replication and recombination of DNA. *Nature* **227**(5265), 1313-1318.
2. Allen, J. R., Lasser, G. W., Goldman, D. A., Booth, J. W., and Mathews, C. K. (1983). T4 phage deoxyribonucleotide-synthesizing enzyme complex. Further studies on enzyme composition and regulation. *J. Biol. Chem.* **258**(9), 5746-5753.
3. Allen, J. R., Reddy, G. P., Lasser, G. W., and Mathews, C. K. (1980). T4 ribonucleotide reductase. Physical and kinetic linkage to other enzymes of deoxyribonucleotide biosynthesis. *J. Biol. Chem.* **255**(16), 7583-7588.
4. Almaula, N., Lu, Q., Delgado, J., Belkin, S., and Inouye, M. (1995). Nucleoside diphosphate kinase from *Escherichia coli*. *J. Bacteriol.* **177**(9), 2524-2529.
5. Aloy, P., and Russell, R. B. (2003). InterPreTS: protein interaction prediction through tertiary structure. *Bioinformatics.* **19**(1), 161-162.
6. Andersson, J., Bodevin, S., Westman, M., Sahlin, M., and Sjöberg, B. M. (2001). Two active site asparagines are essential for the reaction mechanism of the class III anaerobic ribonucleotide reductase from bacteriophage T4. *J. Biol. Chem.* **276**(44), 40457-40463.
7. Ausio, J., Malencik, D. A., and Anderson, S. R. (1992). Analytical sedimentation studies of turkey gizzard myosin light chain kinase and telokin. *Biophys. J.* **61**(6), 1656-1663.
8. Aytuna, A. S., Gursoy, A., and Keskin, O. (2005). Prediction of protein-protein interactions by combining structure and sequence conservation in protein interfaces. *Bioinformatics.* **21**(12), 2850-2855.
9. Belfort, M., Moelleken, A., Maley, G. F., and Maley, F. (1983). Purification and properties of T4 phage thymidylate synthetase produced by the cloned gene in an amplification vector. *J. Biol. Chem.* **258**(3), 2045-2051.

10. Bello, L. J., and Bessman, M. J. (1963a). The enzymology of virus-infected bacteria. IV. Purification and properties of the deoxynucleotide kinase induced by bacteriophage T2. *J. Biol. Chem.* **238**, 1777-1787.
11. Bello, L. J., and Bessman, M. J. (1963b). The enzymology of virus-infected bacteria. V. Phosphorylation of hydroxymethyldeoxycytidine diphosphate and deoxythymidine diphosphate in normal and bacteriophage-infected *Escherichia coli*. *Biochim. Biophys. Acta* **72**, 647-650.
12. Benkovic, S. J., Valentine, A. M., and Salinas, F. (2001). Replisome-mediated DNA replication. *Annu. Rev. Biochem.* **70**, 181-208.
13. Bennett, S. E., Chen, C. Y., and Mosbaugh, D. W. (2004). *Escherichia coli* nucleoside diphosphate kinase does not act as a uracil-processing DNA repair nuclease. *Proc. Natl. Acad. Sci. U. S. A* **101**(17), 6391-6396.
14. Berglund, O. (1972). Ribonucleoside diphosphate reductase induced by bacteriophage T4. II. Allosteric regulation of substrate specificity and catalytic activity. *J. Biol. Chem.* **247**(22), 7276-7281.
15. Berglund, O. (1975). Ribonucleoside diphosphate reductase induced by bacteriophage T4. III. Isolation and characterization of proteins B1 and B2. *J. Biol. Chem.* **250**(18), 7450-7455.
16. Berglund, O., and Eckstein, F. (1972). Synthesis of ATP- and dATP-substituted sepharoses and their application in the purification of phage-T4-induced ribonucleotide reductase. *Eur. J. Biochem.* **28**(4), 492-496.
17. Bernard, M. A., Ray, N. B., Olcott, M. C., Hendricks, S. P., and Mathews, C. K. (2000). Metabolic functions of microbial nucleoside diphosphate kinases. *J. Bioenerg. Biomembr.* **32**(3), 259-267.
18. Berry, M. B., Meador, B., Bilderback, T., Liang, P., Glaser, M., and Phillips, G. N., Jr. (1994). The closed conformation of a highly flexible protein: the structure of *E. coli* adenylate kinase with bound AMP and AMPPNP. *Proteins* **19**(3), 183-198.

19. Brune, M., Schumann, R., and Wittinghofer, F. (1985). Cloning and sequencing of the adenylate kinase gene (*adk*) of *Escherichia coli*. *Nucleic Acids Res.* **13**(19), 7139-7151.
20. Brush, G. S., and Bessman, M. J. (1993). Chemical modification of bacteriophage T4 deoxynucleotide kinase. Evidence of a single catalytic region. *J. Biol. Chem.* **268**(3), 1603-1609.
21. Brush, G. S., Bhatnagar, S. K., and Bessman, M. J. (1990). Bacteriophage T4 deoxynucleotide kinase: gene cloning and enzyme purification. *J. Bacteriol.* **172**(6), 2935-2939.
22. Chiadmi, M., Morera, S., Lascu, I., Dumas, C., Le, B. G., Veron, M., and Janin, J. (1993). Crystal structure of the Awd nucleotide diphosphate kinase from *Drosophila*. *Structure.* **1**(4), 283-293.
23. Chiu, C. S., Cook, K. S., and Greenberg, G. R. (1982). Characteristics of a bacteriophage T4-induced complex synthesizing deoxyribonucleotides. *J. Biol. Chem.* **257**(24), 15087-15097.
24. Chiu, C. S., Ruettinger, T., Flanagan, J. B., and Greenberg, G. R. (1977). Role of deoxycytidylate deaminase in deoxyribonucleotide synthesis in bacteriophage T4 DNA replication. *J. Biol. Chem.* **252**(23), 8603-8608.
25. Cole, J. L., and Hansen, J. C. (1999). Analytical ultracentrifugation as a contemporary biomolecular research tool. *J. Biomol. Techn.* **10**(4), 163-176.
26. Cush, R., Cronin, J. M., Stewart, W. J., Maule, C. H., Molloy, J., and Goddard, N. J. (1993). The Resonant Mirror: a novel optical biosensor for direct sensing of biomolecular interactions. Part I: Principle of operation and associated instrumentation. *Biosensors and Bioelectronics* **8**, 347-353.
27. Dahnke, T., and Tsai, M. D. (1994). Mechanism of adenylate kinase. The conserved aspartates 140 and 141 are important for transition state stabilization instead of substrate-induced conformational changes. *J. Biol. Chem.* **269**(11), 8075-8081.

28. Demeler, B. (2005). UltraScan Software. University of Texas Health Science Center at San Antonio, Department of Biochemistry. [www.ultrascan.uthscsa.edu](http://www.ultrascan.uthscsa.edu).
29. Duckworth, D. H., and Bessman, M. J. (1967). The enzymology of virus-infected bacteria. X. A biochemical-genetic study of the deoxynucleotide kinase induced by wild type and amber mutants of phage T4. *J. Biol. Chem.* **242**(12), 2877-2885.
30. Finer-Moore, J. S., Maley, G. F., Maley, F., Montfort, W. R., and Stroud, R. M. (1994). Crystal structure of thymidylate synthase from T4 phage: component of a deoxynucleoside triphosphate-synthesizing complex. *Biochemistry* **33**(51), 15459-15468.
31. Fivash, M., Towler, E. M., and Fisher, R. J. (1998). BIAcore for macromolecular interaction. *Curr. Opin. Biotechnol.* **9**(1), 97-101.
32. Flanagan, J. B., Chiu, C. S., and Greenberg, G. R. (1977). Inhibitory effect of agents altering the structure of DNA on the synthesis of pyrimidine deoxyribonucleotides in bacteriophage T4 DNA replication. *J. Biol. Chem.* **252**(17), 6031-6037.
33. Flanagan, J. B., and Greenberg, G. R. (1977). Regulation of deoxyribonucleotide biosynthesis during in vivo bacteriophage T4 DNA replication. Intrinsic control of synthesis of thymine and 5-hydroxymethylcytosine deoxyribonucleotides at precise ratio found in DNA. *J. Biol. Chem.* **252**(9), 3019-3027.
34. Fleming, W. H., and Bessman, M. J. (1967). The enzymology of virus-infected bacteria. IX. Purification and properties of the deoxycytidylate deaminase of T6-infected *Escherichia coli*. *J. Biol. Chem.* **242**(3), 363-371.
35. Fontecave, M., Mulliez, E., and Logan, D. T. (2002). Deoxyribonucleotide synthesis in anaerobic microorganisms: the class III ribonucleotide reductase. *Prog. Nucleic Acid Res. Mol. Biol.* **72**, 95-127.
36. Formosa, T., Burke, R. L., and Alberts, B. M. (1983). Affinity purification of bacteriophage T4 proteins essential for DNA replication and genetic recombination. *Proc. Natl. Acad. Sci. U. S. A* **80**(9), 2442-2446.

37. Fournier, H. N., Dupe-Manet, S., Bouvard, D., Lacombe, M. L., Marie, C., Block, M. R., and biges-Rizo, C. (2002). Integrin cytoplasmic domain-associated protein 1alpha (ICAP-1alpha ) interacts directly with the metastasis suppressor nm23-H2, and both proteins are targeted to newly formed cell adhesion sites upon integrin engagement. *J. Biol. Chem.* **277**(23), 20895-20902.
38. Giartosio, A., Erent, M., Cervoni, L., Morera, S., Janin, J., Konrad, M., and Lascu, I. (1996). Thermal stability of hexameric and tetrameric nucleoside diphosphate kinases. Effect of subunit interaction. *J. Biol. Chem.* **271**(30), 17845-17851.
39. Goswami, S. C., Yoon, J. H., Abramczyk, B. M., Pfeifer, G. P., and Postel, E. H. (2006). Molecular and functional interactions between *Escherichia coli* nucleoside diphosphate kinase and the uracil-DNA glycosylase ung. *J. Biol. Chem.*, In press.
40. Gray, J. J., Moughon, S., Wang, C., Schueler-Furman, O., Kuhlman, B., Rohl, C. A., and Baker, D. (2003). Protein-protein docking with simultaneous optimization of rigid-body displacement and side-chain conformations. *J. Mol. Biol.* **331**(1), 281-299.
41. Greenberg, G. R., He, P., Hilfinger, J., and Tseng, M.-J. (1994). Deoxyribonucleoside Triphosphate Synthesis and Phage T4 DNA Replication. In *Molecular Biology of Bacteriophage T4* (J.Karam, J.W.Drake, K.N.Kreuzer, G.Mosig, D.H.Hall, F.A.Eiserling, L.W.Black, E.K.Spicer, E.Kutter, K.Carlson, and E.S.Miller, Eds.), pp. 14-27. American Society for Microbiology, Washington, D.C.
42. Guzman, E. C., Caballero, J. L., and Jimenez-Sanchez, A. (2002). Ribonucleoside diphosphate reductase is a component of the replication hyperstructure in *Escherichia coli*. *Mol. Microbiol.* **43**(2), 487-495.
43. Hall, D. (2001). Use of optical biosensors for the study of mechanistically concerted surface adsorption processes. *Anal. Biochem.* **288**(2), 109-125.
44. Hall, R. H. (2002). Biosensor technologies for detecting microbiological foodborne hazards. *Microbes. Infect.* **4**(4), 425-432.

45. Hama, H., Almaula, N., Lerner, C. G., Inouye, S., and Inouye, M. (1991a). Nucleoside diphosphate kinase from *Escherichia coli*; its overproduction and sequence comparison with eukaryotic enzymes. *Gene* **105**(1), 31-36.
46. Hama, H., Lerner, C., Inouye, S., and Inouye, M. (1991b). Location of the gene (*ndk*) for nucleoside diphosphate kinase on the physical map of the *Escherichia coli* chromosome. *J. Bacteriol.* **173**(11), 3276.
47. Hanson, E. (1994). Bacteriophage T4 ribonucleotide reductase: genes and proteins. Ph.D. Thesis. Oregon State University. Corvallis, Oregon.
48. Hanson, E., and Mathews, C. K. (1994). Allosteric effectors are required for subunit association in T4 phage ribonucleotide reductase. *J. Biol. Chem.* **269**(49), 30999-31005.
49. Hartsough, M. T., and Steeg, P. S. (2000). Nm23/nucleoside diphosphate kinase in human cancers. *J. Bioenerg. Biomembr.* **32**(3), 301-308.
50. Hasunuma, K., Yabe, N., Yoshida, Y., Ogura, Y., and Hamada, T. (2003). Putative functions of nucleoside diphosphate kinase in plants and fungi. *J. Bioenerg. Biomembr.* **35**(1), 57-65.
51. IAsys (1996a). IAsys *Plus* - User's Guide. Affinity Sensors, Saxon Way, Bar Hill, Cambridge, CB3 8SL, England.
52. IAsys (1996b). IAsys Protocols. Affinity Sensors, Saxon Way, Bar Hill, Cambridge, CB3 8SL, England.
53. IAsys (1996c). Methods Guide for IAsys *plus* and IAsys Auto+. Affinity Sensors, Saxon Way, Bar Hill, Cambridge, CB3 8SL, England.
54. IAsys (1996d). Technical Note 3.1: Background Information - The Resonant Mirror. Affinity Sensors, Saxon Way, Bar Hill, Cambridge, CB3 8SL, England.
55. Iwatsuki, N. (1977). Purification and properties of deoxythymidine kinase induced by bacteriophage T4 infection. *J. Biochem. (Tokyo)* **82**(5), 1347-1359.

56. Janin, J. (1993). Shared structural motif in proteins. *Nature* **365**(6441), 21.
57. Janin, J., Dumas, C., Morera, S., Xu, Y., Meyer, P., Chiadmi, M., and Cherfils, J. (2000). Three-dimensional structure of nucleoside diphosphate kinase. *J. Bioenerg. Biomembr.* **32**(3), 215-225.
58. Janin, J., Henrick, K., Moult, J., Eyck, L. T., Sternberg, M. J., Vajda, S., Vakser, I., and Wodak, S. J. (2003). CAPRI: a Critical Assessment of PRedicted Interactions. *Proteins* **52**(1), 2-9.
59. Jarvis, T. C., Paul, L. S., and von Hippel, P. H. (1989). Structural and enzymatic studies of the T4 DNA replication system. I. Physical characterization of the polymerase accessory protein complex. *J. Biol. Chem.* **264**(21), 12709-12716.
60. Ji, J. P., and Mathews, C. K. (1991). Analysis of mutagenesis induced by a thermolabile T4 phage deoxycytidylate hydroxymethylase suggests localized deoxyribonucleotide pool imbalance. *Mol. Gen. Genet.* **226**(1-2), 257-264.
61. Jordan, A., and Reichard, P. (1998). Ribonucleotide reductases. *Annu. Rev. Biochem.* **67**, 71-98.
62. Karlsson, A., Mesnildrey, S., Xu, Y., Morera, S., Janin, J., and Veron, M. (1996). Nucleoside diphosphate kinase. Investigation of the intersubunit contacts by site-directed mutagenesis and crystallography. *J. Biol. Chem.* **271**(33), 19928-19934.
63. Keefe, R. G., Maley, G. F., Saxl, R. L., and Maley, F. (2000). A T4-phage deoxycytidylate deaminase mutant that no longer requires deoxycytidine 5'-triphosphate for activation. *J. Biol. Chem.* **275**(17), 12598-12602.
64. Kim, J. (2005). Organization of the T4 dNTP synthetase complex at DNA replication sites. Ph.D. Thesis. Oregon State University. Corvallis, Oregon.
65. Kim, J., Shen, R., Olcott, M. C., Rajagopal, I., and Mathews, C. K. (2005a). Adenylate kinase of *Escherichia coli*, a component of the phage T4 dNTP synthetase complex. *J. Biol. Chem.* **280**(31), 28221-28229.

66. Kim, J., Wheeler, L. J., Shen, R., and Mathews, C. K. (2005b). Protein-DNA interactions in the T4 dNTP synthetase complex dependent on gene 32 single-stranded DNA-binding protein. *Mol. Microbiol.* **55**(5), 1502-1514.
67. Kimura, N., Shimada, N., Fukuda, M., Ishijima, Y., Miyazaki, H., Ishii, A., Takagi, Y., and Ishikawa, N. (2000). Regulation of cellular functions by nucleoside diphosphate kinases in mammals. *J. Bioenerg. Biomembr.* **32**(3), 309-315.
68. Kimura, N., Shimada, N., Ishijima, Y., Fukuda, M., Takagi, Y., and Ishikawa, N. (2003). Nucleoside diphosphate kinases in mammalian signal transduction systems: recent development and perspective. *J. Bioenerg. Biomembr.* **35**(1), 41-47.
69. Knighton, D. R., Kan, C. C., Howland, E., Janson, C. A., Hostomska, Z., Welsh, K. M., and Matthews, D. A. (1994). Structure of and kinetic channelling in bifunctional dihydrofolate reductase-thymidylate synthase. *Nat. Struct. Biol.* **1**(3), 186-194.
70. Kostyuchenko, V. A., Chipman, P. R., Leiman, P. G., Arisaka, F., Mesyanzhinov, V. V., and Rossmann, M. G. (2005). The tail structure of bacteriophage T4 and its mechanism of contraction. *Nat. Struct. Mol. Biol.* **12**(9), 810-813.
71. Kumar, P., Krishna, K., Srinivasan, R., Ajitkumar, P., and Varshney, U. (2004). *Mycobacterium tuberculosis* and *Escherichia coli* nucleoside diphosphate kinases lack multifunctional activities to process uracil containing DNA. *DNA Repair (Amst)* **3**(11), 1483-1492.
72. Lacombe, M. L., Milon, L., Munier, A., Mehus, J. G., and Lambeth, D. O. (2000). The human Nm23/nucleoside diphosphate kinases. *J. Bioenerg. Biomembr.* **32**(3), 247-258.
73. Lakey, J. H., and Raggett, E. M. (1998). Measuring protein-protein interactions. *Curr. Opin. Struct. Biol.* **8**(1), 119-123.
74. Lamm, N., Wang, Y., Mathews, C. K., and Ruger, W. (1988). Deoxycytidylate hydroxymethylase gene of bacteriophage T4. Nucleotide sequence determination and over-expression of the gene. *Eur. J. Biochem.* **172**(3), 553-563.

75. LaPat-Polasko, L., Maley, G. F., and Maley, F. (1990). Properties of bacteriophage T4 thymidylate synthase following mutagenic changes in the active site and folate binding region. *Biochemistry* **29**(41), 9561-9572.
76. Lascu, I., Chaffotte, A., Limbourg-Bouchon, B., and Veron, M. (1992). A Pro/Ser substitution in nucleoside diphosphate kinase of *Drosophila melanogaster* (mutation killer of prune) affects stability but not catalytic efficiency of the enzyme. *J. Biol. Chem.* **267**(18), 12775-12781.
77. Lascu, I., and Gonin, P. (2000). The catalytic mechanism of nucleoside diphosphate kinases. *J. Bioenerg. Biomembr.* **32**(3), 237-246.
78. Lascu, L., Giartosio, A., Ransac, S., and Erent, M. (2000). Quaternary structure of nucleoside diphosphate kinases. *J. Bioenerg. Biomembr.* **32**(3), 227-236.
79. Laue, T. M., Shah, B. D., Ridgeway, T. M., and Pelletier, S. L. (1992). Computer-aided interpretation of analytical sedimentation data for proteins. In *Analytical ultracentrifugation in biochemistry and polymer science* (S.E.Harding, A.J.Rowe, and J.C.Horton, Eds.), pp. 90-125. Royal Society of Chemistry, Cambridge.
80. Lebowitz, J., Lewis, M. S., and Schuck, P. (2002). Modern analytical ultracentrifugation in protein science: a tutorial review. *Protein Sci.* **11**(9), 2067-2079.
81. Levit, M. N., Abramczyk, B. M., Stock, J. B., and Postel, E. H. (2002). Interactions between *Escherichia coli* nucleoside-diphosphate kinase and DNA. *J. Biol. Chem.* **277**(7), 5163-5167.
82. Logan, D. T., Andersson, J., Sjoberg, B. M., and Nordlund, P. (1999). A glycy radical site in the crystal structure of a class III ribonucleotide reductase. *Science* **283**(5407), 1499-1504.
83. Lombardi, D., and Mileo, A. M. (2003). Protein interactions provide new insight into Nm23/nucleoside diphosphate kinase functions. *J. Bioenerg. Biomembr.* **35**(1), 67-71.

84. Lu, Q., and Inouye, M. (1996). Adenylate kinase complements nucleoside diphosphate kinase deficiency in nucleotide metabolism. *Proc. Natl. Acad. Sci. U. S. A* **93**(12), 5720-5725.
85. Lu, Q., Zhang, X., Almaula, N., Mathews, C. K., and Inouye, M. (1995). The gene for nucleoside diphosphate kinase functions as a mutator gene in *Escherichia coli*. *J. Mol. Biol.* **254**(3), 337-341.
86. MacDonald, N. J., Freije, J. M., Stracke, M. L., Manrow, R. E., and Steeg, P. S. (1996). Site-directed mutagenesis of nm23-H1. Mutation of proline 96 or serine 120 abrogates its motility inhibitory activity upon transfection into human breast carcinoma cells. *J. Biol. Chem.* **271**(41), 25107-25116.
87. Malencik, D. A., Anderson, S. R., Bohnert, J. L., and Shalitin, Y. (1982). Functional interactions between smooth muscle myosin light chain kinase and calmodulin. *Biochemistry* **21**(17), 4031-4039.
88. Maley, F., and Maley, G. F. (1982a). Studies on identifying the allosteric binding sites of deoxycytidylate deaminase. *J. Biol. Chem.* **257**(20), 11876-11878.
89. Maley, G. F., Duceman, B. W., Wang, A. M., Martinez, J., and Maley, F. (1990). Cloning, sequence analysis, and expression of the bacteriophage T4 *cd* gene. *J. Biol. Chem.* **265**(1), 47-51.
90. Maley, G. F., and Maley, F. (1982b). Allosteric transitions associated with the binding of substrate and effector ligands to T2 phage induced deoxycytidylate deaminase. *Biochemistry* **21**(16), 3780-3785.
91. Malmqvist, M., and Karlsson, R. (1997). Biomolecular interaction analysis: affinity biosensor technologies for functional analysis of proteins. *Curr. Opin. Chem. Biol.* **1**(3), 378-383.
92. Mathews, C. K. (1966). On the metabolic role of T6 phage-induced dihydrofolate reductase. Intracellular reduced pyridine nucleotides. *J. Biol. Chem.* **241**(21), 5008-5012.

93. Mathews, C. K. (1972). Biochemistry of deoxyribonucleic acid-defective *amber* mutants of bacteriophage T4. 3. Nucleotide pools. *J. Biol. Chem.* **247**(22), 7430-7438.
94. Mathews, C. K. (1976). Biochemistry of DNA-defective mutants of bacteriophage T4. Thymine nucleotide pool dynamics. *Arch. Biochem. Biophys.* **172**(1), 178-187.
95. Mathews, C. K. (1985). Enzymatic channeling of DNA precursors. *Basic Life Sci.* **31**, 47-66.
96. Mathews, C. K. (1993a). Enzyme organization in DNA precursor biosynthesis. *Prog. Nucleic Acid Res. Mol. Biol.* **44**, 167-203.
97. Mathews, C. K. (1993b). The cell-bag of enzymes or network of channels? *J. Bacteriol.* **175**(20), 6377-6381.
98. Mathews, C. K. (1994). An Overview of the T4 Development Program. In *Molecular Biology of Bacteriophage T4* (J.Karam, J.W.Drake, K.N.Kreuzer, G.Mosig, D.H.Hall, F.A.Eiserling, L.W.Black, E.K.Spicer, E.Kutter, K.Carlson, and E.S.Miller, Eds.), pp. 1-8. American Society for Microbiology, Washington, DC.
99. Mathews, C. K. (1997). Nucleotide and Nucleic Acid Synthesis, Cellular Organization. In *Encyclopedia of Human Biology, 2nd Ed.* pp. 277-290.
100. Mathews, C. K. (2006). DNA precursor metabolism and genomic stability. *FASEB J.* **20**(9), 1300-1314.
101. Mathews, C. K., and Allen, J. R. (1983). DNA Metabolism: Enzymes and Proteins of DNA Metabolism. In *Bacteriophage T4* (C.K.Mathews, E.Kutter, G.Mosig, and P.B.Berget, Eds.), 1st Ed. ed., pp. 59-70. American Society for Microbiology, Washington DC.
102. Mathews, C. K., Moen, L. K., Wang, Y., and Sargent, R. G. (1988). Intracellular organization of DNA precursor biosynthetic enzymes. *Trends Biochem. Sci.* **13**(10), 394-397.

103. Mathews, C. K., and Sinha, N. K. (1982). Are DNA precursors concentrated at replication sites? *Proc. Natl. Acad. Sci. U. S. A* **79**(2), 302-306.
104. Mathews, C. K., Sjöberg, B. M., and Reichard, P. (1987). Ribonucleotide reductase of *Escherichia coli*. Cross-linking agents as probes of quaternary and quinary structure. *Eur. J. Biochem.* **166**(2), 279-285.
105. Mathews, C. K., and Slabaugh, M. B. (1986). Eukaryotic DNA metabolism. Are deoxyribonucleotides channeled to replication sites? *Exp. Cell Res.* **162**(2), 285-295.
106. Mathews, C. K., van Holde, K. E., and Ahern, K. G. (2000). *Biochemistry, 3rd Ed.* The Benjamin/Cummings Publishing Company, Inc., Redwood City.
107. Mathews, C. K., Wheeler, L. J., Ungermann, C., Young, J. P., and Ray, N. B. (1993). Enzyme interactions involving T4 phage-coded thymidylate synthase and deoxycytidylate hydroxymethylase. *Adv. Exp. Med. Biol.* **338**, 563-570.
108. McGaughey, K. M., Wheeler, L. J., Moore, J. T., Maley, G. F., Maley, F., and Mathews, C. K. (1996). Protein-protein interactions involving T4 phage-coded deoxycytidylate deaminase and thymidylate synthase. *J. Biol. Chem.* **271**(38), 23037-23042.
109. Mesnildrey, S., Agou, F., Karlsson, A., Bonne, D. D., and Veron, M. (1998). Coupling between catalysis and oligomeric structure in nucleoside diphosphate kinase. *J. Biol. Chem.* **273**(8), 4436-4442.
110. Mesnildrey, S., Agou, F., and Veron, M. (1997). The in vitro DNA binding properties of NDP kinase are related to its oligomeric state. *FEBS Lett.* **418**(1-2), 53-57.
111. Miller, E. S., Kutter, E., Mosig, G., Arisaka, F., Kunisawa, T., and Rüger, W. (2003). Bacteriophage T4 genome. *Microbiol. Mol. Biol. Rev.* **67**(1), 86-156.
112. Miller, J. H., Funchain, P., Clendenin, W., Huang, T., Nguyen, A., Wolff, E., Yeung, A., Chiang, J. H., Garibyan, L., Slupska, M. M., and Yang, H. (2002). *Escherichia coli* strains (ndk) lacking nucleoside diphosphate kinase are powerful

- mutators for base substitutions and frameshifts in mismatch-repair-deficient strains. *Genetics* **162**(1), 5-13.
113. Milon, L., Meyer, P., Chiadmi, M., Munier, A., Johansson, M., Karlsson, A., Lascu, I., Capeau, J., Janin, J., and Lacombe, M. L. (2000). The human nm23-H4 gene product is a mitochondrial nucleoside diphosphate kinase. *J. Biol. Chem.* **275**(19), 14264-14272.
114. Moen, L. K., Howell, M. L., Lasser, G. W., and Mathews, C. K. (1988). T4 phage deoxyribonucleoside triphosphate synthetase: purification of an enzyme complex and identification of gene products required for integrity. *J. Mol. Recognit.* **1**(1), 48-57.
115. Molina, F., and Skarstad, K. (2004). Replication fork and SeqA focus distributions in *Escherichia coli* suggest a replication hyperstructure dependent on nucleotide metabolism. *Mol. Microbiol.* **52**(6), 1597-1612.
116. Morera, S., LeBras, G., Lascu, I., Lacombe, M. L., Veron, M., and Janin, J. (1994). Refined X-ray structure of *Dictyostelium discoideum* nucleoside diphosphate kinase at 1.8 Å resolution. *J. Mol. Biol.* **243**(5), 873-890.
117. Müller, C. W., and Schulz, G. E. (1992). Structure of the complex between adenylate kinase from *Escherichia coli* and the inhibitor Ap5A refined at 1.9 Å resolution. A model for a catalytic transition state. *J. Mol. Biol.* **224**(1), 159-177.
118. Munoz-Dorado, J., Inouye, M., and Inouye, S. (1990). Nucleoside diphosphate kinase from *Myxococcus xanthus*. I. Cloning and sequencing of the gene. *J. Biol. Chem.* **265**(5), 2702-2706.
119. Narayanan, R., and Ramaswami, M. (2003). Regulation of dynamin by nucleoside diphosphate kinase. *J. Bioenerg. Biomembr.* **35**(1), 49-55.
120. Nayeem, A., Sitkoff, D., and Krystek, S. Jr. (2006). A comparative study of available software for high-accuracy homology modeling: from sequence alignments to structural models. *Protein Sci.* **15**(4), 808-824.
121. Noda, L. (1973). Adenylate kinase. In *The enzymes* (P.D.Boyer, Ed.), 3rd. ed., pp. 279-305. Academic Press, New York.

122. Nordlund, P., and Reichard, P. (2006). Ribonucleotide reductases. *Annu. Rev. Biochem.* **75**, 681-706.
123. North, T. W., Stafford, M. E., and Mathews, C. K. (1976). Biochemistry of DNA-defective mutants of bacteriophage T4. VI. Biological functions of gene 42. *J. Virol.* **17**(3), 973-982.
124. Nossal, N. G., and Peterlin, B. M. (1979). DNA replication by bacteriophage T4 proteins. The T4 43, 32, 44--62, And 45 proteins are required for strand displacement synthesis at nicks in duplex DNA. *J. Biol. Chem.* **254**(13), 6032-6037.
125. O'Donnell, M. (2006). Replisome architecture and dynamics in *Escherichia coli*. *J. Biol. Chem.* **281**(16), 10653-10656.
126. Ogmen, U., Keskin, O., Aytuna, A. S., Nussinov, R., and Gursoy, A. (2005). PRISM: protein interactions by structural matching. *Nucleic Acids Res.* **33**(Web Server issue), W331-W336.
127. Ohtsuki, K., Yokoyama, M., Koike, T., and Ishida, N. (1984). Nucleoside diphosphate kinase in *Escherichia coli*: its polypeptide structure and reaction intermediate. *Biochem. Int.* **8**(5), 715-723.
128. Olcott, M. C., Andersson, J., and Sjöberg, B. M. (1998). Localization and characterization of two nucleotide-binding sites on the anaerobic ribonucleotide reductase from bacteriophage T4. *J. Biol. Chem.* **273**(38), 24853-24860.
129. Ouatas, T., Salerno, M., Palmieri, D., and Steeg, P. S. (2003). Basic and translational advances in cancer metastasis: Nm23. *J. Bioenerg. Biomembr.* **35**(1), 73-79.
130. Parks, R., and Agarwal, R. (1973). Nucleoside diphosphokinases. In *The Enzymes*, 3rd Ed. (P.D.Boyer, Ed.), 3rd Ed. ed., pp. 307-333. Academic Press, New York.
131. Pato, M. L. (1979). Alterations of deoxyribonucleoside triphosphate pools in *Escherichia coli*: effects on deoxyribonucleic acid replication and evidence for compartmentation. *J. Bacteriol.* **140**(2), 518-524.

132. Pazos, F., and Valencia, A. (2001). Similarity of phylogenetic trees as indicator of protein-protein interaction. *Protein Eng* **14**(9), 609-614.
133. Perkins, S. J. (1986). Protein volumes and hydration effects. The calculations of partial specific volumes, neutron scattering matchpoints and 280-nm absorption coefficients for proteins and glycoproteins from amino acid sequences. *Eur. J. Biochem.* **157**(1), 169-180.
134. Phizicky, E. M., and Fields, S. (1995). Protein-protein interactions: methods for detection and analysis. *Microbiol. Rev.* **59**(1), 94-123.
135. Postel, E. H., and Abramczyk, B. M. (2003). *Escherichia coli* nucleoside diphosphate kinase is a uracil-processing DNA repair nuclease. *Proc. Natl. Acad. Sci. U. S. A* **100**(23), 13247-13252.
136. Postel, E. H., and Ferrone, C. A. (1994). Nucleoside diphosphate kinase enzyme activity of NM23-H2/PuF is not required for its DNA binding and *in vitro* transcriptional functions. *J. Biol. Chem.* **269**(12), 8627-8630.
137. Price, A. R., and Warner, H. R. (1969). Bacteriophage T4-induced deoxycytidine triphosphate-deoxyuridine triphosphate nucleotidohydrolase: its properties and its role during phage infection of *Escherichia coli*. *Virology* **39**(4), 882-892.
138. Purohit, S., and Mathews, C. K. (1984). Nucleotide sequence reveals overlap between T4 phage genes encoding dihydrofolate reductase and thymidylate synthase. *J. Biol. Chem.* **259**(10), 6261-6266.
139. Ray, N. B. (1992). Nucleoside diphosphokinase of *Escherichia coli* and its interactions with bacteriophage proteins of DNA synthesis. Ph.D. Thesis. Oregon State University. Corvallis, Oregon.
140. Reddy, G. P., and Mathews, C. K. (1978). Functional compartmentation of DNA precursors in T4 phage-infected bacteria. *J. Biol. Chem.* **253**(10), 3461-3467.
141. Reddy, G. P., Singh, A., Stafford, M. E., and Mathews, C. K. (1977). Enzyme associations in T4 phage DNA precursor synthesis. *Proc. Natl. Acad. Sci. U. S. A* **74**(8), 3152-3156.

142. Reichard, P. (1985). Ribonucleotide reductase and deoxyribonucleotide pools. *Basic Life Sci.* **31**, 33-45.
143. Reichard, P. (1988). Interactions between deoxyribonucleotide and DNA synthesis. *Annu. Rev. Biochem.* **57**, 349-374.
144. Reichard, P. (1993). The anaerobic ribonucleotide reductase from *Escherichia coli*. *J. Biol. Chem.* **268**(12), 8383-8386.
145. Reichard, P. (2002). Ribonucleotide reductases: the evolution of allosteric regulation. *Arch. Biochem. Biophys.* **397**(2), 149-155.
146. Sakiyama, S., and Buchanan, J. M. (1971). *In vitro* synthesis of deoxynucleotide kinase programmed by bacteriophage T4-RNA. *Proc. Natl. Acad. Sci. U. S. A* **68**(6), 1376-1380.
147. Schulz, G. E., Muller, C. W., and Diederichs, K. (1990). Induced-fit movements in adenylate kinases. *J. Mol. Biol.* **213**(4), 627-630.
148. Scott, D., Harding, S. E., and Rowe, A. J. (2006). *Analytical Ultracentrifugation: Techniques and Methods*. Royal Society of Chemistry.
149. Shamoo, Y., Friedman, A. M., Parsons, M. R., Konigsberg, W. H., and Steitz, T. A. (1995b). Crystal structure of a replication fork single-stranded DNA binding protein (T4 gp32) complexed to DNA. *Nature* **376**(6538), 362-366.
150. Shamoo, Y., Friedman, A. M., Parsons, M. R., Konigsberg, W. H., and Steitz, T. A. (1995a). Crystal structure of a replication fork single-stranded DNA binding protein (T4 gp32) complexed to DNA. *Nature* **376**(6538), 362-366.
151. Shen, R. (2006). Protein secondary structure prediction using conditional random fields and profiles. MS Thesis. Oregon State Univeristy.
152. Shen, R., Olcott, M. C., Kim, J., Rajagopal, I., and Mathews, C. K. (2004). *Escherichia coli* nucleoside diphosphate kinase interactions with T4 phage proteins of deoxyribonucleotide synthesis and possible regulatory functions. *J. Biol. Chem.* **279**(31), 32225-32232.

153. Shen, R., Wheeler, L., and Mathews, C. K. (2006). Molecular interactions involving *Escherichia coli* nucleoside diphosphate kinase. *J. Bioenerg. Biomembr.*, In press.
154. Sinev, M. A., Sineva, E. V., Ittah, V., and Haas, E. (1996). Towards a mechanism of AMP-substrate inhibition in adenylate kinase from *Escherichia coli*. *FEBS Lett.* **397**(2-3), 273-276.
155. Sinha, N. K., Morris, C. F., and Alberts, B. M. (1980). Efficient in vitro replication of double-stranded DNA templates by a purified T4 bacteriophage replication system. *J. Biol. Chem.* **255**(9), 4290-4293.
156. Sjöberg, B. M., Hahne, S., Mathews, C. Z., Mathews, C. K., Rand, K. N., and Gait, M. J. (1986). The bacteriophage T4 gene for the small subunit of ribonucleotide reductase contains an intron. *EMBO J.* **5**(8), 2031-2036.
157. Song, H. K., Sohn, S. H., and Suh, S. W. (1999). Crystal structure of deoxycytidylate hydroxymethylase from bacteriophage T4, a component of the deoxyribonucleoside triphosphate-synthesizing complex. *EMBO J.* **18**(5), 1104-1113.
158. Song, S., Pursell, Z. F., Copeland, W. C., Longley, M. J., Kunkel, T. A., and Mathews, C. K. (2005). DNA precursor asymmetries in mammalian tissue mitochondria and possible contribution to mutagenesis through reduced replication fidelity. *Proc. Natl. Acad. Sci. U. S. A* **102**(14), 4990-4995.
159. Song, S., Wheeler, L. J., and Mathews, C. K. (2003). Deoxyribonucleotide pool imbalance stimulates deletions in HeLa cell mitochondrial DNA. *J. Biol. Chem.* **278**(45), 43893-43896.
160. Srere, P. A. (1987). Complexes of sequential metabolic enzymes. *Annu. Rev. Biochem.* **56**, 89-124.
161. Srere, P. A., and Mathews, C. K. (1990). Purification of multienzyme complexes. *Methods Enzymol.* **182**, 539-551.

162. Stafford, M. E., Reddy, G. P., and Mathews, C. K. (1977). Further studies on bacteriophage T4 DNA synthesis in sucrose-plasmolyzed cells. *J. Virol.* **23**(1), 53-60.
163. Sun, X., Harder, J., Krook, M., Jornvall, H., Sjöberg, B. M., and Reichard, P. (1993). A possible glycine radical in anaerobic ribonucleotide reductase from *Escherichia coli*: nucleotide sequence of the cloned *nrdD* gene. *Proc. Natl. Acad. Sci. U. S. A* **90**(2), 577-581.
164. Szabo, A., Stolz, L., and Granzow, R. (1995). Surface plasmon resonance and its use in biomolecular interaction analysis (BIA). *Curr. Opin. Struct. Biol.* **5**(5), 699-705.
165. Tan, S. H., Zhang, Z., and Ng, S. K. (2004). ADVICE: Automated Detection and Validation of Interaction by Co-Evolution. *Nucleic Acids Res.* **32**(Web Server issue), W69-W72.
166. Teplyakov, A., Sebastiao, P., Obmolova, G., Perrakis, A., Brush, G. S., Bessman, M. J., and Wilson, K. S. (1996). Crystal structure of bacteriophage T4 deoxynucleotide kinase with its substrates dGMP and ATP. *EMBO J.* **15**(14), 3487-3497.
167. Thelander, L., and Reichard, P. (1979). Reduction of ribonucleotides. *Annu. Rev. Biochem.* **48**, 133-158.
168. Thylén, C. (1988). Expression and DNA sequence of the cloned bacteriophage T4 dCMP hydroxymethylase gene. *J. Bacteriol.* **170**(4), 1994-1998.
169. Thylén, C., and Mathews, C. K. (1989). Essential role of T4 phage deoxycytidylate hydroxymethylase in a multienzyme complex for deoxyribonucleotide synthesis. *J. Biol. Chem.* **264**(26), 15169-15172.
170. Timmons, L., and Shearn, A. (2000). Role of AWD/nucleoside diphosphate kinase in *Drosophila* development. *J. Bioenerg. Biomembr.* **32**(3), 293-300.
171. Tomich, P. K., Chiu, C. S., Wovcha, M. G., and Greenberg, G. R. (1974). Evidence for a complex regulating the *in vivo* activities of early enzymes induced by bacteriophage T4. *J. Biol. Chem.* **249**(23), 7613-7622.

172. Trakselis, M. A., Mayer, M. U., Ishmael, F. T., Roccasecca, R. M., and Benkovic, S. J. (2001). Dynamic protein interactions in the bacteriophage T4 replisome. *Trends Biochem. Sci.* **26**(9), 566-572.
173. Tseng, M. J., Hilfinger, J. M., He, P., and Greenberg, G. R. (1992). Tandem cloning of bacteriophage T4 *nrdA* and *nrdB* genes and overproduction of ribonucleoside diphosphate reductase (alpha 2 beta 2) and a mutationally altered form (alpha 2 beta 2(93)). *J. Bacteriol.* **174**(17), 5740-5744.
174. Tseng, M. J., Hilfinger, J. M., Walsh, A., and Greenberg, G. R. (1988). Total sequence, flanking regions, and transcripts of bacteriophage T4 *nrdA* gene, coding for alpha chain of ribonucleoside diphosphate reductase. *J. Biol. Chem.* **263**(31), 16242-16251.
175. Villemain, J. L., and Giedroc, D. P. (1996). The N-terminal B-domain of T4 gene 32 protein modulates the lifetime of cooperatively bound Gp32-ss nucleic acid complexes. *Biochemistry* **35**(45), 14395-14404.
176. Villemain, J. L., Ma, Y., Giedroc, D. P., and Morrical, S. W. (2000). Mutations in the N-terminal cooperativity domain of gene 32 protein alter properties of the T4 DNA replication and recombination systems. *J. Biol. Chem.* **275**(40), 31496-31504.
177. Wahba, A. J., and Friedkin, M. (1961). Direct spectrophotometric evidence for the oxidation of tetrahydrofolate during the enzymatic synthesis of thymidylate. *J. Biol. Chem.* **236**, PC11-PC12.
178. Walhout, A. J., Boulton, S. J., and Vidal, M. (2000). Yeast two-hybrid systems and protein interaction mapping projects for yeast and worm. *Yeast* **17**(2), 88-94.
179. Walhout, A. J., and Vidal, M. (2001). Protein interaction maps for model organisms. *Nat. Rev. Mol. Cell Biol.* **2**(1), 55-62.
180. Webb, P. A., Perisic, O., Mendola, C. E., Backer, J. M., and Williams, R. L. (1995). The crystal structure of a human nucleoside diphosphate kinase, NM23-H2. *J. Mol. Biol.* **251**(4), 574-587.

181. Welch, G. R., and Gaertner, F. H. (1975). Influence of an aggregated multienzyme system on transient time: kinetic evidence for compartmentation by an aromatic-amino-acid synthesizing complex of *Neurospora crassa*. *Proc. Natl. Acad. Sci. U. S. A* **72**(11), 4218-4222.
182. Werner, R. (1971). Mechanism of DNA replication. *Nature* **230**(5296), 570-572.
183. Wheeler, L., Wang, Y., and Mathews, C. K. (1992). Specific associations of T4 bacteriophage proteins with immobilized deoxycytidylate hydroxymethylase. *J. Biol. Chem.* **267**(11), 7664-7670.
184. Wheeler, L. J., Ray, N. B., Ungermann, C., Hendricks, S. P., Bernard, M. A., Hanson, E. S., and Mathews, C. K. (1996). T4 phage gene 32 protein as a candidate organizing factor for the deoxyribonucleoside triphosphate synthetase complex. *J. Biol. Chem.* **271**(19), 11156-11162.
185. Williams, R. L., Oren, D. A., Munoz-Dorado, J., Inouye, S., Inouye, M., and Arnold, E. (1993). Crystal structure of *Myxococcus xanthus* nucleoside diphosphate kinase and its interaction with a nucleotide substrate at 2.0 Å resolution. *J. Mol. Biol.* **234**(4), 1230-1247.
186. Young, J. P., and Mathews, C. K. (1992). Interactions between T4 phage-coded deoxycytidylate hydroxymethylase and thymidylate synthase as revealed with an anti-idiotypic antibody. *J. Biol. Chem.* **267**(15), 10786-10790.
187. Young, P., Ohman, M., and Sjöberg, B. M. (1994a). Bacteriophage T4 gene 55.9 encodes an activity required for anaerobic ribonucleotide reduction. *J. Biol. Chem.* **269**(45), 27815-27818.
188. Young, P., Ohman, M., Xu, M. Q., Shub, D. A., and Sjöberg, B. M. (1994b). Intron-containing T4 bacteriophage gene *sunY* encodes an anaerobic ribonucleotide reductase. *J. Biol. Chem.* **269**(32), 20229-20232.
189. Zhang, X., Lu, Q., Inouye, M., and Mathews, C. K. (1996). Effects of T4 phage infection and anaerobiosis upon nucleotide pools and mutagenesis in nucleoside diphosphokinase-defective *Escherichia coli* strains. *J. Bacteriol.* **178**(14), 4115-4121.

190. Zhang, X., and Mathews, C. K. (1995). Natural DNA precursor pool asymmetry and base sequence context as determinants of replication fidelity. *J. Biol. Chem.* **270**(15), 8401-8404.
191. Zhang, Y., and Skolnick, J. (2005). The protein structure prediction problem could be solved using the current PDB library. *Proc. Natl. Acad. Sci. U. S. A* **102**(4), 1029-1034.
192. Zhu, H., Bilgin, M., and Snyder, M. (2003). Proteomics. *Annu. Rev. Biochem.* **72**, 783-812.

**APPENDICES**

## Appendix A. Hm-dCTP Preparation Protocol

Preparation of hm-dCTP is based on the schema depicted in Figure A.1. Deoxycytidine monophosphate (dCMP) is converted to 5-hydroxymethyl-2'-deoxycytidine monophosphate (hm-dCMP) by T4 dCMP hydroxymethylase (gp42) in the presence of tetrahydrofolate and formaldehyde. Hm-dCMP is phosphorylated to hm-dCDP and then hm-dCTP sequentially by T4 dNMP kinase (gp1) and *E. coli* NDP kinase, respectively, with the presence of an ATP regeneration system containing phosphoenolpyruvate and pyruvate kinase.

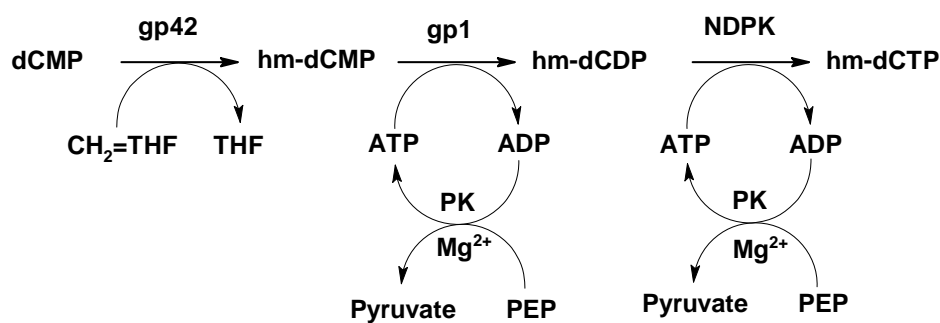


**Figure A.1** Schema for enzymatic preparation of hm-dCTP. PK, pyruvate kinase; gp1, dNMP kinase; gp42, dCMP hydroxymethylase; NDPK, NDP kinase; PEP, phosphoenolpyruvate; THF, tetrahydrofolate; CH<sub>2</sub>=THF, 5,10-methylenetetrahydrofolate.

- **A.1 Enzymatic Production and Purification of hm-dCMP**

- Enzyme reaction (Total volume: 33 ml)

4 ml	1M potassium phosphate buffer, pH 7.0
160 µl	HCHO (37.5% formaldehyde solution)
330 mg	dCMP (330 mg/351.2 mmol/mg = 0.94 mmol)



- Extraction with 2%  $\text{NH}_4\text{OH}$  in 50% ethanol (ethanolic  $\text{NH}_3$ ).  
1<sup>st</sup>, add 35 ml of ethanolic  $\text{NH}_3$  to charcoal, stir for 1 h. Spin down at 3,000 rpm, 30 min. Save the charcoal and supernatant.  
2<sup>nd</sup>, add 20 ml of ethanolic  $\text{NH}_3$  to charcoal, stir for 1 h. Spin down at 3,000 rpm, 30 min. Save the charcoal and supernatant.  
At least 3 times of extraction. Merge the extraction, measure  $A_{283}$  units.
- Dry the extraction with Rotavapor. Re-dissolve in about 4.5 ml  $\text{H}_2\text{O}$ . Measure the  $A_{283}$  units.
- Load it to BioRad AG 50W-X4 (400 mesh) column, pre-equilibrated with  $\text{H}_2\text{O}$  at 0.5 ml/min. Wash with  $\text{H}_2\text{O}$  at 0.5 ml/min. Elute with 0.2 M formic acid at 0.5 ml/min. Pool the fractions of the peaks. If the enzymatic reaction is near complete, the first huge peak should be hm-dCMP.
- Check with TLC to determine which peak is hm-dCMP. See TLC results as shown in Figure A.2.
- Dry the pools by Rotavapor and re-dissolve the pool of huge peak into about 5 ml  $\text{H}_2\text{O}$ . (If it's hard to dissolve, add several drops of  $\text{NH}_4\text{OH}$ ).
- Measure the  $A_{283}$  units. Calculate the hm-dCMP concentration ( $\epsilon_{\text{max}}$  of hm-dCMP: 12,500) and the yield.

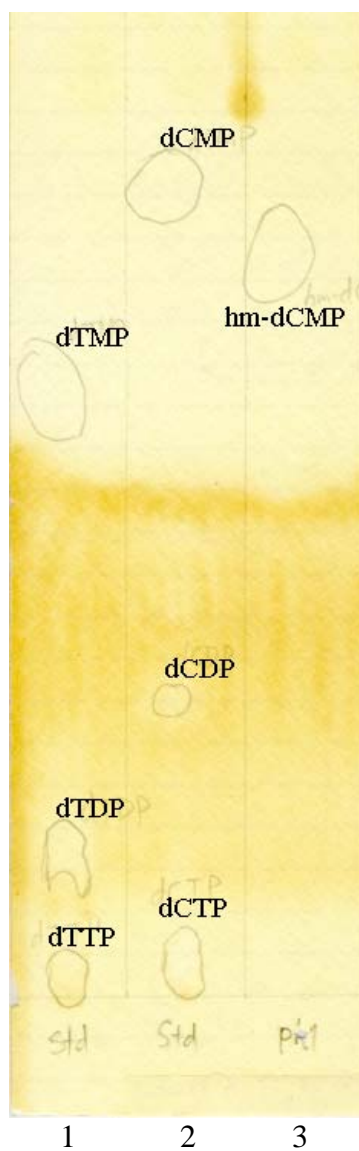


**Figure A.2.** Hm-dCMP production checked by TLC. Lane 1, dTMP, dTDP and dTTP standards; Lane 2, dCMP, dCDP and dCTP standards; Lane 3, hm-dCMP produced in the reaction mixture. PEI-Cellulose F254, 1 M acetic acid + 0.3 M LiCl, 2.5 hr.

- **A.2 Enzymatic Production and Purification of hm-dCTP**

- Enzyme reaction (Total volume: 33 ml)

5 ml	12.7 mM hm-dCMP
25.7 ml	NDPK assay buffer (100 mM Tris-HCl, pH 7.1, 20 mM MgCl <sub>2</sub> (Mg <sup>2+</sup> is critical for phosphorylation), 200 mM KCl)
1.0 ml	T4 gp1 (30-70% ammonium sulfate cut)
1.0 ml	<i>E. coli</i> NDP kinase (45-60% ammonium sulfate cut)
ATP regeneration system:	
165 µl	20 mM ATP (1/127 of the amount of hm-dCMP)
489 mg	PEP (2.5-fold of the amount of hm-dCMP)
40 µl	PK (1,667 nmol/min·µl)
Add H <sub>2</sub> O to 33 ml	

- Incubate at 37°C water bath.
- Take samples at intervals: to 38 µl, add 2 µl of 100% (w/v) TCA to precipitate proteins.
- When the reaction is completed, add 100% (w/v) TCA to 5 %. Store in freezer. Spin down and save the supernatant.
- Run TLC (Cellulose-PEI, F254) in 1 M HAc + 0.3 M LiCl to check hm-dCMP, hm-dCDP and hm-dCTP as shown in Figure A.3. In addition, check with HPLC (Partisil 10SAX, strong anion exchange column).
- Adsorption by activated charcoal. Extraction by 2% NH<sub>4</sub>OH in 50% ethanol just as the steps in hm-dCMP preparation.
- Convert BioRad AG 1-8X-formate (200-400 mesh) column to carbonate type by washing with 650 ml 0.1 M Na<sub>2</sub>CO<sub>3</sub> then with 650 ml H<sub>2</sub>O at 1 ml/min.
- Load the supernatant to the column at 0.3 ml/min. Wash with 150 ml H<sub>2</sub>O at 0.5 ml/min. Then elute with gradient of H<sub>2</sub>O to 0.8 M NH<sub>4</sub>HCO<sub>3</sub> at 0.4 ml/min.

- Pool the fractions of peaks. Dry the pools by Rotavapor. Re-dissolve in 1.5 ml H<sub>2</sub>O.  
Check with TLC and HPLC.
- Calculate the hm-dCTP concentration ( $\epsilon_{\max}$  of hm-dCTP: 12,500) and the yield.

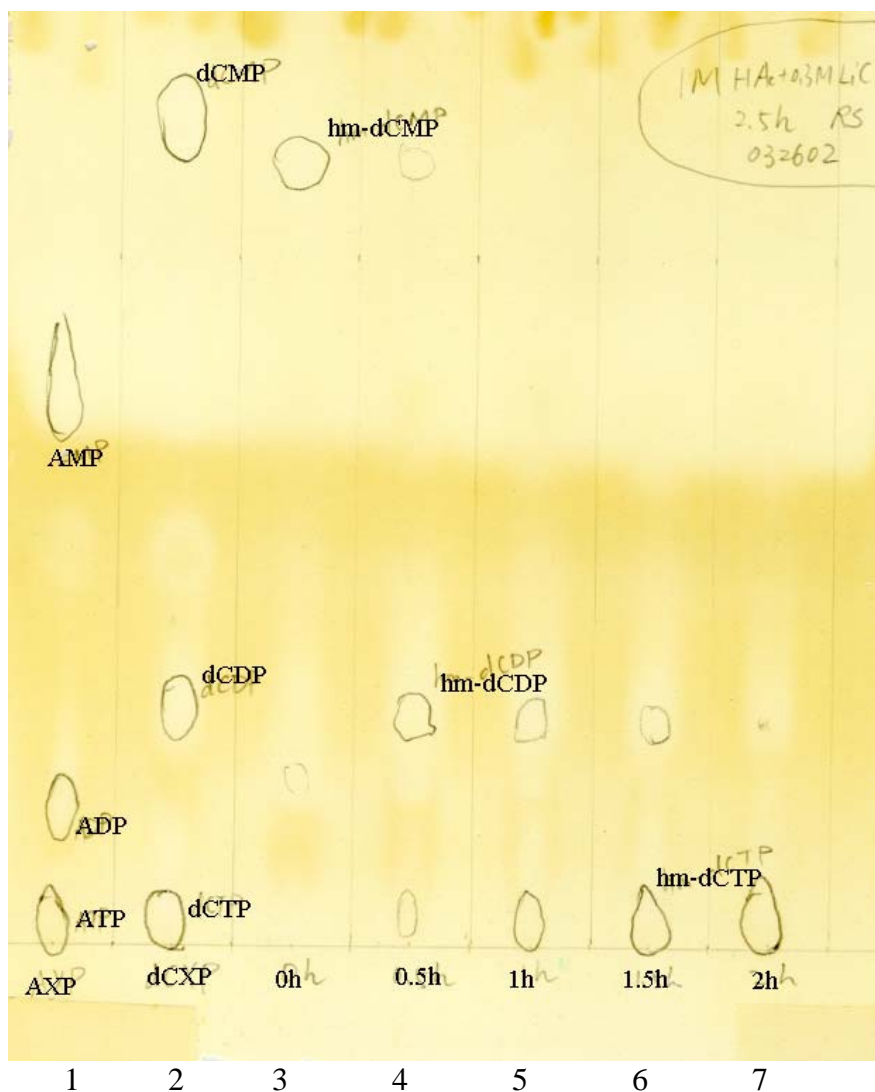


**Figure A.3.** Hm-dCTP production checked by TLC. Lane 1, AMP, ADP and ATP standards; Lane 2, dCMP, dCDP and dCTP standards; Lane 3, reaction at 0 h; Lane 4, reaction at 0.5 h; Lane 5, reaction at 1 h; Lane 6, reaction at 1.5 h; Lane 7, reaction at 2 h. PEI-Cellulose F254, 1 M acetic acid + 0.3 M LiCl, 2.5 hr.

## Appendix B. Raw Data from Analytical Ultracentrifugation

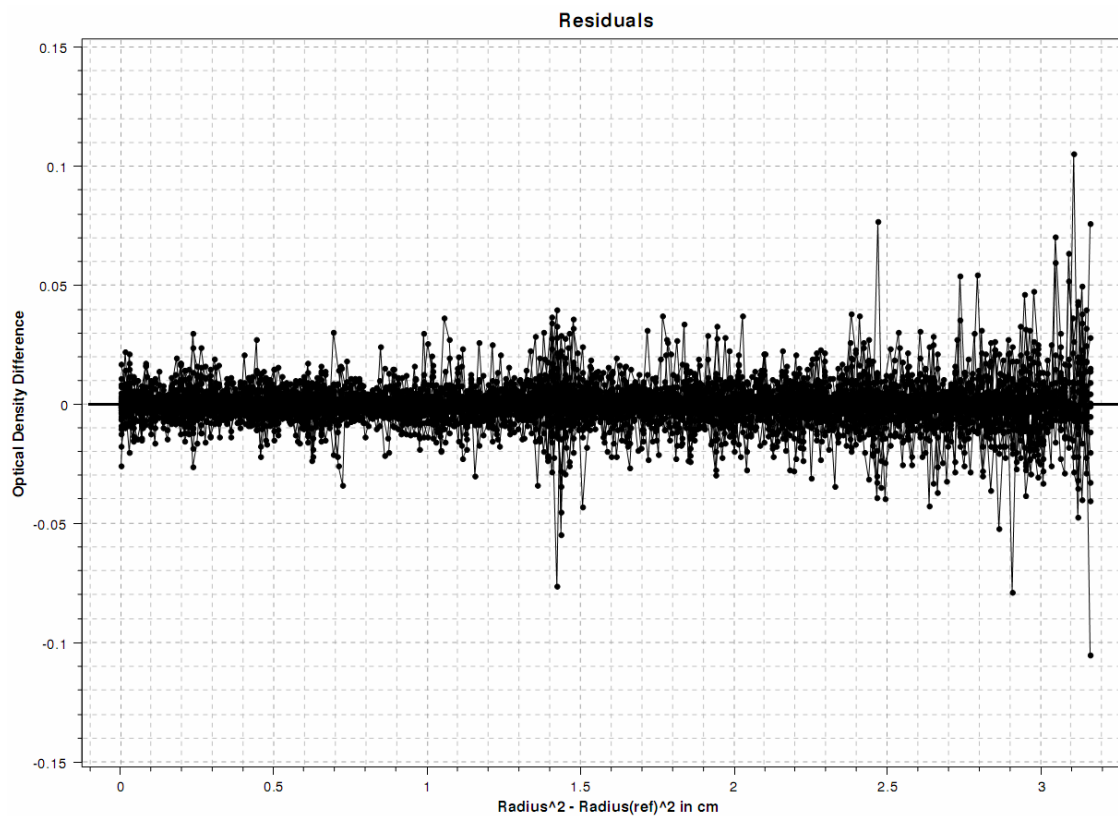


**Figure B.1.** All residual errors in sedimentation equilibrium distribution of *E. coli* NDP kinase. The relative concentration of NDP kinase, measured by its absorbance at 284 nm, was plotted as a function of the radial distance at 15,000 rpm.

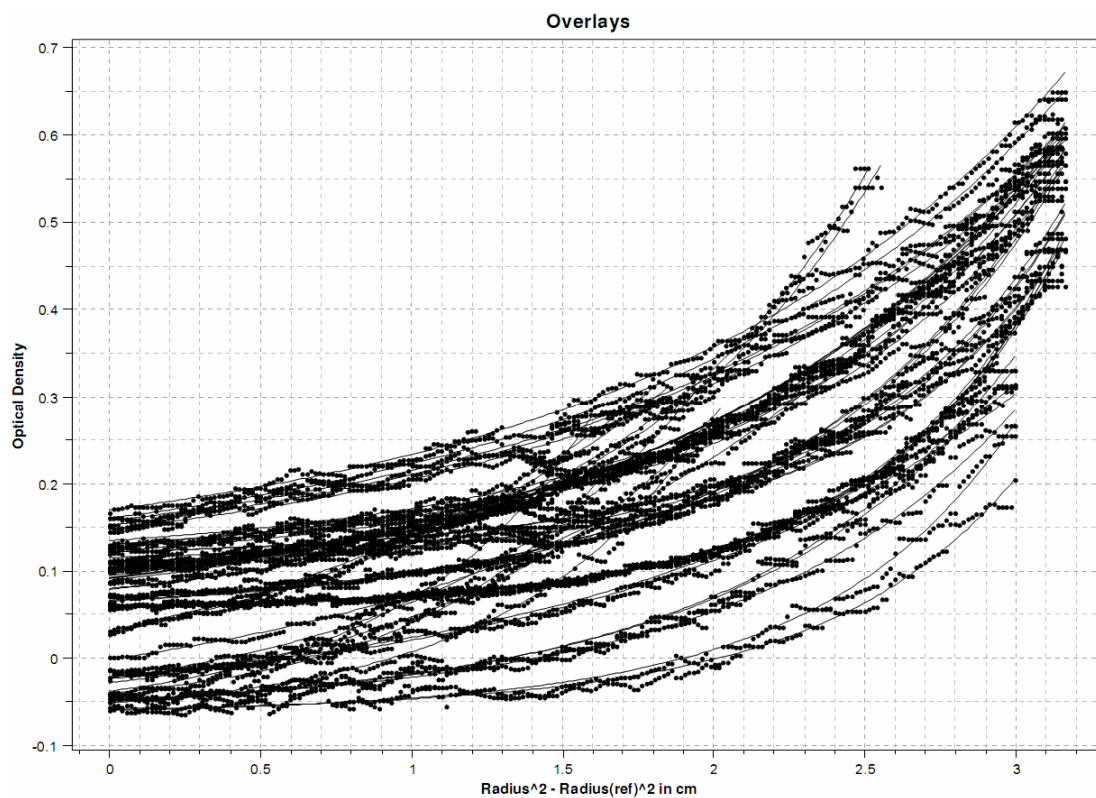
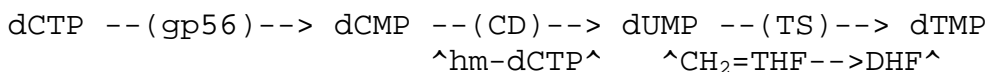


**Figure B.2.** Scan overlays of sedimentation equilibrium distribution of *E. coli* NDP kinase. The relative concentration of NDP kinase, measured by its absorbance at 284 nm, was plotted as a function of the radial distance at 15,000 rpm.

## Appendix C. Computer Simulation of Non-Coupled Assay for Three-Step Pathway: Program in Perl

This Perl program is to show uncoupled reactions as follows:



How to run?

Under command line:

```
perl coupling.pl X
```

assuming the source code is saved as a file name of coupling.pl. X is the folds to the intermediate dCMP concentration, an arbitrary number. X = 1, 2, 4, 10, 50, or other positive integers. By default, X is 1 if X is not provided. That is,

```
perl coupling.pl
```

is the same as

```
perl coupling.pl 1
```

-----The beginning of source code-----

```
#!/usr/bin/perl
use strict;

# The folds of intermediate dCMP
# Default is 1
my $folds = $ARGV[0];

if ($folds == 0) {
    print "Usage: \n perl coupling.pl X\n";
    print " X = 1, 2, 4, 10, 50, or other positive integers\n";
    print " e.g. perl coupling.pl 10\n";
}
```

```

        print "Default is: perl coupling.pl 1\n\n";
        $folds = 1;
    } elsif ($folds < 0) {
        print "Please enter a positive integer!\nProgram now exits!\n";
        exit;
    }

# end time, in min
my $end_time = 6;

# time step (in min), differential variable
my $dt = 1/6000;

# concentration step, (in M), differential variable
my $d_dCTP;
my $d_dCMP;
my $d_dUMP;
my $d_dTMP;

# nucleotide concentration variables, (in M)
my $dCTP = 0.0001;      # initial substrate
my $dCMP;               # intermediate 1
my $dUMP;               # intermediate 2
my $dTMP; # end product

# K_M (Michaelis-Menton constants) variables, (in M)
# These numbers are fixed
my $KM_gp56 = 40 * 10**(-6);
my $KM_CD   = 80 * 10**(-6);
my $KM_TS   = 20 * 10**(-6);

# k_cat values, in min-1 (i.e., s-1 * 60)
my $k_cat_gp56 = 7800;
my $k_cat_CD   = 466 * 60;
my $k_cat_TS   = 11.8 * 60;

# V_max, maximum velocity variables
# V_max = k_cat * [E]t, in M/min

# Concentration of each enzyme is 0.05 uM
my $Et = 0.05 * 10**(-6);
# Assume enzymes are 50% pure and 30% active since enzymes are old
my $relative_activity = 0.5 * 0.3;
my $VMax_gp56 = $k_cat_gp56 * $Et * $relative_activity;
my $VMax_CD   = $k_cat_CD   * $Et * $relative_activity;
my $VMax_TS   = $k_cat_TS   * $Et * $relative_activity;

my $step;
my $step_size;
my $Abs; # Absorbance at 338 nm for dihydrofolate (DHF)

for ( $step = 0; $step_size < $end_time ; $step ++ ) {
    $step_size = $step*$dt;

```

```

# M-M function for gp56
$d_dCTP = -($VMax_gp56*$dCTP/($KM_gp56 + $dCTP) )*$dt;
$dCTP += $d_dCTP;
# this is to ensure [dCTP] >= 0.
if ($dCTP < 0) { $dCTP = 0; }

# M-M function for gp56 and CD
# Assume the intermediate dCMP is concentrated X-fold
#   at X=1, dCMP is not concentrated.
$d_dCMP = ( $VMax_gp56*$dCTP/($KM_gp56 + $dCTP)
  - $VMax_CD*$dCMP*$folds/($KM_CD + $dCMP*$folds) )*$dt;
$dCMP += $d_dCMP;
# this is to ensure [dCMP] >= 0.
if ($dCMP < 0) { $dCMP = 0; }

# M-M function for CD and TS
$d_dUMP = ( $VMax_CD*$dCMP*$folds/($KM_CD + $dCMP*$folds)
  - $VMax_TS*$dUMP/($KM_TS + $dUMP) )*$dt;
$dUMP += $d_dUMP;
# this is to ensure [dUMP] >= 0.
if ($dUMP < 0) { $dUMP = 0; }

# M-M functions   for TS
$d_dTMP = ( $VMax_TS*$dUMP/($KM_TS + $dUMP) )*$dt;
$dTMP += $d_dTMP;

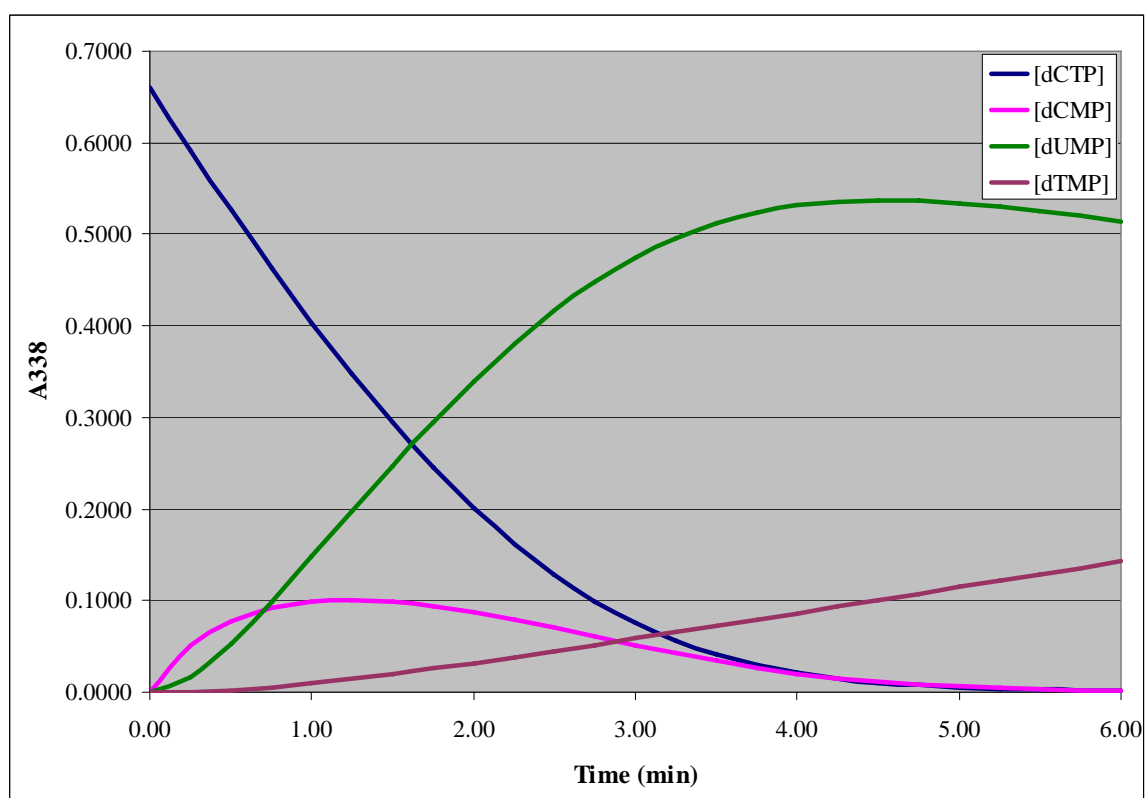
# Absorbance = epsilon * c * l;
# epsilon (338nm) = 6600 M(-1)cm(-1) for DHF
#(Wahba and Friedkin, 1961)
$Abs = 6600 * $dTMP * l;

if ( $step%1500 == 0) {
  # 0.25 min interval is consistent with UV spec
  printf "%5.2f %6.4f %6.4f %6.4f %6.4f \n",
    $step_size, $dCTP*6600, $dCMP*6600, $dUMP*6600, $Abs;
}
}
exit;

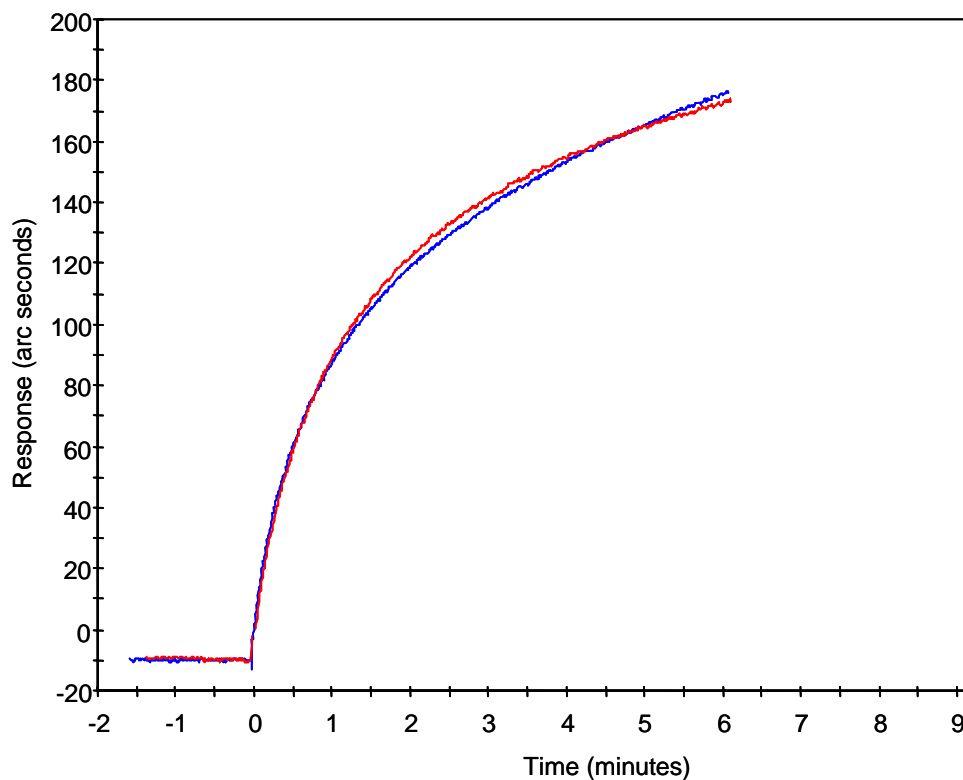
```

-----The end of source code-----

The calculated concentrations of starting substrate, end product and intermediates are shown in Figure C.1.



**Figure C.1.** The calculated concentrations of dCTP, dCMP, dUMP and dTMP.

**Appendix D. Repeatability of IAsys cuvettes.**

**Figure D.1.** The repeatability of an IAsys cuvette. Red curve shows the interaction of T4 gp32 with immobilized *E. coli* NDP kinase, which occurred Blue curve shows the interaction between them after 26 runs of other interaction experiments. Same amount of gp32 were added to the solution in each experiments. Two curves show that not much difference was observed when 26 other runs were conducted in between, suggesting IAsys biosensor possesses good repeatability.